2012 FLEX/Sentinel-3 Tandem Mission Photosynthesis Study

FINAL REPORT
July 2014

ESTEC Contract No. 4000106396/12/NL/AF

Gina H. Mohammed (P & M Technologies, Canada)
Yves Goulas (CNRS – Laboratoire de Météorologie Dynamique, France)
Federico Magnani (University of Bologna, Italy)
Jose Moreno (University of Valencia, Spain)
Julie Olejníčková (Global Change Research Centre AS CR, Czech Republic)
Uwe Rascher (Institute of Bio- and Geosciences, Forschungszentrum Jülich GmbH, Germany)
Christiaan van der Tol (University of Twente, The Netherlands)
Wout Verhoef (University of Twente, The Netherlands)
Alexander Ač (Global Change Research Centre AS CR, Czech Republic)
Fabrice Daumard (CNRS – Laboratoire de Météorologie Dynamique, France)
Alexander Gallé (Forschungszentrum Jülich, Germany; Bayer CropScience NV, Belgium)
Zbyněk Malenovský (Global Change Research Centre AS CR, Czech Republic)
Dan Pernokis (P & M Technologies, Canada)
Juan Pablo Rivera (University of Valencia, Spain)
Jochem Verrelst (University of Valencia, Spain)
Matthias Drusch (ESTEC, The Netherlands)

Study Manager:
Dr. Gina H. Mohammed
Research Director
P & M Technologies, 66 Millwood Street,
Sault Ste. Marie, Ontario P6A 6S7
Canada

ESA/ESTEC Technical Manager:
Dr. Matthias Drusch
Land Surfaces Principal Scientist
Mission Science Division (EOP-SME)
European Space Agency, ESTEC
Earth Observation Programmes
Postbus 299, 2200 AG Noordwijk
The Netherlands

2012 FLEX/Sentinel-3 Tandem Mission Photosynthesis Study — Final Report

2012 FLEX/Sentinel-3 Tandem Mission Photosynthesis Study — Final Report		
ESA/ESTEC Contract No: 4000106396/12/NL/AF	**Subject:** Final Report – July 2014	**Contractor:** P & M Technologies, Canada
***ESA CR( ) No:**	**No. of volumes:** 1	**Contractor's reference:** 39451 (Bidder code); ESA ESTEC ITT AO/1-7088/12/NL/AF

ABSTRACT:
The Photosynthesis Study developed a mechanistically-based model (and a customized GUI) to link steady-state chlorophyll fluorescence with photosynthesis. The study identified steady-state or solar-induced fluorescence features useful as indicators of certain critical stress effects. A key finding was the inherent value of having both red and far-red fluorescence emission peaks for applications, underscoring the unique advantages of FLEX and its FLORIS sensor. A conceptual framework was developed to provide strategic guidance in applying space-based fluorescence to stress detection and planning future research.

Names of authors:

Gina H. Mohammed (P & M Technologies, Canada)
Yves Goulas (CNRS – Laboratoire de Météorologie Dynamique, France)
Federico Magnani (University of Bologna, Italy)
Jose Moreno (University of Valencia, Spain)
Julie Olejníčková (Global Change Research Centre AS CR, Czech Republic)
Uwe Rascher (Institute of Bio- and Geosciences, Forschungszentrum Jülich GmbH, Germany)
Christiaan van der Tol (University of Twente, Netherlands)
Wout Verhoef (University of Twente, Netherlands)
Alexander Ač (Global Change Research Centre AS CR, Czech Republic)
Fabrice Daumard (CNRS – Laboratoire de Météorologie Dynamique, France)
Alexander Gallé (Forschungszentrum Jülich, Germany; currently, Bayer CropScience NV, Belgium)
Zbyněk Malenovský (Global Change Research Centre AS CR, Czech Republic)
Dan Pernokis (P & M Technologies, Canada)
Juan Pablo Rivera (University of Valencia, Spain)
Jochem Verrelst (University of Valencia, Spain)
Matthias Drusch (ESTEC, Netherlands)

ESA Study Manager: Matthias Drusch **Division: **Directorate:	****ESA Budget Heading:**

* To be completed by ESA
** Information to be provided by ESA Study Manager

Table of Contents

Acknowledgements

Funding for the 2012 FLEX/Sentinel-3 Tandem Photosynthesis Study was provided by the European Space Agency through ESTEC Contract No. 4000106396/12/NL/AF.

Helpful contributions to Study activities & reports were provided by Sabrina Raddi, Marijke van der Tol, Antonio Volta, Elena Mezzini, Karel Klem, Frantisek Zemek, Ismael Moya, Anke Schickling, Luis Alonso, and Jesús Delegido Gómez. We also thank the many researchers and organizations who permitted access to their datasets, and especially Jaume Flexas and Albert Porcar-Castell.

Valuable inputs and feedback were obtained from the FLEX Mission Advisory Group, including Elizabeth Middleton, Andreas Huth, Ladislav Nedbal, and Franco Miglietta. We also thank ESA's Stefan Kraft, Umberto Del Bello, and Dirk Schuettemeyer for sharing their insights on FLEX/FLORIS and related campaigns.

Abstract

Within the context of ESA's Phase A/B1 assessments of the FLuorescence EXplorer (FLEX) Earth Explorer 8 candidate mission, the Photosynthesis Study developed and tested a mechanistically-based model to link steady-state chlorophyll fluorescence with photosynthesis. The photosynthesis model developed was an advancement of the SCOPE (Soil Canopy Observation of Photochemistry and Energy fluxes) canopy model and comprises state-of-the-art modules connecting leaf fundamental physiology to top-of-canopy outputs of fluorescence and photosynthesis. Tests of the model show successful simulation of canopy primary productivity comparable to that obtained by eddy flux towers, and sensitivity tests revealed the essential parameters needed to optimize computational speed and efficiency. For convenience of usage, a Graphic User Interface called *A-SCOPE* was created and customized for the new SCOPE v1.53 model, with full user documentation and manuals.

Development of simplified algorithms linking fluorescence to photosynthesis was accomplished based on the model. Relatively simple regression models based on Gaussian processes regression and polynomial & rational functions were able to predict photosynthetic products (e.g., net photosynthesis of the canopy, gross primary productivity, light use efficiency, absorbed photosynthetically active radiation by chlorophyll) in unstressed C3 and C4 species. Noteworthy was the finding that in regression models for C3 and C4 plants, the F685 fluorescence emission peak was more informative than the far-red fluorescence. Nonetheless, relationships were stronger when both bands were included and, for C4 plants, the full fluorescence emission profile was essential to meet an error threshold of 10%.

A second component of the research identified steady-state or solar-induced fluorescence features useful as indicators of stress effects from water deficit, temperature extremes, and nitrogen insufficiency. Red and far-red fluorescence peaks and their ratios were found responsive for the detection of physiological strain from these stresses. Novel stress indices were introduced here as well and require further testing. These included the Stress Intensity Fluorescence Index (SIFI), the Temperature Stress Fluorescence Index (TSFI), the Water Stress Fluorescence Index (WSFI), and the Nitrogen Stress Fluorescence Index (NSFI). In addition, the photosynthesis model and its simplified formats and related algorithms also could provide stress indices based on ratios of actual to potential photosynthesis.

Analysis of knowledge gaps with respect to stress applications indicated the topics of vegetation canopy structural effects, environmental heterogeneity, combined stresses, and sources of variability or error as among the highest priority for study. A conceptual framework was then developed to provide strategic guidance in applying space-based fluorescence to stress detection and in planning future research.

Overall, the findings of this study revealed the inherent value of having a minimum of both the red and far-red fluorescence emission peaks, and in C4 plants the full fluorescence profile. This underscores the unique advantages of FLEX, since its FLORIS sensor would be optimized to extract these spectral features with appropriate spatial and spectral detail.

Executive Summary

Background

Chlorophyll fluorescence (CF) is a natural spectral emission resulting from the interaction of plant chlorophyll pigment with visible light (typically 400-700 nm). In photosynthesizing tissues, red and far-red light can be emitted from any chlorophyll-containing plant tissues which are exposed to light: primarily foliage, but also green stems, green exposed roots, floral structures, many fruits, and green seeds. This emission of chlorophyll fluorescence caused by sunlight is termed 'solar-induced' or 'sun-induced' fluorescence (SIF), and its measurement technique is deemed to be passive as no artificial excitation light is used to induce the fluorescence.

The capacity to observe SIF presents a totally novel option for space-based remote sensing: extracting information on the actual workings of the photosynthetic machinery of plant canopies. Because the production of chlorophyll fluorescence is related to the function of the two photosystems responsible for photosynthetic initiation in green plants, it provides a glimpse into the dynamics of the photosynthetic process itself, an insight not available from existing methodologies involving the usual vegetation reflectance indices.

Momentum is building within the scientific community to apply SIF to quantify terrestrial vegetation photosynthesis – including for the modelling of gross primary productivity (GPP). A second major application area is in detection of stress effects, especially before visual damage is apparent. Stress applications do not necessarily require quantification of photosynthetic rates or GPP, but instead may be able to utilize simple SIF indices.

Promising results in recent years from other investigators indicate that it is indeed possible to discriminate the subtle SIF signal from satellite platforms; however, existing satellite sensors are not optimized spatially or spectrally for SIF retrievals and applications. This presents a unique advantage for the FLuorescence EXplorer (FLEX), which is being designed specifically for the purpose of capture and usage of SIF from terrestrial vegetation. Key to that initiative is the development of methods to derive quantitative photosynthetic information from SIF.

Goals of the Photosynthesis Study

The Photosynthesis Study analysed the relationship between steady-state chlorophyll fluorescence and photosynthesis, and developed and tested a mechanistically-based model to derive photosynthesis from FLEX/Sentinel-3 Tandem Mission (FLEX/S3) measurements and auxiliary data. A secondary goal was to identify health & stress indicators from steady-state fluorescence features.

This dual focus allows full exploitation of the breadth of information potentially contained in the fluorescence signal from space.

Science tasks

The Photosynthesis Study was divided into four major tasks:

1. **Review of model availability and datasets: model/module assessment, comparison, and gap analysis.** A comprehensive review was conducted of available models linking photosynthesis and steady-state chlorophyll fluorescence. Sixty-five datasets were gathered into a database for model testing. Then based on performance results and suitability for the aims of the study, recommendations were made on the appropriate constitution of the consolidated model.
2. **Model implementation, validation, sensitivity analysis, and error quantification.** Software and documentation were produced for the model, which was then verified and validated for internal consistency and performance against field data. Sensitivity tests were performed to support model simplification, and error quantification was done for output variables versus uncertainties in input data.
3. **Algorithm development based on models.** Development of a Level-2 prototype algorithm was investigated to derive measures of photosynthesis from the FLEX/S3 tandem mission using this simplified approach.
4. **Fluorescence as an indicator of vegetation health and stress resilience.** A review was completed of SIF indicators for detection of water deficit, temperature extremes, and nitrogen insufficiency. Knowledge gaps were identified and prioritized, and a conceptual framework was formulated for SIF application in stress detection.

Model development

Because of the timeframe of the Study and the fact that previous studies have made progress in model development, the emphasis here was on utilizing existing models/modules, then integrating them into a consolidated program.

Evaluation of promising models/modules identified in the literature produced a shortlist of candidates which were tested for their capacity to link fluorescence and photosynthesis, and their suitability for the study's goals.

Based on the findings of the model review and testing, the final consolidated model was designated to contain:

1. **for leaf biochemistry:** the MD12 model (developed by F. Magnani and colleagues) is an advanced model capturing fundamental processes in the leaf photosynthetic centres and containing routines for C3 and C4 vegetation, linking steady-state fluorescence and photosynthesis;
2. **for leaf radiative transfer:** the Fluspect optical model (developed by W. Verhoef) is a relatively simple model that operates efficiently and quickly due to its fast layer doubling algorithm;

3. **for canopy radiative transfer:** the SCOPE canopy model (developed by C. van der Tol and colleagues) links all modules in the chain and represents propagation of the fluorescence signals and fluxes to the top of the vegetation canopy.

The SCOPE model, first developed and published in 2009, was significantly updated here to its current version 1.53 – with new functionality, improved modularity, and up-to-date user documentation and manuals. Modules are usable individually or in combination, thus allowing for flexibility. (The model package also includes two leaf-level physiology modules that are empirically-calibrated and require fewer parameters than MD12.)

SCOPE v1.53 was automated in the PS Study to produce the Graphic User Interface A-SCOPE v1.53, which improves user-friendliness for aspects such as data input, storage, graphics and output management (Figure 1).

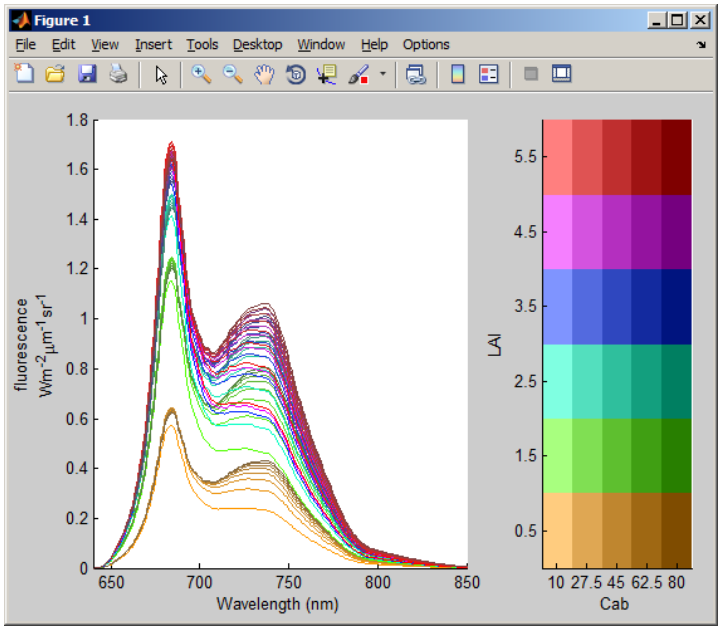

Figure 1. Example of Fluorescence graphic output from SCOPE/A-SCOPE, with color variations based on a broad range of two variables (Cab, LAI).

Model simplification and validation

SCOPE is a complex model with over 50 parameters, necessitating significant run times when all variables are in play. By identifying driving and non-driving parameters, the latter may be kept fixed (to default values) in most situations, thereby simplifying the model and increasing computational speed. Sensitivity analyses identified 10 to 12 core driving parameters for fluorescence and photosynthesis in the consolidated model (Table 1). Furthermore, if co-varying parameters are considered, the model can be streamlined even further. This does not mean that the full parameter matrix will not provide advantages in addressing diverse terrestrial vegetation canopies and conditions, hence, the full complement of variables is maintained at this time for greatest versatility.

Table 1. Major driving parameters of the SCOPE model for fluorescence and photosynthesis.

Driving parameters for fluorescence and photosynthesis	
• maximum carboxylation capacity	• leaf chlorophyll content
• Ball-Berry parameter ***m*** (stomatal conductance)	• dry matter content[1]
• **'Beta'** (fraction of photons partitioned to PSII)	• leaf area index
• rate of sustained non-photochemical quenching **kNPQs** (protection against high-light damage)	• incoming shortwave radiation
• fraction of functional reaction centres **qLs** (photodamage: a lower fraction=higher risk)	• air temperature
• **'stressfactor'**	• atmospheric vapour pressure (optional: C3 species only)

[1]Consistently important for fluorescence only.

The model was tested against field canopy data from a published study of winter wheat. In general, SCOPE was able to simulate canopy photosynthesis behaviour over the course of the day and with respect to the shape of the fluorescence emission. The model was able to simulate steady-state fluorescence especially in the O_2-A (far-red) band, but preliminary indications are that it may be overestimating fluorescence in the O_2-B (red) band. This will require further testing with additional datasets and fine-tuning of parameter settings and/or modules as appropriate.

Algorithms relating fluorescence and photosynthesis

Algorithm development based on the model was also investigated, including the possibility to deduce relatively simple relationships between SIF and GPP or net canopy photosynthesis (NPC). Model inversion work indicated that inclusion of fluorescence data resulted in substantive improvement in algorithm performance for the estimation of NPC. The two types of statistical algorithms – Gaussian processes regression (or GPR) and polynomial & rational functions fitting (or PRF) – gave highly accurate results for retrieval of canopy photosynthesis in the case of C3 plants, while with C4 plants excellent results were obtained using GPR (lower success with PRF). PRF using only simple optical data in a low number of channels was able to predict photosynthetic products (GPP, LUE, APARChl) for C3 plants in a non-stressed case with high performance; for C4 plants, only APARChl could be predicted with high accuracy. Both fluorescence bands were needed to predict GPP and LUE using PRF, meaning that the two bands do not carry the same information. Using GPR, although relationships were obtained using only the second emission peak F740, the most information apparently is contained within the first emission peak F685. An error threshold of 10% was already achievable with the F685 emission band in C3 species using GPR; including more bands, the whole fluorescence profile, and additional biophysical variables optimally yielded R^2 of 0.95 in C3 plants. In C4 plants, GPR required the full fluorescence profile to meet the error threshold. Neither reflectance data nor solely biophysical variables (Chl, LAI, *f*APAR) led to meaningful relationships with NPC. However, it is prudent to take chlorophyll content into account due to its effects on light absorption

(which influences photosynthesis and fluorescence radiance positively) and reabsorption (which decreases fluorescence emission).

Although the models tested in this study were simple and used a limited number of variables, they proved their efficacy to predict photosynthetic products, at least in the absence of severe stress. Further investigations should be undertaken to test the robustness of the retrievals, preferentially with canopy SIF data such as that recently made available from the *HyPlant* airborne sensor, designed as an airborne prototype for FLORIS.

In the case of one-variable models, F760 surprisingly was found to be non-predictive for any products, regardless the plant type (C3, C4). This is in contrast with the previously reported high correlation between far-red fluorescence and GPP deduced from experimental data (Guanter *et al.* 2012; Berry *et al.* 2013; Frankenberg *et al.* 2011b; Rossini *et al.* 2010).

Stress detection

SIF was evaluated for use in detecting stress effects from water deficit, temperature extremes, and nitrogen deficiency. A random-effects meta-analysis identified clear benefits of the red and far-red fluorescence bands and the ratio of these bands for detection of stress-induced strain. Results of the meta-analysis were that:

- water deficit generally causes the red and far-red fluorescence at leaf and canopy levels to decrease;
- both types of temperature stresses cause the ratio of red to far-red fluorescence (stress to control ratio) to decrease;
- nitrogen deficit increases the red to far-red ratio.

Several novel fluorescence-based stress indices have been proposed here to assess stress intensity as well as stress quality in relation with water, temperature, and nitrogen stress. Further investigations and evaluations of these new stress indicators should be undertaken. These indicators are in addition to simple indices already known to be effective for identification of stress, most notably the ratio of red to far-red fluorescence (particularly expressed as a ratio of stressed:control values). The importance of normalizing SIF features was evident, which can be achieved through the use of control values as shown here, or, as others have shown, through the use of incident or absorbed PAR. Furthermore, with FLEX, the repeated measurements would create a change detection system whereby initial retrievals can serve as a baseline for comparison of subsequent retrievals. And finally, the photosynthesis model or its simplified formats – and the F-GPP algorithms developed in this study – provide even further choices for stress indices based on ratios of actual to potential photosynthesis.

Information gaps highlighted the need for better understanding of the effects of canopy structural complexity, environmental heterogeneity, stress interactions, and sources of error, among other factors. Sources of variability or error may be broadly categorized as arising from vegetation factors, environmental factors (including stresses), and instrumental or data processing factors. In remote sensing of SIF, clearly it is more practical to control instrumental

or data processing methods than vegetation and environmental factors, necessitating the availability of adequate supporting and ground-truthing information to assist investigations.

To advance utilization of SIF, a conceptual framework has been formulated for application of remote SIF for stress detection (Figure 2), which also identified priorities for further study. Major elements of the framework include determination of goals and target applications; prioritization of vegetation sites; delineation of likely stresses and associated sources of variability/error; selection of SIF indicators; and definition of supporting measures needed for calibration, validation, data processing, and interpretation.

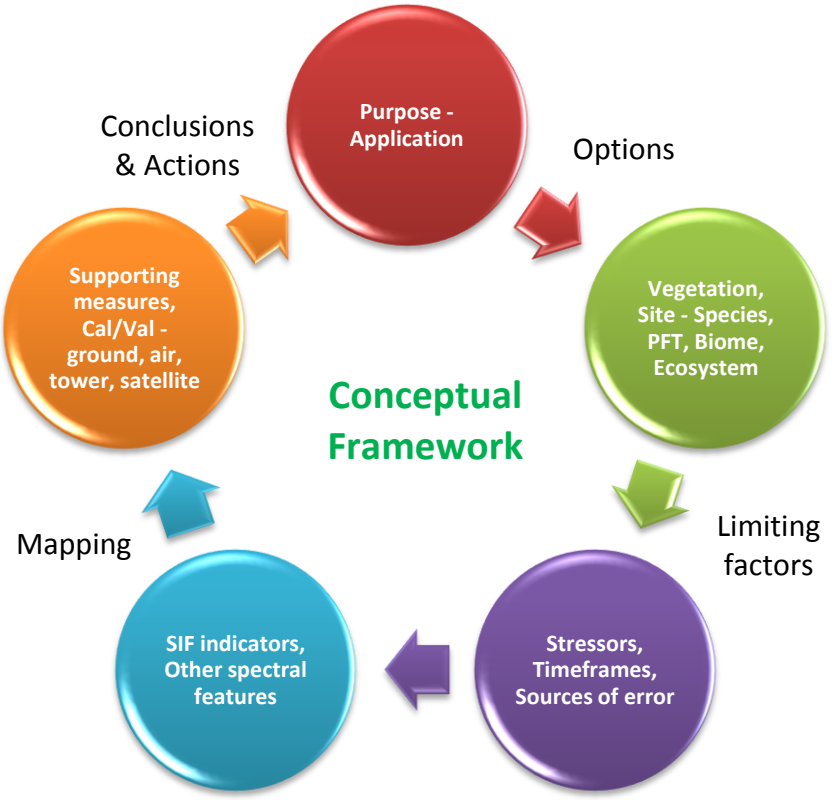

Figure 2. Conceptual framework for the use of remote SIF in stress detection.

Priorities for future study include consideration of the full range of potential applications, identification of the most suitable SIF indicators for different situations, understanding potential sources of variability and errors, establishment of ancillary technologies, and characterization and establishment of site networks for remote and ground-based assessments. Development of calibration and validation strategies and tools is a crucial subject that warrants concerted attention.

Significance for the FLEX mission

Outputs from the Photosynthesis Study that are of key relevance to the FLEX mission include:

1. **model advances** – the availability now of a powerful consolidated model for linking canopy SIF and photosynthesis, making it possible to derive photosynthesis from FLEX fluorescence retrievals (upon conversion to top-of-canopy signals);
2. **model GUI for users** – development of the new A-SCOPE Graphic User Interface, greatly facilitating usage of the photosynthesis model and opening the door to a potentially broad range of users for FLEX-derived products;
3. **calibration/validation tool** – availability of the SCOPE v1.53 model for calibration and validation activities during mission deployment;
4. **processing advancements** – demonstration of streamlining options for the photosynthesis model, thereby making more feasible the execution of large-volume analyses to be triggered from FLEX data;
5. **support of FLORIS spectral strategy** – substantiation in the model inversion work of the inherent value of both fluorescence peaks and the full fluorescence profile for estimating net photosynthesis of the canopy, thus conferring a singular advantage to the FLORIS sensor scheme to extract the complete emission profile;
6. **algorithms** – indications that simple regression models were able to predict photosynthetic products (NPC, GPP, LUE, APARChl) with high performance for C3 and C4 plants in a non-stressed case;
7. **stress applications** – development of novel stress indices, and confirmation of the benefits of having both red and far-red peaks for tracking strain induced by the stresses of water deficit, temperature extremes, and nitrogen insufficiency, which are all issues of contemporary concern in food production and management of significant vegetation systems worldwide;
8. **strategic approach** – depiction of a conceptual framework to support application of SIF to issues involving vegetation stresses and resource management.

Next steps

To build upon the findings of the Photosynthesis Study, the following developments are recommended:

- **advanced model parameterization** – advances in parameterization within the model of strategic physiological variables such light energy distribution between the photosystems, quantification of photoprotective quenching, and photodamage;
- **comprehensive model testing** – evaluation of model performance under a broader range of field situations, including stress scenarios;
- **algorithm testing** – evaluation of the robustness of simple regression models found here to relate SIF and photosynthetic products;

- **expanded stress detection** – consideration of a wider range of stresses – including multiple-stress situations – for which SIF might serve as an indicator, and identification of additional features from the full spectral emission profile that could be used;
- **stress indices testing & validation** – prototype stress indices have been suggested by the study activities which merit further testing and validation under various conditions and with a range of species and functional types;
- **calibration & validation** – development of a thorough strategy for calibration and validation of SIF from FLEX so that accurate interpretations may be drawn in the various application areas;
- **analysis & mitigation of errors** – elucidation of sources of variability and potential errors arising from biological and environmental factors which may constrain interpretations of SIF behaviour in response to stress, and presentation of strategies to mitigate errors and misinterpretation.

A comprehensive suite of recommendations has been developed for actions and studies which could span the timeframe leading up to and during FLEX deployment. These needs serve to underscore a significant reality: SIF from space is truly a fresh and emerging arena for understanding real-time photosynthetic behaviour of land vegetation – a possibility not envisaged before the prospect of the FLEX mission.

Even now, with intensifying efforts from researchers endeavouring to extract SIF data from non-optimized satellite platforms such as GOSAT, GOME-2, OCO-2, etc., it is evident that the FLEX mission would be unique and advantageously positioned to fully engage this extraordinary signal. FLEX and its sensor FLORIS would be the vanguard for this new way to view the actual functioning of terrestrial vegetation from space.

1. Introduction

Chlorophyll fluorescence (CF) is a photobiological phenomenon resulting from the interaction of the chlorophyll in green plant tissues with light. In photosynthesizing tissues, red and far-red light may be emitted from any chlorophyll-containing tissues exposed to light: primarily foliage, but also green stems, green exposed roots, floral structures, many fruits, and green seeds. This emission of chlorophyll fluorescence caused by sunlight is termed 'solar-induced' or 'sun-induced' fluorescence (SIF), and its measurement technique is deemed to be passive. This is in contrast to active techniques which use artificial light sources such as lasers, light-emitting diodes, or halogen lamps to stimulate fluorescence via application of pulses and/or continuous illumination. In natural or artificial light, CF in healthy vegetation achieves a stable low emission or 'steady-state' at a given light intensity.

The capacity to observe SIF presents a totally novel option for space-based remote sensing: extracting information on the real-time workings of the photosynthetic machinery of plant canopies. Because the fluorescence emission is related to the function of the two photosystems active during photosynthetic initiation in green plants, it provides a glimpse into the actual dynamics of the photosynthetic process.

Over the last few decades, CF has been used extensively in thousands of studies and in operational situations to probe the health and stress status of terrestrial and aquatic vegetation. In terrestrial studies, it has been applied in laboratory and field studies in agriculture, horticulture, forestry, and natural ecosystem science. Whereas most of this work has utilized active techniques using near-contact instrumentation, in the last 15-20 years there has been an upsurge in near-remote-scale work using passive and active approaches. More recently, there has been heightened interest in remote passive measurement of canopy SIF from airborne and spaceborne platforms. Some excellent reviews of CF theory and stress applications are available in the literature (Ač *et al.* 2012; Fernandez-Jaramillo *et al.* 2012; Tremblay *et al.* 2012; Rodriguez *et al.* 2011; Rohacek *et al.* 2008; Theisen 2002; Schreiber *et al.* 1994; Krause & Weis 1991; Lichtenthaler & Rinderle 1988).

CF and photosynthesis

The special advantages of CF information reside in its intimate association with photosynthesis and the capacity of CF to reveal non-destructively (unlike most other physiological techniques) whether that process is being compromised, and passive (by definition) does not interfere at all with the instantaneous process being observed or measured. According to current photobiological theory, CF emission is one of several ways by which plants partition absorbed light. Other major paths are heat production and photosynthetic electron transport. CF emission is low (< 5% of absorbed PAR) in comparison to these other routes, and it is considered a dissipation pathway that allows plant tissues to harmlessly shed light energy that may be excessive for photosynthesis and which could otherwise damage tissues.

Although the fluorescence emission is small, it is discernible with sufficiently sensitive instrumentation and suitable retrieval methodologies, and thus CF analysis has been used

widely and successfully to track onset and recovery from stress, even using remote systems deployed from towers or air. Nonetheless, the kinetics of CF emission are complex, and confidence in CF usage traditionally has depended upon using not just one but various CF parameters and by including complementary measures of physiology and environmental variables to assist interpretation (Daumard *et al.* 2010; Malenovský *et al.* 2009).

Fluorescence retrievals from space

The great opportunity for CF is the transition from its proven place as a ground tool and more recently an airborne-based tool to a spaceborne platform capable of monitoring terrestrial vegetation biology on a global scale. Early results with satellites have been intriguing and point to a small but retrievable signal, so far measured in the far-red extremes of the emission. Scientists at NASA's Goddard Space Flight Center and the Jet Propulsion Lab along with their colleagues have published several papers in recent years reporting early SIF retrievals from sensors on-board the Japanese satellite, GOSAT. These data have been used to generated global fluorescence maps, albeit acknowledging the uncertainties and challenges working with a non-optimized platform (Joiner *et al.* 2013, 2012, 2011; Frankenberg *et al.* 2011a,b). Such efforts complement longer-standing investigations of SIF feasibility by the European Space Agency which, over the course of a decade or more, have culminated in the proposed FLuorescence EXplorer (FLEX), a candidate now undergoing Phase A/B1 assessments as an Earth Explorer 8 mission.

Momentum is building within the scientific community to apply SIF to quantify terrestrial vegetation photosynthesis – including for the modelling of gross primary productivity (GPP) (Berry *et al.* 2013). The other main application area is in the early detection of stress effects and recovery from physiological strain. Such evaluations do not necessarily require quantification of photosynthetic rates *per se* but could potentially utilize changes over time of fluorescence-based indices indicative of health or strain (e.g., Fernandez-Jaramillo *et al.* 2012; Tremblay *et al.* 2012; Rodriguez *et al.* 2011).

Goals of the Photosynthesis Study

The Photosynthesis Study analysed the relationship between steady-state chlorophyll fluorescence and photosynthesis, and developed and tested a mechanistically-based model to derive photosynthesis from FLEX/Sentinel-3 Tandem Mission (FLEX/S3) measurements and auxiliary data. A secondary goal was to identify health & stress indicators from steady-state fluorescence features.

The challenge

Photosynthesis is a highly complex process consisting of many biophysical sub-processes and chemical reactions. Oxygenic photosynthesis involves two light reactions operating simultaneously at the reaction centers of both photosystems (PSI and PSII). Light energy is absorbed by the photosystems, then converted into chemical energy used to split water and generate high-energy molecules and reducing agents, ultimately servicing the production of vital organic molecules (Stirbet and Govindjee 2011). These internal processes are constantly

adjusting their efficiencies in response to the environment and the overall physiological status of the plant. Consequently, actual photosynthetic efficiency in green tissues varies considerably, even over very short timescales.

Estimating actual photosynthesis from numerical simulations therefore necessitates a complex modelling approach. Traditionally, photosynthesis models have been driven by standard meteorological variables of rainfall, incident global radiation, wind speed, minimum and maximum air temperature, and mean relative air-humidity. Atmospheric CO_2 concentration also must be known. Models are highly parameterised with a large number of coefficients – factors which are not well defined at large spatial scales and which often rely on fixed look-up table values. Uncertainties in the forcing data introduce further errors into model estimates.

But more recently, process-based tools have emerged which introduce novel elements such as fluorescence. In 2009, C. van der Tol and colleagues presented a canopy model that takes into account SIF and photosynthesis of C3 and C4 vegetation (Van der Tol *et al.* 2009b). [Their SCOPE model (Soil Canopy Observation of Photochemistry and Energy fluxes) has become a useful and well-received tool to support the modelling of water, carbon dioxide, and energy fluxes at the land surface.] These researchers noted that the responsiveness of fluorescence makes it the most direct measure of instantaneous vegetation growth that is currently available for remote sensing. The SCOPE model helps to explain the behaviour of the relationship between CF and photosynthesis reported in the literature. As evidenced through simulations, sensitivity analysis, and measurements, SCOPE shows that variations in total fluorescence correlate with changes in actual photosynthesis under certain conditions. To calculate the actual photosynthesis rate, an estimate of maximum carboxylation capacity is also needed.

The Photosynthesis Study examined the use of SIF for quantifying photosynthesis and in assessing vegetation health and stress status. This dual focus was chosen to exploit the range of information that might be contained in the fluorescence signal from space. On the modelling side, the study identified the most promising developments in photosynthetic process-based modelling and consolidated these best-of-class modules into an integrated platform that is both versatile and user-friendly. [Because of the timeframe of the study and the fact that previous studies have made progress in model development, the emphasis here was on existing models/modules that could be integrated and optimized into a consolidated platform.]

Science tasks

1. **Review of model availability and datasets: model/module assessment, comparison, and gap analysis.** A comprehensive review was conducted of available models linking photosynthesis and steady-state chlorophyll fluorescence. Sixty-five datasets were gathered into a database for model testing. Then, based on performance results and suitability for the aims of the study, recommendations were made as to the best combination of modules for the consolidated final model.

2. **Model implementation, validation, sensitivity analysis, and error quantification.** Software and documentation were developed for the consolidated model. The model was tested for internal consistency and validated against field data. Local

and global sensitivity tests were conducted to simplify the model. Finally, error quantification was done for output variables versus uncertainties in input data.

3. **Algorithm development based on models.** Development of a Level-2 prototype algorithm was undertaken to derive measures of photosynthesis from FLEX/S3 tandem mission using simplified algorithms.

4. **Fluorescence as an indicator of vegetation health and stress resilience.** A review was conducted of steady-state fluorescence indicators for detection of water deficit, temperature extremes, and nitrogen insufficiency. Knowledge gaps were identified and prioritized, and a conceptual framework was formulated for SIF application in stress detection.

Benefits: Applications of SIF

The PS Study supports advances in these areas:

- **photosynthesis modelling** – estimation of canopy physiology, primary productivity; algorithm development; contributions relevant to parameterization of vegetation carbon models;
- **calibration/validation tools** – capacity to provide expected canopy SIF values to gauge veracity of FLEX retrievals;
- **stress applications** – tracking of vegetation responses to stress, including resilience and recovery from natural or human-induced perturbations;
- **gap analysis** – identification of science information gaps that are high priorities for research;
- **strategic planning** – formulation of a conceptual framework for use of remote SIF information, with recommendations for implementation.

2. Data sets and model availability review: model/module assessment, comparison, and gap analysis

2.1 Introduction

This task laid the foundation for the modelling component of the Photosynthesis Study by conducting:

1. a review of existing models and modules that link steady-state (ambient) chlorophyll fluorescence and photosynthesis;
2. a review of available datasets and generation of a database that may be used in testing the models/modules;
3. testing and verification of the modules;
4. development of a model design framework.

Recommendations from this component were applied in the activities that follow on model implementation.

2.2 Review and comparison of existing modules

The main focus was on models addressing: (i) the functional link between photosynthesis and ambient fluorescence in the O_2-B and O_2-A spectral band; the upscaling of (ii) leaf biochemistry and photosynthetic rates, and (iii) ambient fluorescence from leaf to canopy level.

A list of available models that can be provided to ESA was generated, and for each model/module, the following information assembled:

1. description of the individual modelling framework;
2. description of the level of the models/modules (i.e., leaf, canopy, ecosystem);
3. references/publications;
4. availability of the model/module to the Consortium;
5. description of the code/language of the model/modules, if available, or of the algorithms to be coded;
6. explicit list of input parameters for the models/modules;
7. description of the input and output variables of the models/modules;
8. contact information for the Principle Investigator responsible for each model/module;
9. explicit list and description of the test-data that were used for testing the model, and of additional data that could be available for such purposes.

As a first step, a thorough literature search was carried out. Although the focus was on process-based or physically-based models, other empirical models were also briefly reviewed. While all spatial scales were addressed – including the levels of photosystems and single leaves – special emphasis was given to the canopy scale, and the analysis was restricted to 1-D canopy models, i.e., models assuming canopy horizontal homogeneity.

The review also considered models and modules suitable for the prediction of other key parameters to be modelled in the subsequent task (Chapter 3), including:

- radiative transfer and reflectance in the red-edge spectral region, as related to chlorophyll content and canopy leaf area index (LAI);
- Photochemical Reflectance Index (PRI);
- Absorbed Photosynthetically Active Radiation (APAR);
- canopy temperature.

Possible alternatives and improvements over the modules already used in the SCOPE model (Van der Tol *et al.* 2009b) were identified and analysed, also considering the gap analysis already carried out in previous ESA studies.

2.2.1 Results

The search identified a total of **15 leaf-level models** (12 process-based and 3 empirical or semi-empirical models; Table 2.1), **8 radiative transfer models** for the representation of solar-induced fluorescence at leaf and canopy scale (Table 2.2) and **5 empirical models** for the representation of the relationship between solar-induced fluorescence (or fluorescence peak ratio) and photosynthetic or functional processes at canopy scale (Table 2.3).

Each model was further evaluated for relevance and suitability for the aims of the project and the overall mission; strengths, weaknesses, opportunities; availability to the consortium; and critical issues for validation. This process produced a short-list of chloroplast- or leaf-level models (SG95, RS98, TV09, MD12, TB12) and radiative transfer models (FluorMODleaf, Fluspect, SCOPE) for further consideration and testing in the proceeding sections.

Table 2.1. Summary of leaf-level candidate models.

Model #	Name/ acronym	Processes [§]	Type *	Details ^	References	Language	Code avail.	Description avail.	PI contacts
1	SG95	ETR / Fs	PB	PSII, SS	(Srivastava *et al.* 1995a,b)	Algorithm	n.a.	Full	R.J. Strasser, Univ Geneva, CH
2	RS98	ETR / Fs	PB	PSII, SS	(Rosema *et al.* 1998)	Algorithm	n.a.	Full	A. Rosema, EARS, NL
3	AC00	T / FR	E	PSI+II, VFS	(Agati *et al.* 2000)	Algorithm	n.a.	n.a.	G. Agati, CNT, IT
4	FE02	gs, A / Fs	E	PSI+II	(Flexas *et al.* 2002)	Curve	n.a.	n.a.	J. Flexas, Univ. Baleares, E
5	LB02	ETR / Fs	PB	PSI+II,FSD	(Lebedeva *et al.* 2002)	Algorithm	n.a.	Full	A.B. Rubin, Moscow State Univ, RU
6	ZG05	ETR / Fs	PB	PSII, FD	(Zhu *et al.* 2005)	Algorithm	n.a.	Full	S.P. Long, Univ Illinois, USA
7	AP08	Fs / FR	PB	PSI+II, VFS, SS	(Agati *et al.* 2008)	Algorithm		Partial	G. Agati, CNT, IT
8	AR08	ETR / Fs	PB	PSII,FD	(Antal & Rubin 2008)	Algorithm	n.a.	Full	A.B. Rubin, Moscow State Univ, RU
9	TV09	ETR, A / Fs	PB	PSII, SS	(Van der Tol *et al.* 2009a)	MATLAB	Yes	Full	C. van der Tol, ITC, NL
10	L09	ETR / Fs	PB	PSII, FD	(Lazar & Jablonsky 2009)	Algorithm	n.a.	Full	D. Lazár, Palacky Univ, Olomouc, CZ
11	MD09	ETR, A / Fs	PB	PSII, SS	(Magnani *et al.* 2009)	MATLAB	Yes	Full	F. Magnani, UNIBO, IT
12	TT10	PAR / FR	SE	PSI+II	(Thoren *et al.* 2010)	Algorithm	n.a.	Full	U. Schmidhalter, TUM, DE
13	MD12	ETR, A / Fs	PB	PSII, SS	(Magnani & Dayyoub 2014)	Algorithm	Yes	Full	F. Magnani, UNIBO, IT
14	TB12	ETR, A / Fs	PB	PSII, SS	(Van der Tol *et al.* 2014; Berry *et al.* 2013)	MATLAB	Yes	Full	C. van der Tol, ITC, NL
15	ZA12	PAR, ETR / Fs	PB	PSII, FSD	(Zaks *et al.* 2012)	Algorithm	n.a.	Full	G.R Fleming, UC Berkeley, USA

[§] A, gross photosynthesis; PAR, photosynthetically active radiation; T, temperature; ETR, electron transport rate; FR, fluorescence ratio; Fs, solar-induced fluorescence; gs, stomatal conductance.

*PB, process-based; E, empirical; SE, semi-empirical.

^ SS, steady state fluorescence; FD, fast (OJIP) fluorescence dynamics; FSD, fast and slow fluorescence dynamics; PSII, only photosystem II contribution to fluorescence; PSI+II, contributions from both photosystems represented; VFS, variable fluorescence spectrum.

Table 2.2. Candidate up-scaling models.

Model #	Name/ acronym	Processes [§]	Level	Type *	Functional module	Details ^	References	Language	Code avail.	Description avail.	PI contacts
16	FLSAIL	PAR, LAI / Fs, FR, ρ	TOC	RT	fixed Φf	FFS, SL	(Rosema *et al.* 1991)	Fortran	yes	Partial	W. Verhoef, ITC, NL
17	OM92	PAR, LAI / Fs, FR, ρ	TOC	RT	fixed Φf	FFS, SL	(Olioso *et al.* 1992)		no	Partial	A. Olioso, INRA, FR
18	SLOPE	PAR, LAI / Fs, FR, ρ	TOC	RT	fixed Φf	FFS, SL	(Maier 2000)	C	yes	Full	S.W. Maier, Charles Darwin Univ, AU
19	FluorSAIL 2	PAR, LAI / Fs, FR, ρ	TOC	PB, RT	RS98	VFS	(Miller *et al.* 2005)	Fortran	yes	Full	W. Verhoef, ITC, NL
20	FluorMOD leaf	PAR, Chl / Fs, FR	Leaf	RT	RS98	VFS, AL	(Pedrós *et al.* 2010; Miller *et al.* 2005)	C	yes	Full	Y. Goulas, CNRS, FR
21	SCOPE 1.2.1	PAR, LAI, T, RH, CO_2, Chl, N%, Ψ, GPP/ Fs, FR, ρ, canopy temperature	Leaf, TOC	PB, RT	TV08, MD09	FFS, SL	(Magnani *et al.* 2009; Van der Tol *et al.* 2009b)	MATLAB	yes	Full	W. Verhoef, ITC, NL
22	Fluspect	PAR, Chl / Fs, FR	Leaf	RT	RS98	VFS, AL	(Verhoef 2010)	Visual Basic (Fortran, MATLAB)	Yes	Full	W. Verhoef, ITC, NL
23	SCOPE 1.3.4	PAR, LAI, T, RH, CO_2, Chl, N%, Ψ, GPP/ Fs, FR, ρ, canopy temperature	Leaf, TOC	PB, RT	TV08, MD09, Fluspect	VFS, AL	-	MATLAB	yes	Full	W. Verhoef, ITC, NL

[§] PAR, photosynthetically active radiation; T, temperature; FR, fluorescence ratio; Fs, solar-induced fluorescence; GPP, gross primary production; ρ, reflectance; Ψ, soil water potential or content; LAI, leaf area index; Chl, chlorophyll content; RH, air humidity; N%, leaf N concentration; CO_2, air CO_2 concentration

* PB, process-based; RT, radiative transfer/energy balance

^ FFS, fixed fluorescence spectrum; VFS, variable fluorescence spectrum; SL, symmetric leaf; AL, asymmetric leaf

Table 2.3. Additional canopy-scale empirical models.

Model #	Name/ acronym	Processes [§]	Level ^	References	Details	PI contacts
24	FC02	A / FR	TOC	(Freedman *et al.* 2002)	from data	A. Freedman, Aerodyne, USA
25	LI05	Fv/Fm / Fs	TOC	(Liu *et al.* 2005)	Algorithm	L. Liu, Chinese Academy Sciences, CN
26	PP05	Ψ / Fs	TOC	(Perez-Priego *et al.* 2005)	Algorithm	P. Zarco-Tejada, IAS-CSIC, E
27	D10	GPP/ Fs	TOC	(Damm *et al.* 2010)	Algorithm	U. Rascher, IBG2, D
28	FR11	GPP / Fs	TOA	(Frankenberg *et al.* 2011b)	Algorithm	C. Frankenberg, JPL, CalTech, USA

[§] A, gross photosynthesis; FR, fluorescence ratio; Fs, solar-induced fluorescence; GPP, gross primary production; Fv/Fm maximum (dark-adapted) PSII photochemical yield; Ψ, predawn water potential.
^ TOC, top of canopy; TOA, top of atmosphere

2.3 Database generation

This activity reviewed existing datasets for evaluation and testing of modules that might constitute the bricks of the integrated numerical model on which photosynthesis retrieval will be based. Each dataset should be a coordinated set of concurrent environmental, physiological and radiative measurements, possibly complemented by a thorough characterization of structural and biochemical characteristics, at either leaf or canopy level, acquired under either ambient or controlled conditions.

Datasets of interest contained one or more of these types of data:

1. laboratory measurements of leaf-level photosynthesis and ambient fluorescence (i.e. fluorescence level is controlled only by ambient environmental parameters) under variable and controlled conditions;
2. laboratory measurements of leaf-level photosynthesis and pulse-modulated fluorescence under variable and controlled conditions;
3. field measurements of leaf-level photosynthesis and ambient or pulse-modulated fluorescence under variable conditions;
4. field measurements of canopy ambient fluorescence and GPP under variable conditions;
5. field measurements of canopy profiles of biochemical and physiological properties.

The datasets were required to contain all relevant parameters suitable to test the different model approaches and to fulfill a proper comparison of the models. With respect to points 1-4 above, each dataset was required to contain four independent sub-datasets:

1. an environmental dataset;
2. a dataset of ancillary variables (if needed);
3. an input dataset;
4. a verification dataset (for model comparison).

Datasets were located by searching the Web of Knowledge for the topics:

((ambient) OR (steady state) OR (solar induced) OR (sunlight induced)) AND fluorescence AND photosynthesis

2.3.1 Results

The literature search resulted in a total of 65 datasets (Table 2.4), of which 22 were acquired by the Fraunhofer line discrimination technique, 24 by laser-induced fluorescence technique and 22 by the modulated fluorescence technique; several datasets included measurements by a combination of techniques. A total of 29 studies contained data on fluorescence radiances, 32 on fluorescence yields and 30 on fluorescence peak ratios (or fluorescence spectra). A total of 47 datasets investigated leaf level processes, and 22 related to others scales (tree, canopy, global). With respect to environmental factors studied, 10 studies addressed the effects of drought, 4 the response to variable levels of atmospheric CO_2, and 11 the effects of N fertilization or nutrient stress.

Regarding the availability of datasets to the consortium, 11 were already available to project partners, whilst 10 others could be readily accessible through contacts with principal investigators. For the remaining 42 datasets, data could be derived from tables or figures already published in the open literature.

The database was made available to the Consortium on the PS Study website.

Table 2.4. Summary of available datasets for the PS Study.

Data-set #	Code	Reference	Variables addressed*	Scale	Method^	Instrument‡	Applied conditions	Species	Data availability§				PI contacts
									envir.	ancillary	input	valid.	
1	MW80	(McFarlane *et al.* 1980)	Ψ, Fs	canopy	FLD	custom	drought	*Citrus maxima*	n.a.	n.a.	tables	tables	-
2	HS91	(Havaux *et al.* 1991)	Φp, Φf	leaf	MF	Hansatech	light, age	*Pisum sativum, Spinacia oleracea*	tables	n.a.	tables	tables	-
3	WW86	(Wong & Woo 1986)	A, ETR, Φf	leaf	MF	custom	CO_2, DCMU	*Gossypium hirsutum, Brassica chinensis, Helianthus annuus*	tables	n.a.	tables	tables	-
4	CT90	(Carter *et al.* 1990)	A, Fs	leaf	FLD	PerkinElmer	Kautsky, ambient	*Zea mays, Liquidambar styraciflua, Pinus taeda*	n.a.	n.a.	tables	tables	-
5	LH90	(Lichtenthaler *et al.* 1990)	Chl, FR	leaf	LIF	custom	pollution	*Picea abies, Acer pseudoplatanus*	n.a.	n.a.	tables	tables	-
6	RC92	(Rosema *et al.* 1992)	Φf	leaf	LIF	custom	ozone	*Pseudotsuga menziesii, Populus spp.*	tables	n.a.	n.a.	tables	-
7	GD94	(Gunther *et al.* 1994)	A, Chl, Φp,Φf, FR	leaf	LIF	DlidaR-2	drought	*Quercus pubescens*	n.a.	n.a.	tables	tables	-
8	MC94	(McMurtrey III *et al.* 1994)	ρ, A, Φf, FR	leaf	LIF	custom	N%	*Zea mays*	n.a.	n.a.	n.a.	tables	E. Middleton, NASA, USA
9	SM94	(Subhash & Mohanan 1994)	Φf, FR	leaf	LIF	custom	nutrients	*Oryza sativa*	n.a.	n.a.	n.a.	tables	-
10	VC94	(Valentini *et al.* 1994)	A, Φf, FR	leaf	LIF	FLIDAR, LEAF	ambient, PAR, CO_2, drought	*Quercus ilex, Populus alba, Fagus sylvatica*	tables	n.a.	tables	tables	R. Valentini, Univ Tuscia, I
11	AM95	(Agati *et al.* 1995)	Φf, FR	leaf	LIF	LEAF	ambient, Chl, PAR, T	*Ficus benjamini, Lycopersicon esculentum, Epipremnum aureum, Juglans regia, Fagus sylvatica*	tables	n.a.	tables	tables	G. Agati, CNT, IT
12	BU95	(Buschmann 1995)	Φf, FR	leaf	MF, LIF	Walz PAM, LITWaF	Aurea mutants, PAR	*Nicotiana tabacum*	n.a.	n.a.	tables	tables	C. Buschmann, Univ Karlsruhe, DE
13	SG95	(Srivastava *et al.* 1995a)	Φp, Φf, FR	leaf	MF	Hansatech	PAR, age	*Pisum sativum, Nerium oleander, Ficus spp.*	tables	n.a.	tables	tables	R.J. Strasser, Univ Geneva, CH
14	AM96	(Agati *et al.* 1996)	Fv/Fm, Φf, FR	leaf	LIF	LEAF	T	*Phaseolus vulgaris, Pisum sativum*	tables	n.a.	tables	tables	G. Agati, CNT, IT

15	BL96	(Babani & Lichtenthaler 1996)	A, Fv/Fm, Φp, FR	leaf	FM, LIF	LITWaF	ageing, Chl	*Hordeum vulgaris*	n.a.	n.a.	tables	tables	H.K. Lichtenthaler, Univ Karlsruhe, DE
16	CG96	(Cerovic *et al*. 1996)	Φp, Φf, τ	leaf	TRF	-LIDAR	Light, water stress, C3/C4/ CAM	*Beta vulgaris, Zea mays, Kalanchoë sp.*	tables	n.a.	tables	tables	Y. Goulas, CNRS, F
17	SM97	(Subhash & Mohanan 1997)	Φf, FR	leaf	LIF	custom	Nutrient stress	*Helianthus annuus*	n.a.	n.a.	tables	tables	C.N. Mohanan, CESS, IND
18	AG98	(Agati 1998)	Φf, FR	leaf	LIF	custom	T, PAR	*Lycopersicon esculentum, Phaseolus vulgaris, Pisum sativum, Vicia faba*	tables	n.a.	tables	tables	G. Agati, CNT, IT
19	PF98	(Pfundel 1998)	Fv/Fm, FR (77K)	leaf	FM, SF	Walz PAM 101-103, PerkinElmer	C3/C4 photosyn-thesis	*Flaveria spp.* (C3 and C4), *Zea mays*	tables	tables	tables	tables	E. Pfundel, Heinz Walz GmbH, DE
20	RS98	(Rosema *et al.* 1998)	A, Φp, Φf	leaf	LIF, MF	EARS-PPM	PAR, drought, ozone	*Populus nigra*	data	data	data	data	C. van der Tol, ITC, NL
21	FE99	(Flexas *et al.* 1999)	PAR, T, Ψ, A, ETR, Φf	leaf	FM	Walz PAM-2000	ambient, drought	*Vitis vinifera*	tables	n.a.	tables	tables	J. Flexas, Univ. Baleares, E
22	GB99	(Gitelson *et al.* 1999) (Gitelson *et al.*, 1998)	Chl, FR	leaf	SF	PerkinElmer	species, season	*Fagus sylvatica, Ulmus minor, Parthenocissus tricuspidata*	n.a.	n.a.	tables	tables	C.Buschmann, Univ Karlsruhe, DE
23	KT99	(Kebabian *et al.* 1999)	Chl, Fs, FR	leaf	LIF	PFS	N fertilization	*Phaseolus vulgaris*	n.a.	tables	tables	tables	A. Freedman, Aerodyne, USA
24	MB99	(Morales *et al.* 1999)	Chl, Φp, Φf, τ	leaf	LIF, TRF	-LIDAR	season, Fe-deficiency	*Beta vulgaris*	n.a.	n.a.	tables	tables	Y. Goulas, CNRS, F
25	AC00	(Agati *et al.* 2000)	Φf, τ, FR	leaf	TRF	Cerovic	T	*Phaseolus vulgaris, Pisum sativum*	tables	n.a.	tables	tables	G. Agati, CNT, IT
26	SS00	(Saito *et al.* 2000)	Chl, FR	tree	LIF	custom	season	*Ginkgo biloba*	n.a.	n.a	tables	tables	Y. Saito, Shinshu Univ, JP
27	OE01	(Ounis *et al.* 2001)	Φf	leaf	MF	Laser-PAM	ambient	*Vitis vinifera*	n.a.	n.a.	tables	tables	Y. Goulas, CNRS, F
28	PO01	(Peterson *et al.* 2001)	A, Φf, FR	Leaf	MF	Walz PAM-101 modified	Kautsky	*Helianthus annuus, Sorghum bicolor*	n.a.	n.a.	tables	tables	A. Laisk, Tartu Univ, EE
29	FC02	(Freedman *et al.* 2002)	A, FR	canopy	FLD	PFS	CO_2, N%	*Quercus hemispherica*	n.a.	n.a.	tables	tables	A. Freedman, Aerodyne, USA

30	FJ02	(Franck *et al.*2002)	Φf, FR	Chloroplasts	SF	PerkinElmer	Kautsky	*Hordeum vulgare*	n.a.	n.a.	tables	tables	R. Popovic, U. Quebec, CA
31	FL02	(Flexas *et al.* 2002)	A, Φp, Φf	leaf	MF	Walz PAM-2000	ambient, drought	*Vitis vinifera*	data	n.a.	data	data	J. Flexas, Univ. Baleares, E
32	CM03	(Corp *et al.* 2003)	Chl, LAI, FR	leaf, canopy	SF, LIF	FIS, LIFIS	N%	*Zea mays*	contact	contact	contact	contact	E. Middleton, NASA, USA
33	ZP03	(Zarco-Tejada *et al.* 2003)	Chl, DPi, Φf	canopy	DPD, MF	ASD FieldspecPro, Walz PAM-2000	T stress, drought	*Acer negundo*	tables	n.a.	tables	tables	P. Zarco-Tejada, IAS-CSIC, E
34	CF04	(Carter *et al.* 2004)	A, Chl, Fs, FR	leaf	FLD	PFS	bromicil	*Zea mays, Glycine max*	n.a.	n.a.	tables	tables	G.A. Carter, NASA, USA
35	ME04	(Evain *et al.* 2004; Moya *et al.* 2004)	A, Fs, PRI, Φp, Φf	leaf	FM, LIF	Laser-PAM, FIPAM	PAR, DTT, ambient	*Vitis vinifera*	data	data	data	data	I.Moya, CNRS, F
36	AK05	(Ananyev *et al.* 2005)	A, Φp, Φf	leaf	LIF, MF	LIFT, Walz MiniPAM	ambient	*Populus deltoides, Inga spp., Pterocarpus spp.*	tables	n.a.	tables	contact	U. Rascher, IBG2, D
37	LI05	(Liu *et al.* 2005)	Fv/Fm, Fs	canopy	FLD, MF	ASD Fieldspec, OptiScience OS1-FL	ambient	*Triticum aestivum, Parthenocissus tricuspidata*	n.a.	n.a.	tables	tables	L. Liu, Chinese Academy Sciences, CN
38	PP05	(Perez-Priego *et al.* 2005)	Φp,Fs	canopy	FLD, MF	OceanOptics HR-2000, Walz PAM-2100	drought	*Olea europaea*	n.a.	n.a.	tables	tables	P. Zarco-Tejada, IAS-CSIC, E
39	SIFLEX02	(Louis *et al.* 2005)	Fs, PRI, GPP	canopy	FLD	PMFD	ambient	*Pinus sylvestris*	contact	n.a.	contact	contact	I. Moya, CNRS, F
40	LO06	(Louis *et al.* 2006)	FR, ASFY	leaf	SF	Cary Eclipse, Variant	ambient	*Phaseolus vulgaris*	n.a.	n.a.	data	data	Y. Goulas, CNRS, F
41	CM06	(Corp *et al.* 2006)	Chl, Chl a:b, N, A, LAI, Fs, FR	canopy	FLD, SF	ASD FieldspecPro, Spex Fluorolog-II	N%	*Zea mays, Glycine max, Liriodendron tulipifera, Acer rubrum, Liquidambar styraciflua*	n.a.	n.a.	tables	tables	E. Middleton, NASA, USA
42	MC06	(Meroni & Colombo 2006)	Fs	leaf	FLD	OceanOptics HR-2000	ambient, DCMU	*Phaseolus vulgaris*	contact	n.a.	contact	contact	R. Colombo, UMB, I
43	BB08	(Borisov & Bykov 2008)	Fs, FR	leaf	SF	OceanOptics S-2000	Kautsky	*Acacia spp.*	n.a.	n.a.	tables	tables	B.A. Borisov, Russian Acad Sciences, RU
44	CA08	(Campbell *et al.* 2008)	Fs, FR	leaf	FLD	ASD FieldspecPro	ambient, N%	*Zea mays, Glycine max, Acer rubrum*	contact	contact	contact	contact	E. Middleton, NASA, USA
45	MC08	(Middleton *et al.* 2008)	Fs, FR	leaf, canopy	FLD, SF	ASD Fieldspec FR	N%	*Zea mays*	contact	contact	contact	contact	E. Middleton, NASA, USA
46	PC08	(Porcar-Castell *et al.* 2008a)	A, Φp, Φf	leaf	MF	Walz Moni-PAM	season	*Pinus sylvestris*	contact	contact	contact	contact	A. Porcar-Castell, Univ. Helsinki, FI

47	PM08	(Peguero-Pina *et al.*2008)	PRI, A, DEPS, gs, Φp, Φf	leaf	MF	Walz PAM-2000,	ambient, drought	*Quercus coccifera*	n.a.	n.a.	tables	tables	J. Flexas, Univ. Baleares, E
48	SC08	(Soukupová *et al.* 2008)	A, Fv/Fm, Φp, Φf	leaf	MF	PSInstruments FluorCam	season, tempera-ture	*Picea abies, P. omorika*	tables	n.a.	tables	tables	L. Nedbal, Univ South Boemia, CZ
49	SEN2-FLEX	(Alonso *et al.* 2008)	A, Fs, Φp, Φf	leaf	FLD	ASD Fieldspec FR	ambient	*Triticum aestivum, Zea mays*	contact	contact	contact	contact	L. Alonso, UVAL, E
50	SZ08	(Suarez *et al.* 2008)	gs, NDVI, PRI, Tc, Fs	canopy	FLD	AHS, Walz PAM-2100	ambient	*Olea europaea*	n.a.	n.a.	tables	tables	P. Zarco-Tejada, IAS-CSIC, E
51	CEFLES2a	(Damm *et al.* 2010; Rascher *et al.* 2009)	A, GPP, Fs, Φp, Φf	Leaf, canopy	FLD, LIF, MF	AirFLEX, AHS, HYPER, ASD FieldspecPro, FLIDAR, OceanOptics HR-2000+ / HR4000, SpectroFLEX, Walz Mini-PAM	ambient	*Pinus pinaster, Triticum aestivum, Zea mays*	data	data	data	data	U. Rascher, IBG2, D A. Damm
52	CEFLES2b	(Rascher *et al.* 2009)	FCO_2, Fs	canopy	FLD, LIF, MF	AirFLEX, AHS, HYPER, ASD FieldspecPro, FLIDAR, OceanOptics HR-2000+ / HR4000, SpectroFLEX, Walz Mini-PAM	ambient	*Pinus pinaster, Triticum aestivum*	data, contact	data	data	data, contact	U. Rascher, IBG2, D Y. Goulas, CNRS, F F. Miglietta, IBIMET-CNR, IT
53	MP09	(Meroni *et al.* 2009)	A, PRI, Fs	Leaf, canopy	FLD	OceanOptics HR-2000	ozone, ambient	*Trifolium repens, Populus deltoides*	n.a.	n.a.	tables	tables	R. Colombo, UMB, I
54	DAU10	(Daumard *et al.* 2010)	Chl, PRI, NDVI, Fs, FR	canopy	FLD	TriFLEX (OceanOptics HR-2000+)	ambient	*Sorghum bicolor*	data	data	data	data	Y. Goulas, CNRS, F
55	LI10	(Liu & Cheng 2010)	A, GPP, Fs	canopy	FLD	ASD FieldspecPro	ambient	*Triticum aestivum, Zea mays*	n.a.	n.a.	tables	tables	L. Liu, Chinese Academy Sciences, CN
56	TT10	(Thoren *et al.* 2010)	PAR, T, A, FR	leaf	LIF	Planto	PAR	*Triticum aestivum*	tables	tables	tables	tables	U. Schmidhalter, TUM, DE
57	ROS10	(Rossini *et al.* 2010)	Fs, GPP, fAPAR	canopy	FLD	HR4000	ambient	*Oryza sativa*	contact	contact	contact	contact	R. Colombo, UMB, IT
58	DM11	(Dayyoub 2011)	A, Φp, Φf	leaf	MF	Walz PAM-2000	CO_2, PAR, N%	*Populus x euroamericana*	data	data	data	Data	F. Magnani, UNIBO, IT

59	FF11	(Frankenberg *et al.* 2011b)	GPP, Fs	satellite	FLD	GOSAT-FTS	ambient	global	n.a.	n.a.	MPI-BGC, MODIS CASA	contact	C. Frankenberg, JPL, CalTech, USA
60	JY11	(Joiner *et al.* 2011)	Fs	satellite	FLD	GOSAT-FTS	ambient	global	n.a.	n.a.	n.a.	contact	E. Middleton, NASA, USA
61	PC11	(Porcar-Castell 2011)	Φp, Φf, NPQs, NPQr	leaf	MF	Walz Moni-PAM	ambient	*Pinus sylvestris*	data	data	data	data	A. Porcar-Castell, Univ. Helsinki, FI
62	FD12	(Fournier *et al.* 2012)	PAR, Fs, FR, ρ	leaf, canopy	SF, FLD	LSF, SpectroFLEX	canopy structure, LAI, ambient	*Holcus lanatus, H. mollis*	n.a.	n.a.	tables	tables	Y. Goulas, CNRS, F
63	GF12	(Guanter *et al.* 2012)	GPP, Fs	satellite	FLD	GOSAT-FTS	ambient	global	n.a.	n.a.	MPI-BGC, MODIS	contact	C. Frankenberg, JPL, CalTech, USA
64	DAU12	(Daumard *et al*. 2012)	Fs687, Fs760	leaf, canopy	FLD	TriFLEX (OceanOptics HR-2000+)	ambient, Chl, LAI	*Sorghum bicolor*	data	data	data	data	Y. Goulas, CNRS, F
65	JU12	n.a.	A, Φp, Φf, FR	leaf	MF	Walz PAM-2000, ASD	CO_2, PAR	*Nicotiana tabacum*	data	data	data	data	U. Rascher, IBG2, D

[§]data, dataset available to the Consortium in electronic format at www.FLEX-photosyn.ca; tables, dataset can be derived from published tables/graphs available to the Consortium in pdf format; contact, dataset available from PI upon request; n.a., not available. *Fs, steady-state fluorescence; A, photosynthesis; FR, fluorescence ratio; GPP, gross primary production; Φp, photochemical yield; Φf, fluorescence yield; ASFY, Apparent Spectral Fluorescence Yield; PRI, photochemical reflectance index; NDVI, normalized difference vegetation index; Tc, canopy temperature; τ, fluorescence lifetime; DPi, double-peak index; LAI, leaf area index, N, leaf N concentration; Chl, chlorophyll content; Chl a:b, chlorophyll a:b ratio. ^ MF, modulated fluorescence; FLD, Fraunhofer Line Discrimination; LIF, laser-induced fluorescence; SF, field or laboratory spectrofluorometer; TRF, time-resolved fluorometer; DPD, double-peak detection

[‡] Laser-PAM, (Ounis *et al.* 2001); FIPAM, (Flexas *et al.* 2000); τ-LIDAR, (Cerovic *et al.* 1996); LEAF, (Cecchi *et al.* 1994); FLIDAR, (Cecchi *et al.* 1994); DlidaR-2, (Gunther *et al.* 1994); LITWaF (Lichtenthaler & Rinderle 1988); τ-LIDAR, (Moya *et al.* 1995); PMFD, (Evain *et al.* 2001); AirFLEX, (Rascher *et al.* 2009); SpectroFLEX, (Fournier *et al.* 2012); PFS, (Kebabian *et al.* 1999); FIS, (Corp *et al.* 2003); LIFIS, (Corp *et al.* 2003); LIFT, (Ananyev *et al.* 2005)

2.4 Test and verification of modules: A-SIF

Various alternative modules were compared, based on their agreement with experimental data from the database and consistency with current understanding of PSII functioning (in order to ensure generality of the results, as well as the broad acceptability of results to the scientific community). The test was based on experimental data obtained under a wide range of environmental conditions, including stress conditions.

The exercise also resulted in a gap analysis, which highlighted processes are not currently well-represented. Because of the planned time frame of the task, however, no *ex-novo* module development was mandated, although one of the modules (MD12) was re-formulated so as to include the effects of long-term changes (photoinhibition and photoacclimation).

Datasets (Section 2.3) were screened for suitability quantitative testing of the leaf-level modules. Several datasets did not contain quantitative data of fluorescence and photochemical yields under variable conditions. This was considered a necessary requisite, since:

1. The aim of the modelling component of this study is to ascertain the relationship between fluorescence and photosynthetic rates, not the response of fluorescence to environmental conditions *per se*;
2. Both fluorescence radiance and electron transport (and hence photosynthesis) are known to be strongly associated with incoming and absorbed irradiance. Although this constitutes one of the main advantages of measuring fluorescence radiance remotely (making it possible to estimate photosynthesis without side measurements of irradiance), such a co-variation would obscure any other effects and make the testing of process-based models all but impossible. A reliable test of the functional relationship between fluorescence and photochemistry therefore should be based on the comparison of yields, rather than radiances and fluxes;
3. Fluorescence yields are related to competing processes taking place in the photosystem, notably photochemistry. Although photochemistry will eventually affect photosynthesis, in C3 species the latter is also strongly affected by photorespiration, which is itself dependent upon a number of factors (e.g., temperature, atmospheric CO_2, stomatal and mesophyll conductance). Fluorescence yields should be therefore better tested against PSII photochemical yields, rather than photosynthetic yields and gas exchange;
4. Short- and long-term (i.e. seasonal) processes could affect yields in different ways. It would be therefore desirable to test the models both against short-term measurements under controlled conditions and against long-term measurements under natural conditions;
5. Finally, datasets should have a suitable sample size, in terms both of interval covered by measurements and of number of replicates.

Ultimately, three datasets were selected for a thorough test of models, focusing on the main environmental drivers of short-term changes (irradiance, temperature and atmospheric CO_2,

capturing also the effects of drought and stomatal closure) and on long-term dynamics under field conditions:

- DM11 consists of parallel measurements of fluorescence and photochemical yields (and photosynthesis) under controlled irradiance and atmospheric CO_2 conditions in two contrasting broadleaf species, and is representative of short-term responses to changing environmental variables;
- JU12 consists of parallel measurements of fluorescence radiance, fluorescence and photochemical yields (and photosynthesis) under controlled irradiance and temperature conditions in a third broadleaf species, and is representative of short-term responses to changing environmental variables;
- PC11 consists of year-long measurements of fluorescence and photochemical yields in mature conifer needles under boreal conditions.

The five models fitted onto the selected datasets were: SG95 (Srivastava *et al.* 1995a), RS98 (Rosema *et al.* 1998), TV09 (Van der Tol *et al.* 2009a), TB12 (Van der Tol *et al.* 2014; Berry *et al.* 2013) and MD12 (Magnani & Dayyoub 2014; Dayyoub 2011). The MD09 model was not tested here, as it has been superseded by its newer development.

Model testing determined to what extent individual models were able to capture and reproduce the observed relationship between photochemical and fluorescence yield, under a range of environmental conditions – in practical terms, it amounted to model calibration.

Model validation assessed the possibility to extrapolate model predictions to novel conditions. Two data-splitting procedures were applied. In the first, each model was calibrated against one half of the data, and validated against the other half. A second procedures was also applied In the case of short-term datasets acquired under a range of controlled environmental conditions: models were first calibrated against data at one level, then validated against the remaining dataset (e.g., data at 10°C for calibration, data at 20 and 30°C for validation); the procedure was repeated for each available level of environmental conditions.

Comparison between models was based on: (i) qualitative analysis of model R^2, RMSE, slope and intercept of the least-squares regression between predicted and observed yields (Mayer & Butler 1993; Willmott 1981), and (ii) the ratio between observed differences in model MSE and the variance of mean squared errors (Wallach & Goffinet 1989).

Model calibration was done using the non-linear regression NLIN procedure of SAS statistical package (SAS Institute Inc., Cary, NC), using a Marquardt algorithm with a wide initial grid search, using photochemical yield as a dependent variable; when possible, both steady-state modulated fluorescence (F_t) and fluorescence yield (Φ_f) were used as independent variables. "Fluorescence yield" was computed as the ratio between fluorescence radiance at 740 nm and incoming PAR.

2.4.1 Results

Although not exhaustive, the three tests permitted evaluation of the potential of the proposed models for the prediction of short- and long-term changes in photochemical yield from measurements of steady-state fluorescence.

The SG95 model was unable to capture the joint effects of PAR and CO_2 on photochemical yields (Figure 2.1, Tables 2.5, 2.6). This problem arises from its assumption of a unique relationship between photochemical and fluorescence yields irrespective of exciton pressure and irradiance. SG95 was, therefore, not included in further testing.

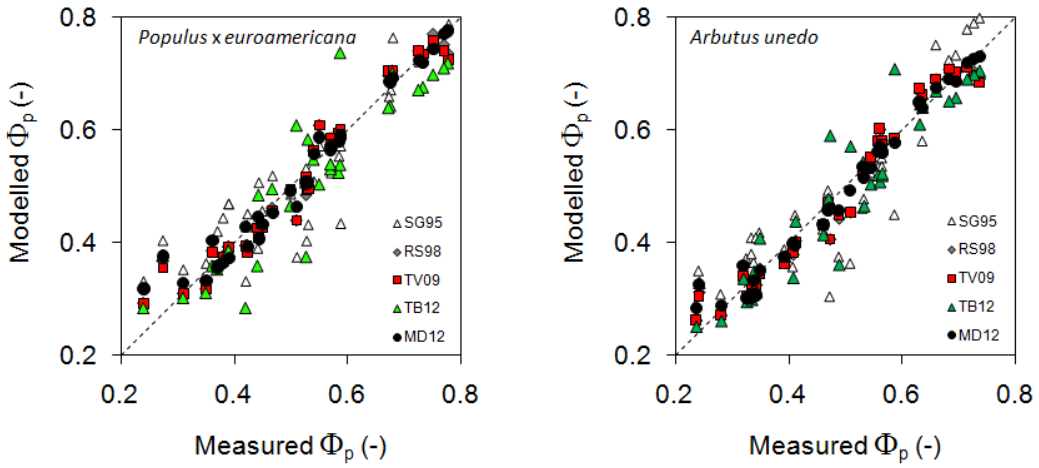

Figure 2.1. Model goodness-of-fit comparison. Comparison of observed photochemical yields with predictions by the five models in *Populus* x *euroamericana* and *Arbutus unedo* leaves. The dashed line corresponds to the 1 : 1 relationship.

Under short-term conditions, the RS98 and TV09 models yielded very similar results. In fact, short-term results suggested that RS98 could simply be collapsed onto TV09 because of the negligible value of the parameter involved in the response to light of heat dissipation. The conclusion was not supported, however, by results against long-term data, and the RS98 model appeared to perform slightly better in this case.

The TB12 model performed almost consistently worse than the remaining models, both qualitatively and quantitatively. This was the result of: (i) the single relationship assumed in the model between photochemical and fluorescence yield, not further modulated by co-occurring levels of absorbed irradiance, which prevented it from capturing the interactive effects of irradiance and stomatal closure (as simulated by variable CO_2 levels); (ii) its more empirical nature, which made it impossible to take into account the indirect effects of temperature mediated by changes in potential electron transport rates. Nevertheless, TB12 was retained because of the interest it has recently suscitated in the modelling community, so as to further test its heuristic value.

Table 2.5. Summary of model statistics for *Populus* x *euroamericana*. For each model, the values of R^2, adjusted R^2, RMSE and systematic (MSE_s) and unsystematic (MSE_u) mean-squared error components (Willmott 1981) are presented. The intercept (a) and slope (b) of the comparison of fitted and observed yields are also presented.

	SG95	RS98	TV09	TB12	MD12
R^2	0.799	0.955	0.954	0.831	0.970
Adj R^2	0.793	0.953	0.952	0.826	0.959
a	0.078	0.012	0.009	0.041	0.027
b	0.850	0.976	0.980	0.887	0.948
MSE	4.2E-03	9.3E-04	9.6E-04	3.6E-03	8.2E-04
RMSE	6.5E-02	3.1E-02	3.1E-02	6.1E-02	2.9E-02
MSE_s	4.6E-04	1.2E-05	9.4E-06	5.3E-04	5.5E-05
MSE_u	3.7E-03	9.2E-04	9.5E-04	3.2E-03	7.7E-04

Table 2.6. Summary of model statistics for *Arbutus unedo*. For each model, the values of R^2, adjusted R^2, RMSE and systematic (MSE_s) and unsystematic (MSE_u) mean-squared error components (Willmott 1981) are presented. The intercept (a) and slope (b) of the comparison of fitted and observed yields are also presented.

	SG95	RS98	TV09	TB12	MD12
R^2	0.804	0.959	0.959	0.885	0.966
Adj R^2	0.798	0.958	0.958	0.881	0.965
a	0.05	0.01	0.01	0.03	0.03
b	0.91	0.98	0.98	0.91	0.95
MSE	4.8E-03	9.4E-04	9.5E-04	2.7E-03	7.9E-04
RMSE	7.0E-02	3.1E-02	3.1E-02	5.2E-02	2.8E-02
MSE_s	2.3E-04	1.2E-05	8.8E-06	2.1E-04	6.0E-05
MSE_u	4.6E-03	9.3E-04	9.4E-04	2.5E-03	7.3E-04

Quantitatively, the MD12 model performed only slightly better than RS98 or TV09 against short-term data (although in qualitative terms it better captured the pattern observed under low light conditions). Under some circumstances (notably, *A. unedo* in the DM11 dataset), however, the RS98 and TV09 models behaved significantly worse than MD12. Against long-term data, moreover, MD12 proved significantly better at representing the observed pattern both on a daily and on an annual basis, explaining more than 78% of the overall annual variability in photochemical yields based on fluorescence measurements (Figure 2.2).

All three models (MD12, RS98, TV09) performed worse when calibrated against data for saturating light conditions (possibly as a result of photoinhibition, not accounted for in the models), with potential implications for the optimal illumination conditions and overpass time of the proposed satellite.

Direct effects of temperature on the relationship between fluorescence and photochemical yields are well explained by the modulation of enzymatic processes controlling potential electron transport rates, and are conveniently captured by the modified Arrhenius-type equation (Kattge & Knorr 2007) already implemented in SCOPE as applied in previous modelling projects.

The comparison with the PC11 dataset also highlighted the need to further refine the models, to predict and account for long-term changes in sustained NPQ and reaction centre photoinhibition under severe stress conditions, as could be observed under boreal or Mediterranean conditions. Inclusion in the model of sustained NPQ, in particular, proved particularly important, accounting for most of the interannual variability observed at the site.

A prediction of seasonal changes in PSII photodamage cannot be included in the model for the time being. Reaction centre photoinhibition or photodamage is known to be affected by the total amount of light absorbed (Tyystjärvi & Aro 1996), possibly interacting with winter temperature because of its effects on protein synthesis and PSII repair. A few process-based models have been proposed in the literature for the representation of PSII damage and repair in phytoplankton (Garcia-Camacho *et al.* 2012; Ross *et al.* 2008; Marshall *et al.* 2000); in higher plants, however, the process has been modelled only for conditions preventing PSII repair (Tyystjärvi *et al.* 2005). An extension of such models to more realistic conditions appears worthwhile and timely.

To the best of our knowledge, no mechanistic models have been proposed for the representation of sustained NPQ and PSII photoprotection, although the process is known to play an important role under low temperature (Porcar-Castell 2011; Demmig-Adams *et al.* 1998; Adams *et al.* 1995) and drought conditions (Baraldi *et al.* 2008; Adams & Demmig-Adams 2004). Because of the rather conservative response of fluorescence to low-light, this long-term component could be effectively estimated through ancillary measurements under such conditions, but this solution seems to be impractical for remote sensing applications given the low signal-to-noise ratio that could be achieved.

In summary, available models appear to be adequate for the representation of the relationship between fluorescence and photochemical yield in response to short-term changes of a number of environmental conditions. Further studies are needed for modelling long-term changes in:

1. PSII photoinhibition in response to low temperatures (and potentially high temperatures and drought, and high-light conditions);
2. photoprotection (zeaxanthin retention and sustained NPQ) under low temperature and drought conditions.

Future experimental studies should also focus on long-term measurements under field conditions, at both leaf and canopy level, to assess the role of seasonal acclimation and test the ability of the models to account for them.

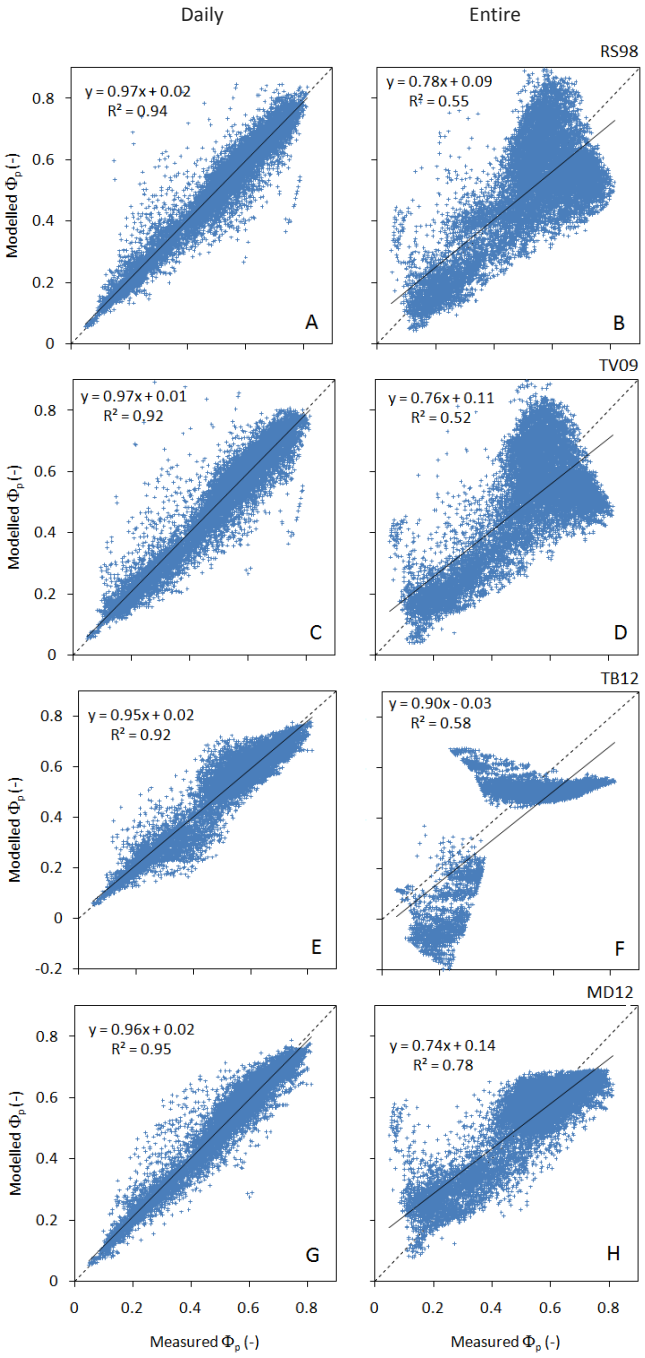

Figure 2.2. Model test against annual fluorescence data from *P. sylvestris* needles at the SMEAR site (PC11 dataset): calibration of the four models. Photochemical yield (Φ_p) predicted from fluorescence yields after model calibration independently on individual daily datasets (A, C, E, G) and on the entire annual dataset (B, D, F, H) for the models RS98 (A, B), TV09 (C, D), TB12 (E, F) and MD12 (G, H). Continuous lines represent best-fit linear regression; dotted lines mark the 1:1 relationship.

2.5 Test and verification of modules: radiative transfer and SIF upscaling

This component tested the performance of different modules presently available for radiative transfer and up-scaling of ambient solar induced fluorescence (SIF) from photosystem, to the leaf, canopy and satellite level. The report focusses on assessing whether the available set of instruments is sufficient for the purpose of FLEX, and whether the model components provide realistic results.

A complete model includes radiative transfer of both incident and internally generated radiation (heat and fluorescence) in the leaf and in the canopy. The following components are needed:

- the radiative transfer inside the leaf;
- radiative transfer of incident radiation (the excitation source);
- radiative transfer of internally generated thermal radiation;
- radiative transfer of internally generated fluorescence;
- an aerodynamic and stomatal conductance scheme to calculate leaf boundary meteorological conditions;
- a biochemical model for fluorescence yield (Sections 2.2 and 2.4) and photosynthesis.

This evaluation consists of three steps: (1) overview of the literature on each of these components, (2) verification of modules by contrasting simulations with data, (3) a gap analysis of the present state-of-the art. (In addition, a sensitivity analysis of the coupled system was performed but is not included here as such analyses are the focus of Chapter 3).

Fluorescence radiative transfer inside the leaf

The two available models for radiative transfer of fluorescence inside the leaf (FluorMODleaf and Fluspect) are both based on the leaf optical properties model PROSPECT (Jacquemoud & Baret 1990). FluorMODleaf was developed during an ESA study (Miller *et al.* 2005), and it has been published by Pedrós *et al.* (2010). This model has been programmed in the C language and in Mathematica.

The second model, Fluspect (Verhoef 2010) differs from FluorMODleaf in that fluorescence is calculated using a fast doubling algorithm, by applying a Kubelka-Munk (KM) type of radiative transfer approach at the photosystem level including fluorescence. The model has been programmed in the languages Visual Basic 5, Fortran and MATLAB, which facilitates its incorporation into the canopy level model SCOPE (versions 1.33 and later).

For radiative transfer of fluorescence from leaf to canopy, we presently have only models based on SAIL (developed by W. Verhoef). These include FluorSAIL, developed during an ESA study between 2002-2005 (Miller *et al.* 2005; Verhoef 2004); and SCOPE (Van der Tol *et al.* 2009b).

Because of the limited availability of alternative model formulations for fluorescence radiative transfer, we focussed the verification on assessing whether the concepts presently incorporated in the models are sufficient for the purpose of FLEX, and where they require modification.

2.5.1 Results

Models identified in the literature are listed in Table 2.7.

Table 2.7. Radiative transfer and most widely used energy balance models in the literature.

Component	Model	References
Fluorescence radiative transfer inside the leaf	FluorMODleaf Fluspect[1]	Miller *et al.* (2005), Pedrós *et al*. (2010) Verhoef (2010)
Transfer of incident radiation	Sun/shade model SAIL[1] DART *+ many other*	Pury & Farquhar (1997) Verhoef (1984) Gastellu-Etchegorry *et al*. (1995)
Leaf energy balance		
- *Aerodynamics*	Goudriaan Wallace and Verhoef[1]	Goudriaan (1977) Wallace & Verhoef (2000)
- *Stomatal regulation*	Conceptual 'economic' model [1] Coupled model A-Ci-E model [2] Coupled A-Ci-E model *+ many other*	Cowan (1977) Ball *et al.* (1987) Leuning (1995)
Fluorescence radiative transfer	RTMf[1,3]	Verhoef (2004), Van der Tol *et al*. (2009b)

[1] included in SCOPE,[2] included in SCOPE version 1.34 and higher, [3] the radiative transfer of fluorescence in FluorSAIL is identical to RMTf.

A full validation of leaf level models was not feasible in this study. As a necessary first step a qualitative comparison was done of the model against measurements of reabsorption reported by Gitelson *et al.* (1998) within the leaf. They found that, with an excitation source wavelength of 430 nm, the ratio of fluorescence in the two peaks (at 680 and 735 nm) decreased with chlorophyll concentration as a function of chlorophyll concentration. The ratio of absorbed radiation in these wavelengths showed a similar relation with chlorophyll concentration.

Fluspect output of these quantities across a range of chlorophyll concentrations also shows a decrease of backward fluorescence and absorption ratio with chlorophyll concentration, but there are two differences. First, the simulated fluorescence peak ratio (1.6) does not reach values as high as those in the measurements (3.1). At longer excitation wavelengths (green and red), the measured fluorescence peak ratios were lower (Gitelson *et al.* 1998), and the model was in better agreement with the simulations for these excitation wavelengths. Second, the simulated fluorescence peak ratio reaches a minimum at a chlorophyll concentration (Cab) of 40 mg m^{-2}, whereas observations suggest a saturation at Cab> 40 mg m^{-2}.

Radiative transfer from leaf to canopy, and the energy balance

The canopy-level models listed in Table 2.2 are based on the SAIL model concept, which has the limitation of horizontally homogeneous canopy structure. Other radiative transfer models, such as DART (Gastellu-Etchegorry *et al.* 1995), do not have this limitation, but these models lack a fluorescence module. Because it was not feasible in this study to develop a 3-D model for

fluorescence, only the consequences of this limitation of SAIL have been evaluated in this project.

Timmermans *et al.* (2011) showed that the quality of the calculation of bi-directional reflectance is mainly a function of the vegetation cover fraction (the vertical projection of crowns on the surface). For partially vegetated areas (cover fraction <85%), SAIL fails to reproduced the azimuthal dependencies of the upwelling radiance.

The two canopy-levels in Table 2.2 that include a variable fluorescence are FluorSAIL and SCOPE. Both models share the radiative transfer from leaf to canopy in the optical domain, including fluorescence. The first difference between the models is that SCOPE also calculates thermal radiation and photosynthesis, taking into account the interdependence of thermal radiation and photosynthesis. The second difference is the use of the leaf model FluorMODleaf in FluorSail, and Fluspect in SCOPE.

Given the large overlap between the existing models, the SCOPE output of radiation, photosynthesis and temperature was verified by comparison to observations on *Zea mays* canopy in Sonning, United Kingdom. The following conclusions were drawn:

- Reflectance as a function of solar zenith angle is well reproduced with the SAIL concept, confirming that the 4-stream radiative transfer model concept works for closed canopies;
- Thermal outgoing radiance and component temperatures of leaves were well reproduced. This is relevant for the photosynthesis calculation, which is a function of temperature;
- Measured surface energy balance components of net radiation, ground heat flux, sensible heat flux and latent heat flux were reproduced. This indicates that the SCOPE model has similar capabilities as Soil-Vegetation-Atmosphere Transfer (SVAT) models commonly used in the scientific community.

The capability of SCOPE to reproduce observed top-of-canopy fluorescence was evaluated, using the measurements in the database (see Section 2.3) as collected during the CEFLES campaign. Measurements consisted of fluorescence retrieved from an ASD spectrometer and net CO_2 exchange with an eddy covariance system (Damm *et al.* 2010). SCOPE was used with the available meteorological and crop data collected in the field (LAI = 2.8; Cab = ~40 mg cm^{-2}), and the diurnal cycle of the energy balance, photosynthesis and fluorescence in the O_2-A band between 770 and 785 nm for three consecutive days (5-7 September 2007) was assessed. Since incoming longwave radiation was not measured, it was estimated from air temperature and humidity using an empirically calibrated function (Allen *et al.* 1998). For parameters for which no information was available (some PROSPECT parameters, photosynthetic capacity), default values were used.

Figure 2.3 shows the diurnal cycles of three energy balance components (R_n, λE and H), modelled net photosynthesis with measured net CO_2 exchange (including soil respiration), and fluorescence derived using the O_2-A band at 760 nm. Fluorescence was calculated in NADIR and assumed that this value was representative for the field of view of 25^o of the instrument (an

ASD Fieldspec spectrometer). The magnitude of the simulated fluxes agrees with the measurements. Fluorescence was overestimated (Cab of 40 µg cm^{-2} used here; but Damm *et al.* (2010) describe a vertical profile of Cab with the lowest values at the top). Orders of magnitude and diurnal cycles of all simulated fluxes including fluorescence agree with observations, although differences still exist.

Gap analysis

At present, two leaf level and two canopy level models for radiative transfer are readily available. The representation of fluorescence radiative transfer in the two canopy level models, SCOPE and FluorSAIL, is equal.

The main limitations of these models are (see also Table 2.8):

- The available scaling models assume horizontally homogenous, layered vegetation. This is inaccurate in sparse or strongly clumped vegetation.
- It is not clear if and how PSI fluorescence is regulated. At present PSI fluorescence matrices are assumed constant (but in SCOPE v1.34, PSI varies together with PSII by default; this was changed for future releases into a constant PSI and shared with the FLEX group).
- Neither of the available models is a TOA simulator, because
    - FluorSAIL lacks a physiological model for photosynthesis and an energy balance routine
    - SCOPE lacks an algorithm to translate TOC fluorescence to TOA algorithm. However, this aspect has recently been addressed in the PARCS study, and a TOA simulator has been built.
- SCOPE assumes vertically constant leaf optical properties, and vertically constant aerodynamic resistances. The vertically constant aerodynamic resistance causes some error in the simulated leaf temperatures; these errors affect the thermal signal mainly, but they also have a small effect on the fluorescence signal.
- Although most building blocks have been validated as they have been published individually, neither of the coupled models has been systematically validated against measurements.
- The effect of PRI is not included in Fluspect, although absorbance spectra of leaves are available for vegetation under various conditions (not discussed in this report).

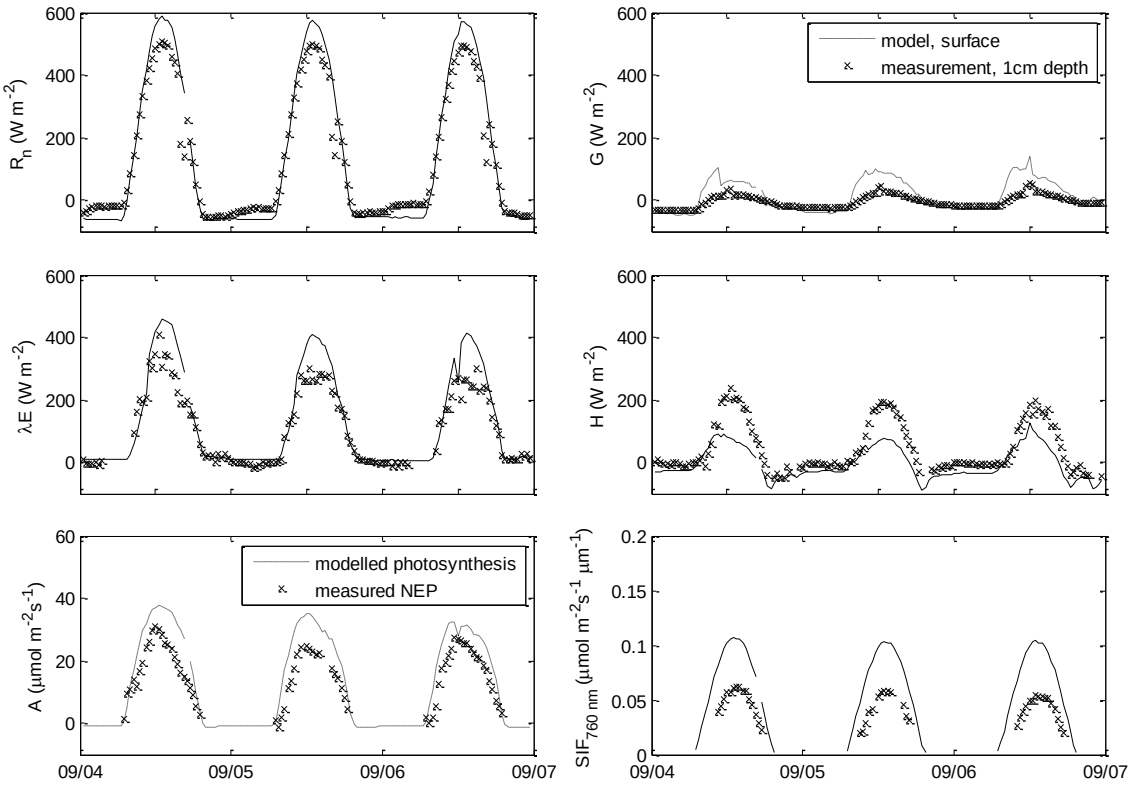

Figure 2.3. Comparison between measured (symbols) and SCOPE modelled (lines) fluxes measured over a maize field during the CEFLES campaign (Damm *et al.* 2010). Solid lines refer to a direct comparison where the simulated variable was the same as the measured one, while dashed lines refer to an comparison of different variables. Clockwise from top left: net radiation, ground heat flux at the surface (modelled) and at 1 cm depth (measured), sensible heat flux, solar induced fluorescence in the O_2-A band (760 nm, aggregated over a FOV of 25°), net photosynthesis of all leaves (simulated) and net ecosystem exchange – including soil respiration – (measurements), and latent heat flux.

Table 2.8. Gap analysis of present radiative transfer models. A distinction is made between elements critical for an end-to-end simulator and elements not critical, and between elements that are easily implemented as part of this project, and elements that require a separate study.

	Feasible to implement in this study	Not feasible to implement in this study
Critical	- Choice of biochemical model - PSI/PSII separate responses - Coupling with atmosphere - Validation of leaf measurements using existing data	- PRI in Fluspect/ FluorMODleaf and biochemical modules - Full validation against leaf and canopy level measurements using new experimental work.
Not critical	- Vertical profile of chlorophyll concentration	- 3-Dimensional vegetation (row crops, cones), comparison with ray tracing models.

We recommend focussing on these issues first in the present study:

- implementation of separate responses for PSI and PSII and using experimental evidence to parameterize these responses correctly;
- validation of Fluspect and FluorMODleaf against observations, ideally combined with a validation of the leaf biochemistry (photosynthesis) models simultaneously;
- coupling with atmosphere, which would involve the following steps:
    - defining and preparing realistic atmospheric profiles, bottom of atmosphere irradiance and meteorology, and optical properties of the atmosphere;
    - simulation of TOA fluorescence radiance by coupling of SCOPE input and output with MODTRAN atmospheric profiles;
    - translating TOA output to the satellite level using band characteristics of the instruments.

Two other issues, including PRI effects and validation against airborne and tower measurements, are also aspects that need to be addressed, but due to the resources needed they should be done in parallel research projects. Adding further complexity to the models by including different aspects of the heterogeneity of the vegetation (such 3-D radiative transfer for row crops) are relevant for the interpretation of the signal, but this is not considered critical for the present study.

2.6 Model design framework

2.6.1 Structure

This section addresses elements of model structure, including which chains of individual or integrated modules would allow investigation of the relationship between ambient fluorescence and photosynthesis at canopy scale. A modular model set-up was proposed, so as to: (i) improve model readability, (ii) help in module development, and (iii) make it possible in the future to replace model components/modules with alternative ones if new modelling insights become available.

Existing limitations and gaps in the forward modelling are also summarized.

As agreed during the 1st Progress Meeting, the model should be a development of the existing SCOPE (Soil Canopy Observation, Photochemistry and Energy fluxes) model (Verhoef 2011; Van der Tol *et al.* 2009b), of which it retains the general concept and model structure. It is suggested that the model should retain a 1-D structure, i.e., represent the vegetation as a horizontally homogeneous canopy, extending infinitely in all directions. In the vertical direction, the canopy is divided into a number of layers. For the description of canopy architecture, the same inputs as the ones used in the SAIL models (Verhoef 1998; Verhoef 1984) are applied. The model distinguishes between modules for radiative transfer (of incident light, internally generated thermal radiation and chlorophyll fluorescence), and the energy balance (Figure 2.4). It was decided that the input and output structure of the SCOPE model should be updated such

that it is easier to implement new modules for leaf radiative transfer and leaf physiology, such as the MD12 model, in the structure.

The modules are executed in the order from top to bottom of Figure 2.4:

1. RTMo, a semi-analytical radiative transfer module for incident solar and sky radiation, based on four-stream SAIL extinction and scattering coefficients (Verhoef & Bach 2007; Verhoef 1984): calculates the TOC (top of canopy) outgoing radiation spectrum (0.4 to 50 µm), as well as the net radiation and absorbed photosynthetically active radiation (PAR) per canopy surface element.
2. RTMt, a numerical radiative transfer module for thermal radiation generated internally by soil and vegetation, based on Verhoef *et al.* (2007): calculates the TOC outgoing thermal radiation and net radiation per surface element, but for heterogeneous leaf and soil temperatures. Thermal radiative transfer is also described on the basis of the four-stream SAIL extinction and scattering coefficients (Verhoef 1984), but the solution method of SCOPE is of a more numerical nature to allow for a heterogeneous vertical temperature distribution.
3. An energy balance module for latent, sensible and soil heat flux per surface element, as well as photosynthesis, chlorophyll fluorescence and skin temperature at leaf level. Leaf level fluxes are computed as described above, and summed up over the entire canopy (Figure 2.5). In this part, the alternative leaf models for the fluorescence yields as described in Section 2.2 can be implemented.
4. RTMf, a radiative transfer module for chlorophyll fluorescence based on the FluorSAIL model (Miller *et al.* 2005): calculates the TOC radiance spectrum of fluorescence from leaf level chlorophyll fluorescence (calculated in step 3) and the geometry of the canopy.

Iteration between the thermal radiative transfer module (RTMt) and the energy balance module is carried out to match the input of the radiative transfer model with the output of the energy balance model (skin temperatures), and vice-versa: the input of the energy balance model with the output of the radiative transfer model (net radiation).

The radiative transfer modules predict the distribution of irradiance and net radiation over surface elements (leaves and the soil), as an input for the energy balance module. The energy balance module, in turn, calculates the fate of net radiation (i.e., the turbulent energy fluxes, latent heat fluxes and photosynthesis) as well as surface temperatures, which are input for the radiative transfer model. The energy balance is preserved at all times, except for the small contribution of chlorophyll fluorescence.

For computational efficiency, the radiative transfer of chlorophyll fluorescence (RTMf) is carried out at the end of the cascade, and canopy outgoing fluorescence eventually is added to TOC reflectance. This implies that the contribution of chlorophyll fluorescence to the energy balance is neglected. Note that this only applies to the radiative transfer of fluorescence through the

canopy, which is computationally demanding. The chlorophyll fluorescence at leaf level is calculated at every iteration step as a result of estimated leaf photosynthesis (step 3).

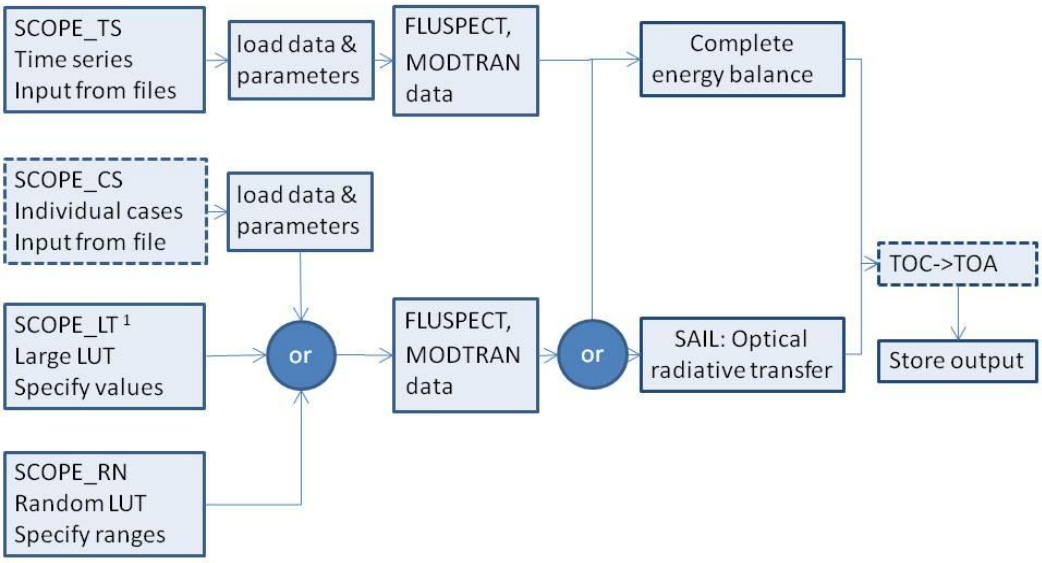

Figure 2.4. General workflow of SCOPE. The routines 'SCOPE_xx' represent optional modes for running SCOPE: as time series (e.g., hourly changing meteorology specified in files), for individual cases with parameters specified as a file, or for Lookup table generation with parameters or ranges specified. Either the complete energy balance routine including photosynthesis can be executed, or the radiative transfer of direct and diffuse light (with the SAIL model) only. The dashed boxes represent routines that are available in versions higher than v1.34. [1]SCOPE_LT is called 'SCOPE.m' in version 1.34.

For the calculation of radiative transfer, the description of the geometry of the vegetation is of crucial importance: in SCOPE the sunlit leaves are discriminated by their orientation with respect to the sun and their vertical position in the canopy layer, as in the FluorSAIL model (Miller *et al.* 2005), whereas in 4SAIL (Verhoef *et al.* 2007) only a differentiation between sunlit and shaded leaves was made.

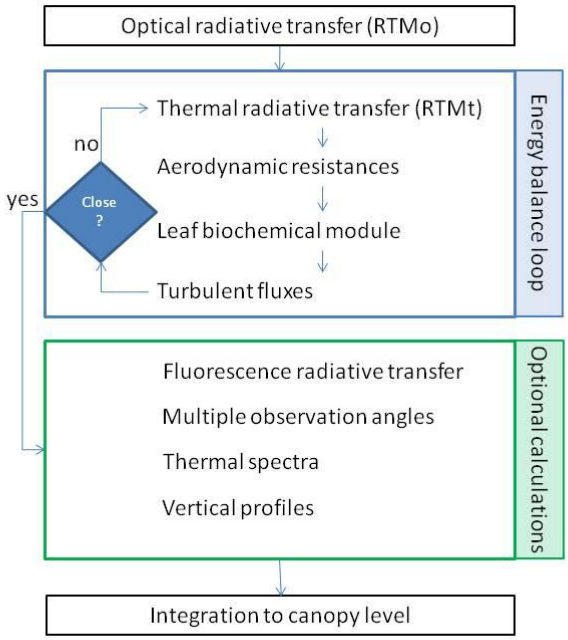

Figure 2.5. Workflow of the full energy balance calculations in SCOPE (function 'ebal.m'). The core is the energy balance loop, in which leaf temperatures for each leaf orientation are calculated. Leaf temperatures are updated every iteration step. The loop breaks when the energy balance closes for all leaf orientations or a user defined maximum number of iteration steps is reached. The optional calculations can be switched off to enhance computation speed.

2.6.2 Key advancements, remaining limitations and gaps

Proposed developments over the baseline SCOPE v1.34 consist of:

1. a revised and tested leaf level model of fluorescence. Two alternative modules (MD12 and TB12) were coded, sharing the same input-output interface;
2. the explicit representation of PSI and PSII fluorescence. This makes it possible to represent dynamic changes in fluorescence spectra and fully exploit fluorescence measurements at different wavelengths in a future mission;
3. representation of VIS spectral changes associated with photochemistry. The representation in the fluorescence model also of reflectance changes associated with xanthophyll DEPS and conformational changes will allow merging of two complementary approaches, providing additional value for the assessment of photosynthesis from space.

Some limitations will still persist that cannot be easily addressed within the project. In particular:

1. The 1-D structure of the model neglects the potential effects of the shadows cast by individual crowns, which are known to have a relevant effect on canopy albedo.

Moreover, the model will not be able to deal with sparse vegetation, or agricultural systems such as vineyards and orchards, although gross trends predicted by the homogeneous model may hold for 3-D structures as well;

2. The model does not include a full water balance, but soil water content has to be prescribed as an external forcing parameter. In perspective, this will restrain the possibility of estimating response functions and functional parameters through the inversion of the model on fluorescence and reflectance measurements;
3. The instantaneous and diagnostic nature of the model should be stressed. Since plant growth and LAI dynamics are not computed internally but prescribed as external forcing values, the model has no prognostic value. While this is convenient for the description of FLEX observations, it should be kept in mind that the model cannot be used to predict the dynamics of plant reflectance and fluorescence in response to future conditions arising from climate and global change.

2.7 Conclusions

Key outputs from this task were:

1. identification of best modules (notably MD12) for leaf-level biochemical processes, and radiative transfer at leaf (Fluspect, FluorMODleaf) and canopy (SCOPE) levels;
2. creation of an extensive database of datasets that were useful in model/module testing;
3. testing & verification of proposed modules at the leaf and canopy levels;
4. design of a model framework and modularized structure, and identification of gaps.

These outputs laid the foundations for the definition and testing of a consolidated model and its implementation in the next task.

3. Model implementation, validation, sensitivity analysis and error quantification

3.1 Introduction

This task addressed implementation and verification of the forward model, local & global sensitivity testing, field validation, and error quantification. Development of the model software and documentation were the main outputs.

3.2 Model consolidation

The main requirement for the consolidated model was suitability for use in the assessment of the FLEX candidate mission. Hence, the model should be able to simulate fluorescence spectra and photosynthesis at the canopy level, as a function of meteorological variables and physiological stress factors. The assignment was limited to top-of-canopy (rather than top-of-atmosphere) fluorescence spectra, because atmospheric correction has been addressed in a different study: FLUSS ("Atmospheric Corrections for Fluorescence Signal and Surface Pressure Retrieval Over Land").

The minimum required model components were:

- a deterministic physiological module quantifying the link between fluorescence and photosynthesis of leaves;
- a deterministic module quantifying the shape of the fluorescence spectrum at leaf level;
- a deterministic module for radiative transfer in the canopy.

Chapter 2 addressed the comparison and evaluation of existing models. The scientific literature revealed that one existing model has all components included and is able to simulate canopy photosynthesis and fluorescence simultaneously: the Soil Canopy Observation of Photochemistry and Energy fluxes (SCOPE) model by Van der Tol *et al*. (2009b). Multiple individual model components for radiative transfer, photosynthesis and fluorescence are available in SCOPE, and some of these have been updated since the model was first published in 2009. The selected modules were connected, using the existing SCOPE model as a platform. Also, the software was modified to make it independent of operating systems.

An important clarification is the difference between photosynthesis (an output of SCOPE) and gross primary production. By definition, GPP is the Net Primary Production (NPP) plus (absolute) plant respiration (Armthor & Baldocchi 2001). The SCOPE output of total photosynthesis is GPP *minus* growth respiration by leaves. This makes it comparable to the quantity measured by eddy flux towers because tower measurements of 'GPP' ignore (do not account for) growth respiration of leaves.

3.2.1 Selection of the model framework

In the earlier FluorMOD project 'Development of a Vegetation Fluorescence Canopy Model', a radiative transfer model for chlorophyll fluorescence and solar & sky radiation was developed (Zarco-Tejada *et al.* 2006; Miller *et al.* 2005). The same radiative transfer scheme was used in the SCOPE model (Van der Tol *et al.* 2009b). In addition, SCOPE includes a calculation of leaf photosynthesis, thermal radiative transfer and turbulent heat exchange. The last two aspects are essential for the estimation of stomatal regulation. Because of these extra elements the SCOPE model was selected as a baseline platform.

Similar to FluorMOD, SCOPE consists of several interacting modules. The strategy followed in this project was on the one hand to improve the modularity of SCOPE, and on the other hand to select state-of-the art approaches for each component.

The core parts of the model are a leaf optical module, a biochemical module and a radiative transfer module for the canopy. Interaction among these modules is depicted schematically in Figure 3.1. Fully integrated leaf optical and biochemical modules did not exist (yet). The available leaf optical models calculate leaf fluorescence spectra as a function of chlorophyll concentration, assuming a constant emission for the two photosystems (PSI and PSII), and assuming a fixed distribution of chlorophyll over the two photosystems. The leaf biochemical modules account for the fact that the fluorescence yield of PSII is subject to active regulation in response to photosynthesis, but they do not predict leaf fluorescence spectra. Hence, a coupling of the two model components was necessary in this project.

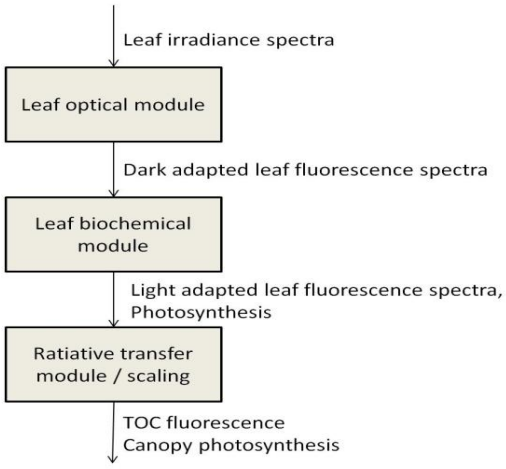

Figure 3.1. Schematic and simplified representation of the calculation of TOC fluorescence in the SCOPE model. The irradiance spectra at leaf level that enter the processing chain have been calculated with the SAIL model.

The following sections describe (1) the selection of a leaf optical module, (2) the selection of a leaf biochemical module, and (3) the coupling of the modules.

3.2.2 Consolidation of the leaf optical model component

At the start of the Photosynthesis Study, FluorMODleaf was discussed as a possible choice for the leaf optical model, since it was already published in the peer-reviewed literature (Pedrós *et al.* 2010), it had already been funded by ESA in a previous project, and it appeared to be the state of the art for radiative transfer of fluorescence within the leaf. However, SCOPE is written in MATLAB™, and for FluorMODleaf there was no MATLAB version available, so it was decided, at least for the time being, to use the Fluspect model instead, because it would be an advantage if the leaf optical model could be called directly from within SCOPE. A possible disadvantage was that this model had only appeared in conference papers, so it has not yet enjoyed the same exposure within the science community as has FluorMODleaf.

Fluspect (Verhoef 2011) was originally introduced in 2004 by W.Verhoef at NLR, the National Aerospace Laboratory of The Netherlands. Originally, it was a demo program written in the Visual Basic 5 language, which is now obsolete. Later versions in Fortran and MATLAB were developed at the ITC. Conceptually the model has always remained the same. Both FluorMODleaf and Fluspect are based on the leaf optical model PROSPECT, to which fluorescence was added by simulating the fluorescence at photosystem level and by propagating the fluorescence spectra originating in PS I and PSII from the internal of the leaf to the leaf's surfaces at top and bottom. The difference between the models is that Fluspect uses a fast layer doubling algorithm for the radiative transfer inside the leaf, whereas in FluorMODleaf the fluorescence contribution is calculated with complex analytical expressions. Fluspect therefore has an advantage in computational speed and simplicity. However, there are also conceptual differences, since in FluorMODleaf the fluorescence was kept separate from scattering processes on the borders of the leaf, while in Fluspect all scattering, absorption and fluorescence processes were homogeneously mixed. This difference in approach also led to differences in the resulting fluorescence spectra. In particular, the fluorescence at the illumination side of the leaf in the red peak at 685 nm might be overestimated by Fluspect, leading to too high values of the red / far-red peak ratio (Section 3.5).

Until recently it was not considered feasible to bridge the conceptual gap between Fluspect and FluorMODleaf regarding the separation between scattering on one hand and absorption/fluorescence on the other. However, since FluorMODleaf might produce more realistic results as a function of the chlorophyll concentration and with respect to the peak ratio, it was attempted (albeit outside the frame of this study) to develop a version of Fluspect that separates the border effects from the internal radiative transfer. This version is called Fluspect_B, and preliminary results indicate it might be producing more realistic peak ratios, and responses as a function of the chlorophyll concentration that would be more similar to those of FluorMODleaf.

The new Fluspect_B model was presented and discussed by the PS Study consortium in January 2014 but, since it was in the last few months of the study and additional time would be needed to test it fully, it was concluded that – while the new development looks to be very promising – it was prudent at the time to continue with the original Fluspect. Another consideration was that modelling results obtained with SCOPE during this study were based on the use of the

original Fluspect model, and introducing a new optical model would create inconsistencies between the SCOPE model version to be delivered to ESA and the simulation results already obtained.

One modification was made to the original Fluspect model at the beginning of the project, notably the separation of the contributions of the two photosystems PSI and PSII. Typical (normalized) photosystem emission spectra of PSI and PSII are used as input data. By default, the quantum efficiency of PSI is fixed at one-fifth that of PSII, as the total spectrally integrated flux of PSII has been reported to be fivefold that of PSI (Franck *et al*. 2002).

3.2.3 Consolidation of the leaf biochemical model component

Of the leaf biochemical models evaluated in the study (Chapter 2), the 'MD12' model was selected as a baseline. This module became available during the project, and tests (Section 2.4) indicated superior performance to other tested modules, albeit at the requirement of the additional parameters qLs, kNPQs and β. SCOPE also contained two empirically calibrated relationships between photochemical and fluorescence yield, one for light and CO_2 response curves of otherwise unstressed vegetation (TB12; Van der Tol *et al*. 2014), and one for experiments of different levels of drought stress (TB12-Drought) (Berry *et al.* 2013). These two equations were maintained as more empirical alternatives in the SCOPE model. The TB12 empirical models are coupled to the photosynthesis models for C3 and C4 vegetation of Collatz *et al.* (1992, 1991); the MD12 model (Magnani & Dayyoub, 2014) is linked to the Farquhar model (Von Caemmerer 2000; Farquhar *et al.* 1980) and the Von Caemmerer model (Von Caemmerer 2013, 2000) for the C3 and C4 photosynthetic pathways, respectively.

3.2.4 Coupling of model components

The biochemical module provides relative variations of the broadband (i.e., spectrally integrated) fluorescence yield of PSII, ϕ_{FII}, as output, but these had to be linked to the absolute, spectrally distributed, fluorescence radiance of the leaf optical model. In the original SCOPE model, the relative yield variations were applied to the whole spectrum (PSI + PSII), but for this project, the contributions to fluorescence *F* of the two photosystems (PSI and PSII) were separated:

$$F = F_I + F_{II} \tag{3.1}$$

where the contributions F_I and F_{II} are the leaf optical model equivalents $F_{I,0}$ and $F_{II,0}$, multiplied by a factor η representing the relative yield variation:

$$F_I = \eta_I \cdot F_{I,0} \tag{3.2}$$

$$F_{II} = \eta_{II} \cdot F_{II,0} \tag{3.3}$$

Because the excitation lifetime and fluorescence yield in PSI are constant, $\eta_I = 1$. For PSII, η is calculated from the biochemical model as:

$$\eta_{II} = \frac{\phi_{FII}}{\phi_{FII0o}} \tag{3.4}$$

where ϕ_{FII0o} is the PSII fluorescence yield of open ('*o*') photosystems in absence of energy excess non-photochemical quenching ('0'). Normalization to ϕ_{FII0o} was chosen because the typical PSI and PSII emission spectra of Franck *et al.* (2002), used in the optical model Fluspect, were defined for this case. Thus, the spectra of Franck *et al.* (2002) are reproduced if $\eta_{II} = 1$. A few lines of code were added to the MD12 model to calculate the factor η. The TB12 and TB12(Drought) models were calibrated to spectrally integrated, active fluorescence measurements that already include the constant F_I contribution. Hence, the models provide

$$\eta' = \frac{\phi_{FI}+\phi_{FII}}{\phi_{FI}+\phi_{FII0o}} \qquad (3.5)$$

Because the ratio of spectrally integrated fluorescence of the two photosystems, PSII:PSI, is 5 for open photosystems in absence of energy excess non-photochemical quenching (Franck *et al*. 2002), the ratio ϕ_{FII0o}: ϕ_{FI} is also 5. Thus, factors η_{II} and η' are related to each other as:

$$\eta_{II} = \frac{6}{5}\eta' - \frac{1}{5} \qquad (3.6)$$

With these additions to the MD12 and TB12(Drought) modules, the biochemical and leaf optical model concepts were linked.

Figure 3.2 illustrates how the fluorescence spectra vary in the resulting coupled leaf optical and biochemical modules, for the shaded side of the leaf (subscript 'fw' for forward direction). Because of the coupling, fluorescence responses to leaf structure, meteorological forcing, and physiological parameters are visible. An increase in chlorophyll concentration Cab and an increase in incident shortwave radiation (R_{in}) may both increase absorbed photosynthetically active radiation. The increase due to R_{in} is spectrally constant, while the increase due to Cab is lower at the shorter wavelengths due to reabsorption of fluorescence in the leaf. The physiology affects only PSII fluorescence through the factor η_{II}, and hence, some spectral changes occur with variations in physiology (right panel).

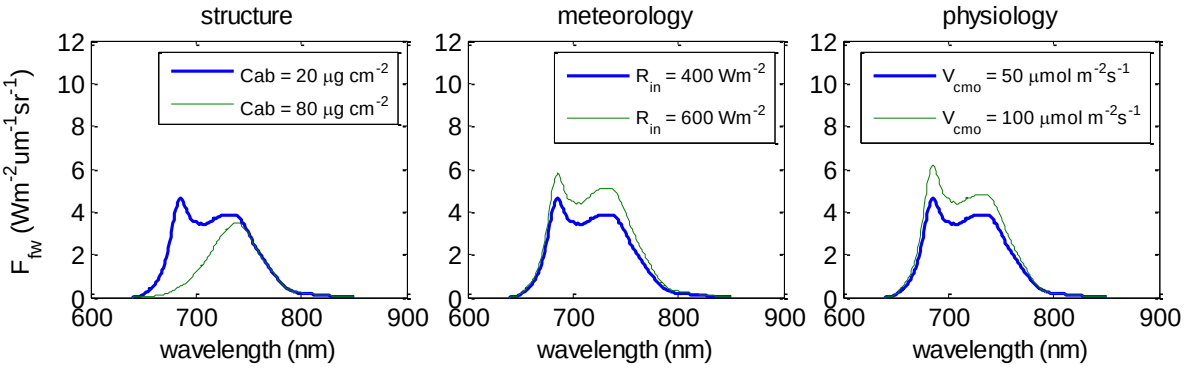

Figure 3.2. Examples of the calculation of fluorescence spectra after the coupling of the leaf optical model (Fluspect) and the leaf biochemical model (for this example: TB12-Drought)

The translation of the leaf level model output to the canopy level and the calculation of the energy balance was unaltered compared to the published version of SCOPE (Van der Tol *et al*. 2009b). However, a few additional features were developed and included during the project:

- the calculation of hemispherically integrated fluorescence W m^{-2} µm, besides the directional flux in W m^{-2} µm sr^{-1}, in the radiative transfer module of fluorescence;
- the possibility to include a vertical gradient of the carboxylation capacity Vcmo from top to bottom of the canopy.

Other changes to the original SCOPE model were made to ensure operating system independency and to increase the number of simulation options.

For the consolidated model for this study, various technical improvements were made to the SCOPE model, as itemized in Section 3.3.1.

In summary, it was concluded that the consolidated version of the SCOPE model (v1.53) for further use in this project would contain:

- the version of Fluspect with separate PSI and PSII contributions, but not the Fluspect_B version of January 2014;
- the mechanistic MD12 model for leaf biochemistry.

The empirically calibrated relations in the alternative TB12 and TB12(Drought) biochemical models, which require fewer parameters, are provided in the software as alternatives.

3.3 Forward model implementation & verification

The different modules for leaf biochemistry, leaf radiative transfer, and canopy radiative transfer were assembled to produce a final software implementation chain for testing activities. Specific objectives were to:

- assemble all modules to produce a single simulation chain;
- implement the required interfaces between modules for automatic communication;
- perform functional and consistency checks of the assembled model;
- develop documentation for the model, including installation & user guides.

3.3.1 SCOPE / A-SCOPE v1.53

SCOPE. The SCOPE model provides the structure within which the modules are integrated. SCOPE v1.53 has been written in MATLAB 7.6 (R2008a). The model also works with version 6.0 (R2006a), 7.5x, but not with version MATLAB 5.1. No special toolboxes are required.

Various improvements were implemented since C. van der Tol and colleagues first published the original SCOPE model (v1.21) in 2009. The Photosynthesis Study adopted SCOPE v1.34 as its baseline and made further updates over the course of the study. The user manual for SCOPE v1.53 by Van der Tol (2014) developed in the study itemizes these improvements since the time of the original paper from Van der Tol *et al.* (2009b).

Briefly, improvements arising from the present study include:

- addition of the leaf level photosynthesis and fluorescence model according to Von Caemmerer (2013, 2000) and Magnani & Dayyoub (2014);
- update of the leaf module Fluspect with separate fluorescence spectra for PSI and PSII;
- addition of hemispherically integrated fluorescence as an output;
- inclusion of C3 and C4 vegetation;
- provision of more options for running only parts of the model;
- major changes in model structure to facilitate data input, and improved user friendliness with the introduction of an Excel spreadsheet for inputting data;
- improved operating-system independency by the introduction of an alternative to the Excel input spreadsheet for MAC and Linux users;
- introduction of additional fluorescence outputs;
- increased simulation options, such as generation of Lookup Tables (LUT) and time series;
- introduction of a verification dataset to test whether model output calculated with default input parameters is affected by changing operating systems or MATLAB version;
- an improved user manual.

The Von Caemmerer-MD12 leaf biochemical model is based on the routines of Farquhar *et al.* (1980) for C3 species, and Von Caemmerer (2000) for C4 species. For the latter, both the full and simplified versions proposed by Von Caemmerer have been coded. The simplified version appears to be almost correct under most (but not all) circumstances and could be used if the full model is too computationally demanding. The model contains parameters for photodamage and sustained photoprotection; an unstressed value of 1 and 0 is currently used, although more specific values could be derived from field measurements and read from a look-up table (LUT).

A-SCOPE. To facilitate usability of the model and to automate the generation of multiple simulations, interfaces were built during the study for automatic communication. This led to the Graphical User Interface (GUI) software package called **A-SCOPE** ('automated SCOPE'). A-SCOPE is an integration of SCOPE into the ARTMO (Automated Radiative Transfer Models Operator, version 3) architecture. More information about ARTMO (version 1.0) is available in Verrelst *et al.* (2012; 2011) and at http://ipl.uv.es/artmo/. ARTMO is designed in a modular way and the present version of the toolbox is customized specifically for running SCOPE v1.53, hereafter referred to as A-SCOPE v1.53 (Figures 3.3, 3.4).

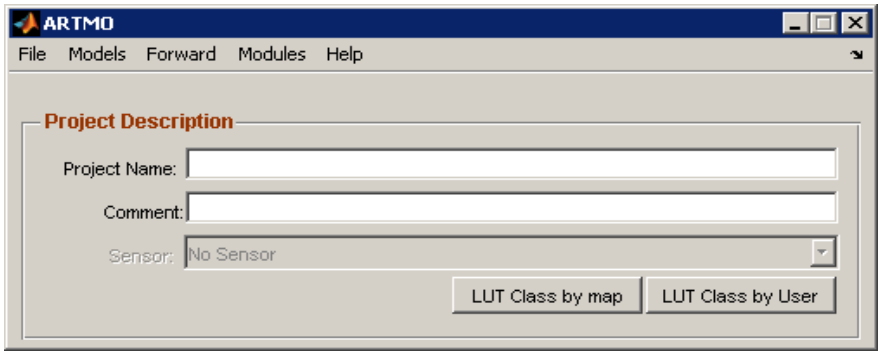

Figure 3.3. ARTMO's main window as configured for A-SCOPE.

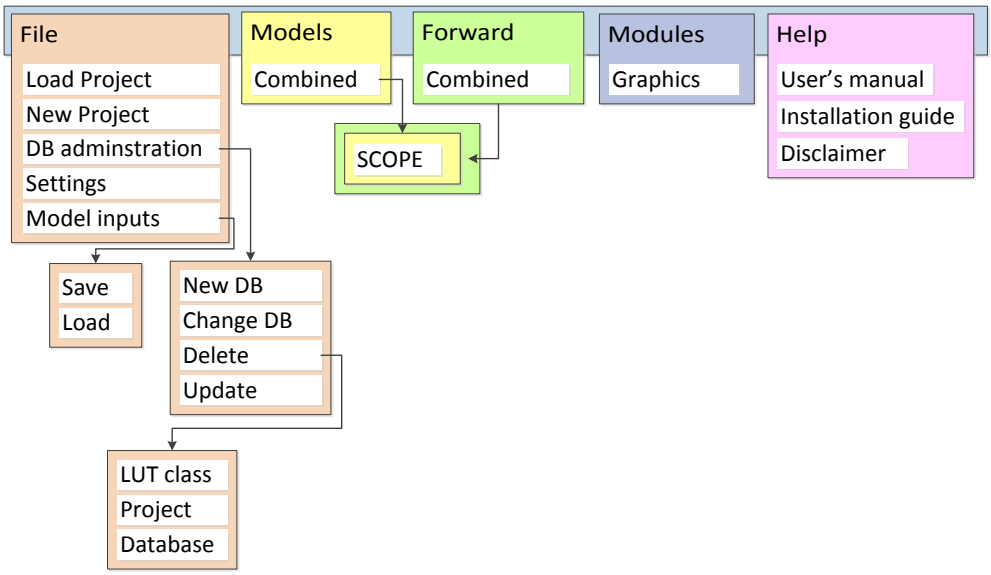

Figure 3.4. ARTMO's hierarchical design as configured for A-SCOPE.

A-SCOPE facilitates the reading of model input parameters through modular GUIs. Several modules need to be configured (Figure 3.5). The leaf biochemical module is dynamic and input parameter choices correspond to the chosen biochemical module – MD12, TB12, or TB12-Drought. As with SCOPE, A-SCOPE's own performance must be tested as well.

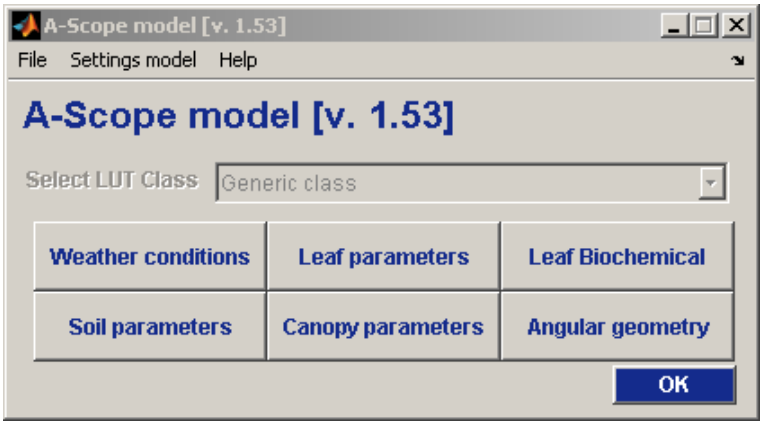

Figure 3.5. A-SCOPE main window.

For each module, default fixed values are provided. In the simplest case each module may simply be confirmed (by clicking 'OK'). Or new values may be entered.

A schematic overview of ARTMO's functioning and data flow is depicted in Figure 3.6.

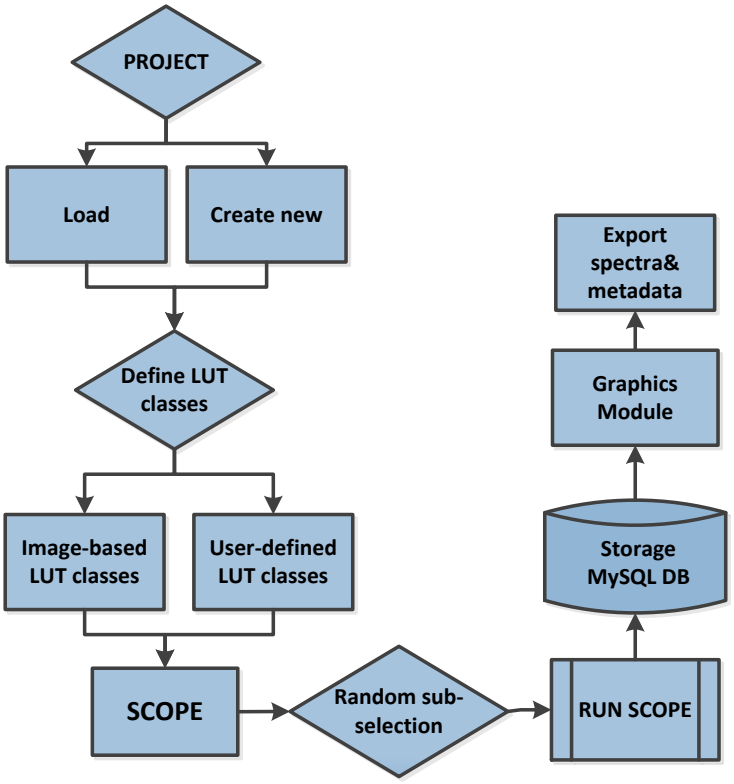

Figure 3.6. ARTMO's data flow chart

A-SCOPE begins by creating or selecting a project, within which multiple LUT-classes may be defined. Data may be entered as a single value (generates one simulation), as a range (generates multiple simulations), and/or as discreet multiple values. The model is run in ARTMO's Forward module. All input data and generated output are automatically stored in the MySQL database, and simulations may be visualized in the Graphics module. SCOPE delivers many types of output plots: fluxes, surface temperature, aerodynamic, radiation, fraction of shaded leaves, spectrum, reflectance, fluorescence, and vertical profiles of fluxes. Figure 3.7 shows an example of a fluorescence output. The Graphics module enables export of selected simulations to a text file for further processing.

While much effort has gone into developing a bug-free toolbox, there may be situations in which errors might still occur during the running of A-SCOPE. Bugs may be reported to Jochem Verrelst (jochem.verrelst@uv.es).

Documentation. For each of SCOPE and A-SCOPE v1.53, comprehensive documentation has been developed to accompany the software, including an Installation Guide, User Manual, Verification Report, and Notes (Van der Tol 2014; Verrelst & Rivera 2014a,b,c).

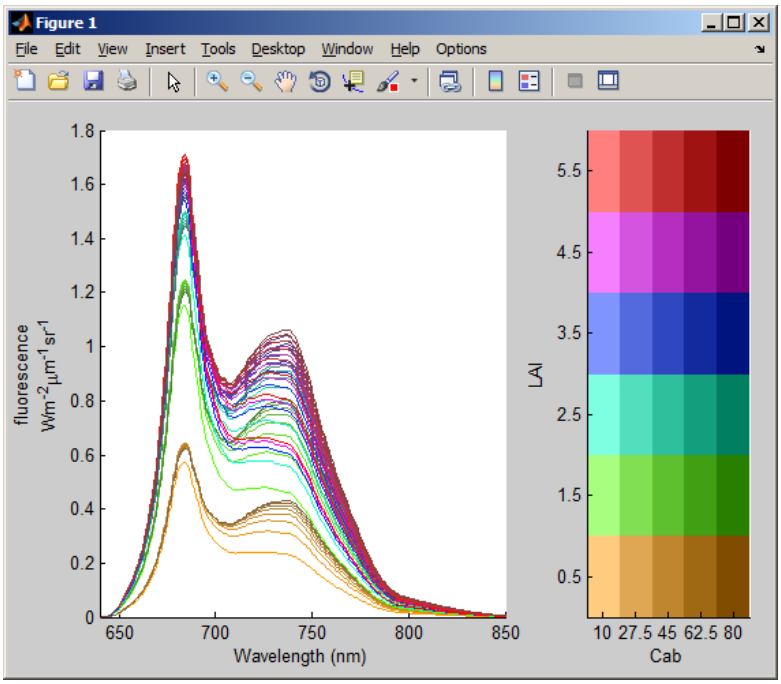

Figure 3.7. An example of Fluorescence graphic output, with color variations based on a broad range of two variables (Cab, LAI).

3.3.2 Verification

SCOPE v1.53 and the A-SCOPE v1.53 software were verified to ensure provision of physically correct outputs and consistency. Verification reports are contained in the documentation. The software successfully handled input data and delivery of outputs. No errors were encountered, and the modules performed consistently. MD12 fluorescence outputs were consistent, but validation tests against field data are required to know if outputs are biologically realistic.

3.4 Model validation based on consistency tests and statistical properties of input/output data

A validation was performed based on internal model performance (MD12 algorithm) for prediction of leaf-level C assimilation and fluorescence in species with C3 and C4 photosynthesis.

Baseline values for all parameters were derived from the literature. Only one parameter (Jmax, maximum electron transport rate) and two environmental variables (*Q*, incoming photosynthetically active radiation; *stress*, the reduction factor for stomatal closure as a result of air and soil humidity) were changed.

The maximum electron transport rate (Jmax) parameter was changed over a range (150-300 µmol e^- m^{-2} s^{-1}) representative of values observed in C3 crop species (Kattge *et al.* 2009) and in the C4 crop maize (Yin *et al.* 2011). Both leaf respiration rates (Rd, in the light) and maximum RuBP carboxylation rates (Vcmo) and (in the case of C4 species) maximum PEP carboxylation rates (V_{pm}) are assumed to co-vary with Jmax, as all four parameters are related to leaf N content (Yin *et al.* 2011; Kattge *et al.* 2009).

Photosynthetically active radiation Q was changed over a range (0.001-1250 μE m^{-2} s^{-1}) spanning both light- and CO_2-limited conditions.

The pooled parameter representing stomatal closure induced by either air relative humidity or soil dryness in the Ball-Berry model (*stress*) was given different values in C3 and C4 species. A value of the parameter equal to 1.6/*m* results in a null CO_2 concentration in intercellular spaces, imposing a physical limit to the range to be explored; because of the different value attributed to the stomatal parameter *m* in C3 and C4 species, the *stress* parameter was scaled differently in the two types, so as to cover the entire range from full stomatal opening to 80% of maximum stomatal closure.

3.4.1 Results

Note: Photochemical yields refer to the ratio between linear electron transport through photosystem II (PSII) and irradiance absorbed by PSII itself (Q_a). Fluorescence yields refer to the ratio between estimated PSII fluorescence radiance and Q_a.

3.4.1.1 Response to irradiance – fluxes and yields

The response of net assimilation rates to a combination of irradiance and environmental stress (air and soil dryness) leading to stomatal closure indicated that saturation occurs much earlier in C3 species, and it is hastened by both stomatal closure and reduced photosynthetic potentials. Saturation is observed in C4 species only at the highest irradiances, thanks to the CO_2 concentrating mechanism which strongly increase carboxylation rates. A similar pattern was predicted for the response of electron transport to irradiance, with two notable differences: (i) the initial slope of the response to irradiance was higher in C3 species; (ii) maximum electron transport rates were quite similar between photosynthetic types, despite differences in net photosynthesis.

A single curvilinear relationship was predicted between linear electron transport and fluorescence radiance, irrespective of the photosynthetic type and level of stomatal limitations. Thus, fluorescence radiance from PSII is predicted to level off as soon as light saturation is achieved. However, a further increase with light was predicted for overall leaf fluorescence radiance, because of the PSI contribution, with a constant fluorescence yield.

The response of both photochemical and fluorescence yields to irradiance was consistent with available experimental evidence (Dayyoub 2011; Flexas *et al.* 2002; Rosema *et al.* 1998; Srivastava *et al.* 1995a).

3.4.1.2 Response to irradiance – mutual relationship between yields and fluxes

The predicted relationship between photochemical and fluorescence yields is dictated by the MD12 algorithm. A negative association was predicted under light-limited conditions, followed by a transition to a positive association under CO_2-limited conditions, in good agreement with experimental evidence. It should be noted that the latter phase is not observed in C4 species

under conditions of high Jmax (i.e., high fertility, because of the known association between Jmax and leaf N content).

Although important for model testing, the analysis of yields is not representative of measurements directly acquired by the proposed FLEX instrument. In this respect, an analysis of fluorescence radiances in terms of photosynthetic rates is much more informative.

In response to changes in irradiance, the relationship between fluorescence radiance from PSII and electron transport rates, as predicted by the MD12 algorithm, is only affected by the level of Jmax (and therefore fertility, or level in the canopy), and not by level of stress or photosynthetic type (Figure 3.8A). The relationship was slightly less straightforward, however, when considering overall fluorescence radiance, including contributions from PSII and from PSI (Figure 3.8B): while the former contribution is predicted by MD12 to saturate together with J under conditions of saturating light, the latter (with constant fluorescence yield, therefore strictly proportional to absorbed irradiance) keeps increasing with light, resulting in the vertical tracks observed in the relationship. Such a decoupling between total fluorescence radiance and electron transport (and assimilation rates; data not shown) under high light conditions suggests a potential limitation of FLEX measurements, that will be discussed further below.

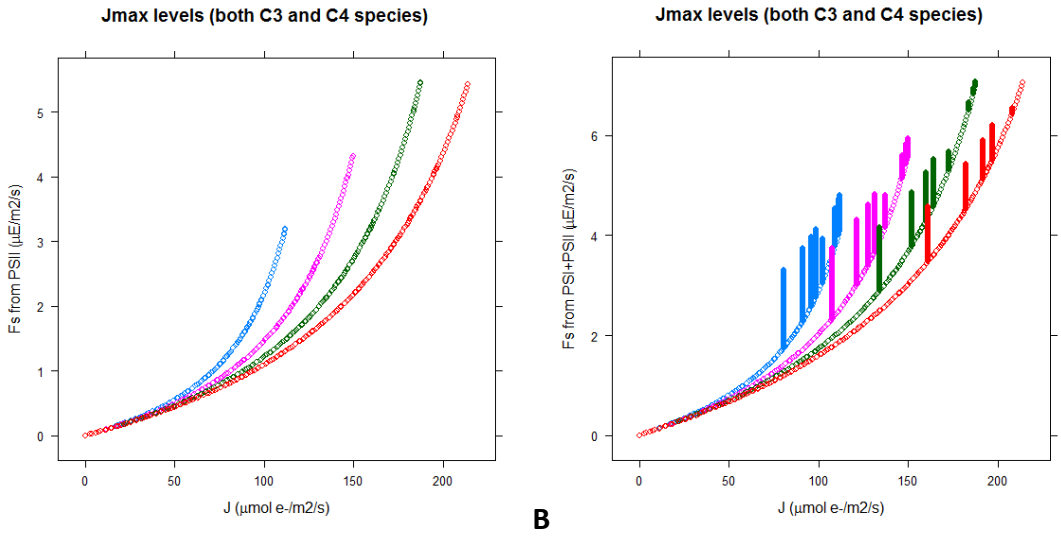

A **B**

Figure 3.8. Predicted relationship between fluorescence radiance (F_s) and electron transport rates (J) in response to changes in irradiance, Jmax and *stress* parameter. A: fluorescence radiance from PSII alone. B: fluorescence radiance from both PSI and PSII. Results for C3 and C4 species are combined; different colours correspond to levels of Jmax.

The relationship between fluorescence radiance from PSII and net assimilation rates is affected by both stomatal limitations and photosynthetic type (Figure 3.9). For each level of Jmax (Figure 3.9A), a unique relationship was predicted for C4 species, as a result of the lack of photorespiration and of the constant partitioning of ATP between RuBP and PEP carboxylation assumed in the Von Caemmerer model. In C3 species, on the contrary, increasing stomatal closure is predicted to result in a slight increase in fluorescence radiance for a given level of net photosynthesis. When pooling together all results (Figure 3.9B), a rather tight curvilinear

relationship was apparent for C3 species, irrespective of fertility and stomatal limitations. The corresponding relationship for C4 species is more disperse, despite the insensitivity to stomatal closure.

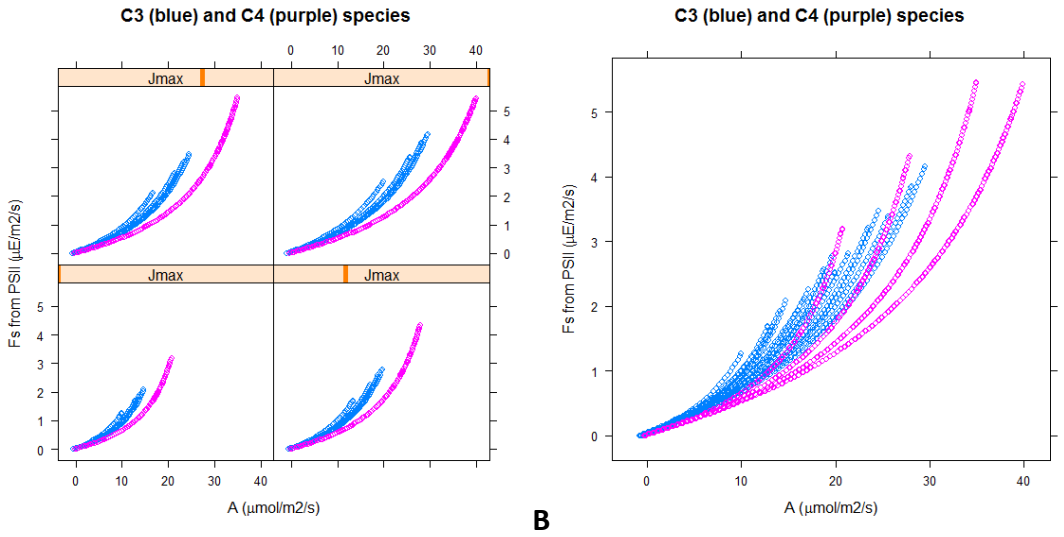

Figure 3.9. Predicted relationship between fluorescence radiance from PSII (F_s) and net photosynthetic rates (*A*) in response to changes in irradiance, Jmax and *stress* parameter. A: results disaggregated by level of Jmax, as shown. B: combined results. Results for C3 (blue symbols) and C4 species (purple symbols) are presented.

3.4.1.3 Response to stomatal closure under high light – mutual relationship between yields and fluxes

Considering the nature of the proposed FLEX mission, of greater interest is the relationship between fluorescence radiance and photosynthetic fluxes under high irradiance. With respect to the relationship between total fluorescence radiance (from both PSI and PSII) and net assimilation rates (Figure 3.10), and considering a single level of saturating light (Figure 3.10A), a rather tight relationship is predicted for C3 species, despite wide changes in stomatal limitations (0-80% stomatal closure) and photosynthetic potential (Jmax = 150-300 µmol e^- m^{-2} s^{-1}). This contrasts with results for C4 species (purple symbols in Figure 3.10A), which despite the more limited effects of stomatal closure show a stacked response, indicative of a strong interaction between Jmax levels and the response to air and soil drought; under conditions of highest fertility, however, stomatal closure appears to have no effect on the relationship, which collapses to a single point. This is consistent with the observation that photosynthesis is always light limited under such conditions, implying a complete insensitivity of all photosynthetic processes to changes in stomatal opening and CO_2 availability.

The expected relationship under a range of high irradiances, representative of midday conditions, is also worth considering (Figure 3.10B), so as to reproduce the response expected in FLEX measurements over the year. For each level of fertility and stomatal closure, the relationship will marginally depend upon the level of irradiance. In the case of C3 species, this is

the result of the contribution from PSI to fluorescence radiance, resulting in an increase in total fluorescence with light despite the constancy in saturated photosynthesis, electron transport and PSII fluorescence. In the case of C4 species, on the contrary, the effects of PSI fluorescence will superimpose over the effects of variable light on photosynthetic processes and PSI fluorescence, as photosynthesis is typically not saturated by light.

As a result, a reasonably tight relationship is predicted for C3 species, despite the wide changes in irradiance, stomatal closure and fertility. A less coherent, stacked relationship is predicted on the contrary for C4 species.

Finally, the model was applied to explore the relationship between PSII fluorescence yield and stomatal conductance; a functional link between the two variables was proposed (Flexas *et al.* 2002) based on the effects of stress-induced stomatal closure under high-light conditions to the development of non-photochemical quenching (NPQ). Model predictions for C3 species were indeed qualitatively consistent with the curvilinear relationship observed by Flexas, as well as with the observed response of fluorescence yield to irradiance. A markedly different relationship was predicted for C4 species, because of the insensitivity of photosynthetic processes to stomatal closure for a wide range of conditions.

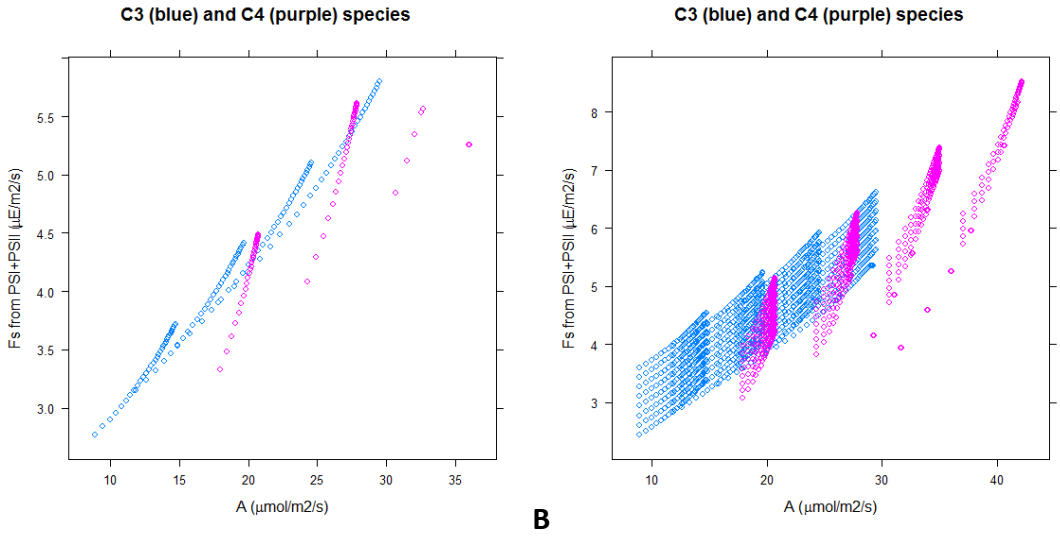

A B

Figure 3.10. Predicted relationship under high light conditions and increasing stomatal limitations between total fluorescence radiance from both PSI and PSII (F_s) and net assimilation rates (A). A: results for a single level of saturating light (Q = 1000 µE m^{-2} s^{-1}). B: light variable between 800-1500 µE m^{-2} s^{-1}), demonstrating the confounding effect of fluorescence radiance from PSI. Results corresponding to four levels of Jmax have been pooled together for C3 (blue symbols) and C4 species (purple symbols).

3.4.1.4 Response to seasonal changes in photodamage (qLs)

The overall effect of increasing levels of photodamage (declining qLs) on the relationship between photochemical and fluorescence yield under saturating light indicated that, in all

cases, photodamage resulted in a strong increase in fluorescence at any given level of photochemical yield and electron transport.

3.4.1.5 Response to seasonal changes in photoprotection (kNPQs)

The predicted effect of sustained photoprotection under high light conditions was a parallel decline in both photochemical and fluorescence yields. Since both photodamage and sustained photoprotection are often observed under extreme environmental conditions, the overall effect on the expected relationship will vary and should be carefully analyzed.

3.5 Model validation based on field measurements and external reference information

A first validation test of the model was conducted with field measurements and external reference information (i.e., meteorological parameters). For comparative purposes, both MD12 and TB12 results were evaluated. In performing this test, it must be recognized that measured data may not correspond exactly to what the model inputs understand for the meaning of variables. Also, external information is assumed to be correct.

A canopy dataset of winter wheat (*Triticum turgidum durum*) was used from a 2010 measurement campaign conducted in Avignon, France (Daumard *et al.* 2010). The site was equipped with a movable crane (height 21 m) for remote assessments. Measurements were made of vegetation radiance (300 nm to 900 nm), CO_2 fluxes (eddy covariance), canopy transmittance, fraction of absorbed PAR, leaf chlorophyll fluorescence, PSII quantum efficiency in the light, apparent electron transport, leaf chlorophyll content (SPAD-502), canopy height, leaf area, instantaneous incident radiation, and air temperature. A TriFLEX fluorosensor and PAM-2000 fluorometer were used to measure passive and active fluorescence, respectively.

Retrieval of reflectance and fluorescence radiances (F687, F760) was done using specific models applicable to the small spectral region around each respective band as described in Daumard *et al.* (2010).

Simulations were conducted using SCOPE v1.53, with parameters set to closely approximate actual measurement conditions. However, since many parameters were not specifically derived during the 2010 campaign, most were kept to default values (Table 3.1).

3.5.1 Results

A few days of measurements were selected from the end of the wheat growth period. These were for clear, sunny days with good variability in environmental conditions (PAR, temperature) and canopy characteristics (LAI 2.5 to 6.5; crop height 0.4 m to 0.9 m).

Both Fs687 and Fs760 increased over the growing period, reaching a maximum on day 137. The increase was stronger for Fs760 than for Fs687, likely a canopy structure effect induced by the reabsorption of Fs687 during its radiative transfer through the canopy (Daumard *et al.* 2012; Fournier *et al.* 2012).

Table 3.1. SCOPE parameters used in the PS Study.

SCOPE parameters	Value	SCOPE parameters	Value
soil_file	default	*SMC*	0.25 (default)
leaf_file	default	*LAI*	**Measurements**
atmos_file	default	*Hc*	**Measurements**
Cab	**Measurements**	*LIDFa*	***Adjusted***
Cdm	0.012 (default)	*LIDFb*	***Adjusted***
Cw	0.09 (default)	*Leafwidth*	0.01
Cs	0 (default)	*z*	1
N	1.4 (default)	*Rin*	**Measurements**
Rho_termal	0.01 (default)	*Ta*	**Measurements**
Tau_thermal	0.01 (default)	*Rli*	809.5 (default)
Vcmo	**Derived from measurements**	*p*	**Measurements**
m	***Adjusted***	*ea*	**Measurements**
Type	0 (C3)	*u*	**Measurements**
kV	0.6396 (default)	*ca*	**Measurements**
Rdparam	0.015 (default)	*oa*	209 (default)
Tparam	default	*zo*	0.1107 (default)
Tyear	15 (default)	*d*	0.603 (default)
Beta	0.507 (default, C3)	*cd*	0.3 (default)
kNPQs	0 (default)	*rb*	10 (default)
qLs	1 (default)	*cr*	0.35 (default)
Stressfactor	1 (default)	*Cd1*	20.6 (default)
Fqe	0.02 (default)	*Psicor*	0.2 (default)
Spectrum	1 (default)	*Cssoil*	0.01 (default)
Rss	500 (default)	*rbs*	10 (default)
Rs_thermal	0.06 (default)	*rwc*	0 (default)
cs	$1.18.10^3$ (default)	*tts*	**Measurements**
Rhos	$1.80.10^3$(default)	*tto*	**Measurements**
Lambdas	1.55 (default)	*psi*	**Measurements**

Both models satisfactorily simulated GPP. Results for DoY 142 are shown in Figure 3.11. Both the TB12 and MD12 models reproduced the diurnal pattern of GPP, although MD12 predicted a slightly higher GPP. In general, GPP was well simulated over the various measurement days, although accuracy varied somewhat depending on the day. Total latent heat flux was also generally well simulated.

The overall shape of the fluorescence diurnal cycle was well captured by the models (Figure 3.11). However, the absolute value of modelled fluorescence at 687 nm was considerably higher than the measured value, especially with TB12 (Table 3.2 shows an analysis of the last 4 days). At 760 nm the simulated fluorescence agreed more closely with measurements.

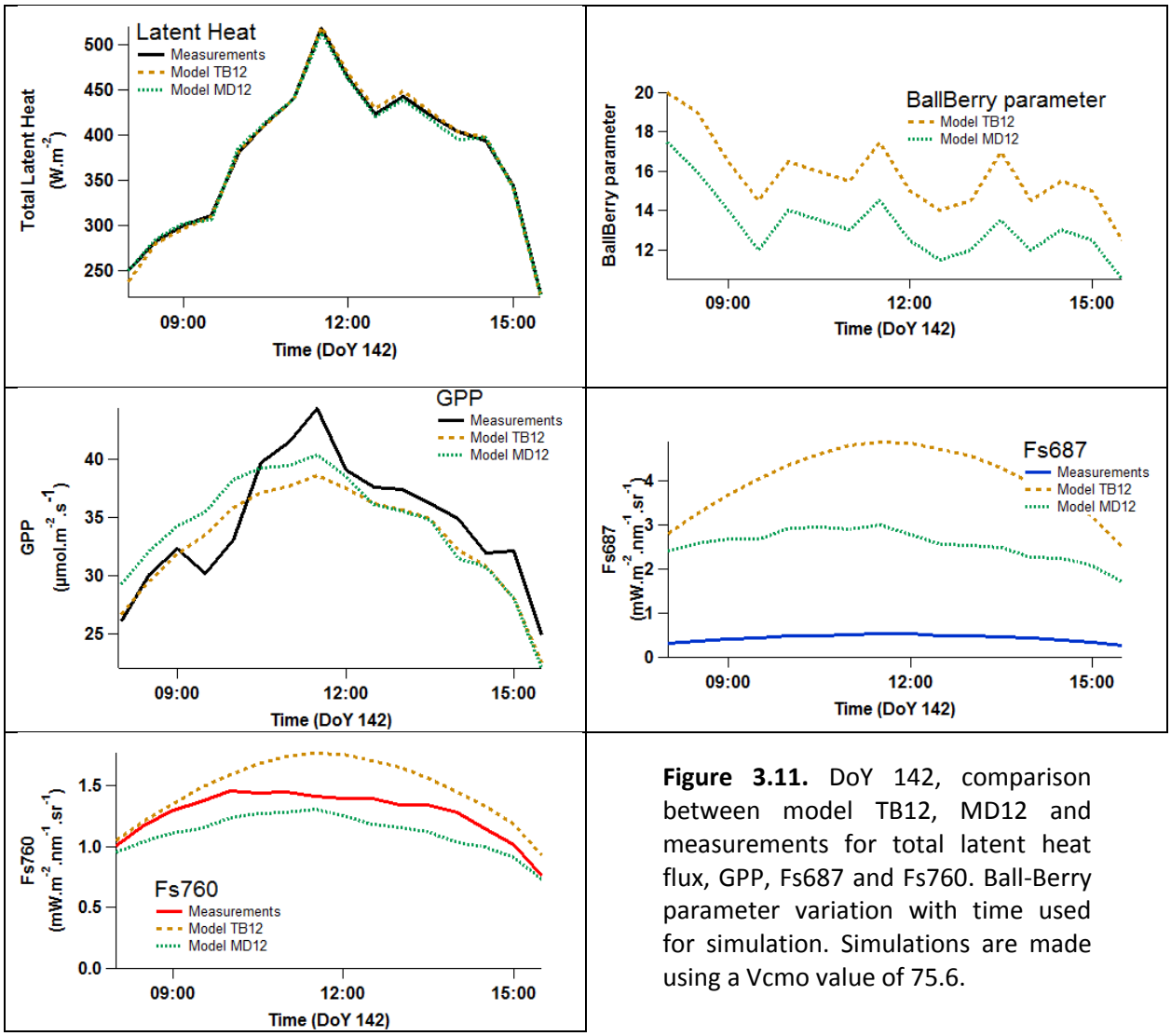

Figure 3.11. DoY 142, comparison between model TB12, MD12 and measurements for total latent heat flux, GPP, Fs687 and Fs760. Ball-Berry parameter variation with time used for simulation. Simulations are made using a Vcmo value of 75.6.

Table 3.2. Scale factor between measured and modelled fluorescence for TB12 and MD12 models. For fluorescence at 687 nm, TB12 model was 8.48 times higher than measured values and MD12 5.8 times higher. For fluorescence at 760 nm, TB12 values were close to measured one (x 1.02) and MD12 values were lower by a factor of 0.82.

	Model TB12	Model MD12
Simulated F687 compared to measurements	x 8.48	x 5.8
Simulated F760 compared to measurements	x 1.02	x 0.82

Using a constant value for the Ball-Berry parameter did not change significantly the quality of the simulation and could account for both the shape and the absolute values of the latent heat flux diurnal cycle. Concerning GPP simulation, the use of a constant Ball-Berry parameter did not have a significant impact.

A linear relationship was obtained between GPP and O_2-fluorescence (Fs760) from measurements, shown in Figure 3.12. Simulations with the models, especially MD12, were also able to capture this linear relationship (Figure 3.13).

In summary, the validation test found that SCOPE v1.53 was able to simulate the O_2-A band feature. A tendency of the MD12 model to slightly underestimate Fs760 might imply that it is too sensitive to the Ball-Berry parameter.

There was a tendency to overestimate fluorescence in the O_2-B band. It is known that during radiative transfer within the canopy, fluorescence in the O_2-B band is reabsorbed whereas that in the O_2-A band is well transmitted or reflected. This results in a decrease of the fluorescence ratio (red over far-red fluorescence) at canopy level compared to leaf level (Fournier *et al.* 2012). Thus a canopy fluorescence ratio close to or less than 1 could be expected. But SCOPE simulations produced a ratio greater than 1. To ensure that the issue did not come from radiative transfer in the canopy, several simulations were made with different canopy architecture settings. Although expected changes in the fluorescence ratios were obtained, the fluorescence flux in the O_2-B band nonetheless was always greater than in the O_2-A band. Therefore, it is possible that the issue with fluorescence absolute value at 687 nm might reside with leaf-level optical fluorescence model. This aspect needs further investigation.

GPP simulations were satisfactory for both models, and good agreement was found between measurements and output of the SCOPE model. Both the TB12 and MD12 models were able to reproduce the absolute value of GPP and its temporal evolution.

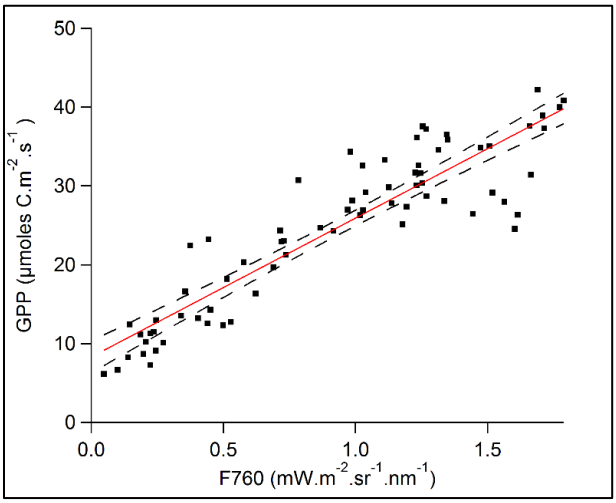

Figure 3.12. Relationship between GPP and sun induced fluorescence radiances in O_2-A (F760) band for daily integrated values (7-15h UTC). Correlation coefficient 0.83.

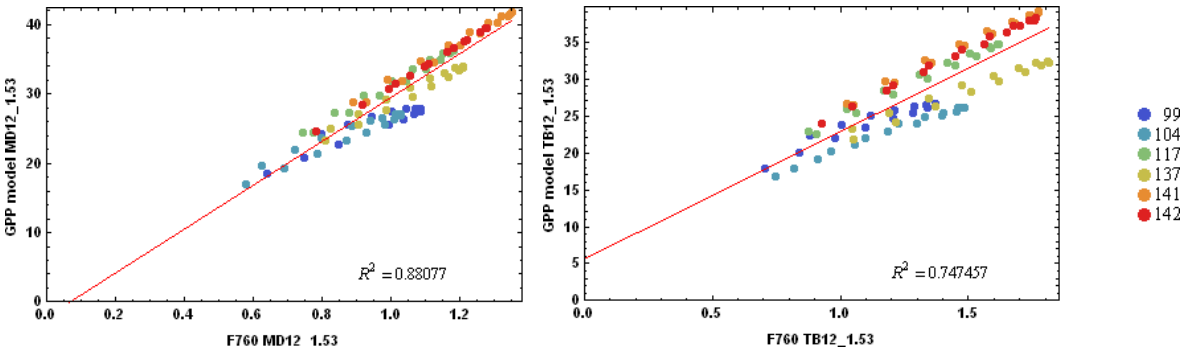

Figure 3.13. GPP vs O_2-A fluorescence relationship from simulated data obtained during the 6 days selected. **Left**: MD12 model, **Right**: TB12 model.

3.6 Sensitivity analysis

Sensitivity analyses in general indicate how responsive a model is to quantitative changes in its parameters or variables. These types of analyses allow identification of driving and non-driving variables, thus making it possible to simplify model parameterization and streamline operation by keeping non-driving variables set to fixed (default) values. This capability greatly expedites the use of a complex, multi-parameter model such as SCOPE.

Two types of sensitivity tests were carried out here: Jacobian and Monte Carlo. Jacobian testing addresses 'local' sensitivity using specific combinations of model parameters. In contrast, Monte Carlo indicates 'global' sensitivity by considering the entire parameter space and the

results from varying multiple parameters in concert. The two analyses can yield rather different dimensions of information about model character and behaviour.

The use of Jacobians to analyse sensitivity does have a few limitations. The first is that the Jacobian is defined locally in the parameter space: it only provides the model sensitivity with a specific combination of parameters. Since the parameter space of the SCOPE model is large, there is a risk of calculating the Jacobian for unrealistic parts of the parameter space, potentially leading to incorrect interpretations regarding model behaviour. To prevent such misleading results, the Jacobian sensitivity analysis was calculated for parameters of specific climate zones and specific plant functional types. In this way, the model sensitivity was obtained in realistic parts of the parameter space. A second limitation is that although Jacobians provide partial derivatives, they actually say little about the absolute effects of each parameter on the output. In order to homogenize the units and compare the elements of the Jacobian matrix, the values have to be normalized by the ranges over which each variable varies. For this purpose it was necessary to collect literature values of these ranges. A third limitation is that the partial derivatives do not take into account that parameters might be dependent and might co-vary in nature. Covariance of the parameters is relevant for the interpretation of variations in the model output (see also Section 3.7). To address this problem, the model was also used to produce output for realistic time series of co-varying parameter values collected from the literature.

3.6.1 Jacobian tests

The Jacobian provides the partial derivatives of the model outputs (*O*) to the parameters and input variables (hereon referred to as 'parameters' (*p*)):

$$J = \begin{bmatrix} \partial O_1/\partial p_1 & \cdots & \partial O_1/\partial p_n \\ \cdots & \cdots & \cdots \\ \partial O_m/\partial p_1 & \cdots & \partial O_m/\partial p_n \end{bmatrix} \qquad (3.7)$$

where *n* is the number of parameters, and *m* the number of output variables.

Jacobian matrices of the consolidated SCOPE model were calculated for five combinations of climate zones and plant functional types (PFTs) (Table 3.3), using published data for climate and PFTs to provide a range in each parameter. Matrices were first calculated for nomimal (mean) mid-season values of the input for the different climatic zones and PFTs. Estimates of the total variation in output were calculated, and individual contributions of each parameter were derived. As the SCOPE model has many parameters, outputs were limited to the most relevant ones for this study: fluorescence output at the two peaks (F685, F745) and canopy photosynthesis.

Climate data. For the climate zones (Köppen's classification), surface incident solar and thermal radiation, air temperature, and dewpoint temperature were obtained from 40-year reanalysis data of ECMWF (http://data-portal.ecmwf.int/). Selection of only these four weather variables

was justified by preliminary sensitivity analysis of the Jacobians indicating other meteorological variables appeared much less influential. Data were processed into 10-calendar-day averages.

PFT data. Structural and physiological data for the PFTs were from literature data (Houborg *et al.* 2013; Asner *et al.* 2003; Kosugi *et al.* 2003; Wilson *et al.* 2001; Reich *et al*. 1998; Wullschleger 1993). Some limitations were that: (i) data were collected in different ways, (ii) data may not have been entirely representative for the respective PFTs, and (iii) data were insufficient to calculate standard deviations of the parameters during the seasonal cycle – nevertheless, it was possible to estimate *annual* means for the different structural and physiological parameters for the purposes of the present tests.

For the parameters, two sets were used. The first set tested all parameters to select the most influential parameters, after which a more detailed analysis over growing seasons was performed for the Jacobians including only those driving parameters.

For the simulations reported here, the consolidated SCOPE v1.53 was used with the MD12 model for biochemistry. Initially all parameters were included to select the most influential parameters. Three influential parameters of the MD12 model, notably β, qLs and kNPQ, were not included in the detailed sensitivity analysis over the growing seasons, for lack of literature data of the parameter values for different plant functional types or climate zones.

Table 3.3. Climate zones and PFTs. Af: tropical everwet. Aw: tropical with dry season. Cf: temperate everwet. Dfd: cold continental climate. EBT: evergreen broadleaf tree. Cab: chlorophyll content. LAI: leaf area index. Vcmo: maximal carboxylation capacity. *m*: Ball-Berry stomatal parameter as calculated from reported Ci/Ca ratios.

Site name	Benjamin Constant	Mato Grosso C4	Mato Grosso C3	Jülich	Salekhard
Lat, Lon	-4,-70	-1,-57	-1,-57	51,6	67,67
Climate	Af	Aw	Aw	Cf	Dfd
PFT	EBT	C4 crop	C4 crop	C3 crop	Grass
Cab (µg cm^{-2})	51±23	31±10	60±10	60±30	17 ± 10
LAI	4.8±1.7	3.6±2.1	3.6±2.1	3.6±2.3	1.9 ± 1.5
Vcmo (µmol m^{-2} s^{-1})	51±35	39±10	39±10	70±26	15 ± 10
m	6.0	5.2	5.2	7.5	7.3

3.6.1.1 Results

Driving variables for fluorescence were:

- leaf and canopy structural parameters: chlorophyll a/b content (Cab), dry matter content (Cdm), senescent material fraction (Cs), leaf thickness parameters (N), leaf area index (LAI) and leaf inclination (LIDFa);
- meteorological parameters: irradiance, vapour pressure and air temperature;
- physiological parameter: maximum carboxylation capacity (Vcmo), and in the tropics the solar zenith angle (tto).

Variations in SIF were driven largely by irradiance, followed by LAI and carboxylation capacity. GPP was sensitive to these factors too, but less to irradiance and more to Vcmo and LAI than SIF. Simulated GPP and SIF were also sensitive to temperature and humidity in a tropical savannah climate, but the effect was stronger on GPP than on SIF. These results indicate that GPP variations due to variations in LAI and Vcmo could be detected with SIF.

Physiology parameters specific for the MD12 module (β, kNPQs and qLs) had a dominant effect on photosynthesis and fluorescence. It should be noted that the ranges for these parameters were rather wide. The sensitivity to kNPQ is intriguing, as it indicates that fluorescence can potentially be used to detect non-photochemical quenching, which is a stress parameter. The parameter qLs had a positive effect on photosynthesis, but a negative effect on fluorescence.

Sensitivity varied according to PFT and climate, but in all cases irradiance had a stronger effect on fluorescence than did other parameters. LAI and Vcmo had similar effects on fluorescence and photosynthesis, while the effect of Cab was opposite (positive effect of Cab on fluorescence, negative effect on photosynthesis).

With respect to the two fluorescence peaks, the red peak (F685) appeared less sensitive to chlorophyll concentration, because any increase in fluorescence emission due to higher chlorophyll content likely was compensated for by an increase in reabsorption at F685. The sensitivity to chlorophyll was non-linear. Local sensitivity analysis only provides the sensitivity at the nominal, relatively high values for the selected PFTs. The global sensitivity (Section 3.6.2) to chlorophyll concentration was found to be stronger. The F685 peak was also less sensitive than the far-red peak to other structural parameters (Cs, Cdm, N) and to irradiance.

The far-red peak, despite a contribution of the more constant fluorescence emission of PSI, was responsive to physiological parameters related to PSII.

In order to account for correlation between parameters, photosynthesis and fluorescence were also calculated for a season with realistically co-varying parameters (Cab, Vcmo and LAI) throughout growing seasons of crops. Seasonal cycles of measured Cab and LAI of three crops (winter wheat, barley and maize) in a temperate climate were used (Houborg & Boegh 2008), and linearly interpolated to daily values, along with one year weather data of the 40-year ECMWF data. The year 2001 was selected, because it was reasonably close to the 40-year average, but obviously with more frequent variations than the 40-year averages. Vcmo was estimated as a linear function of Cab following Houborg *et al.* (2013). All other structural parameters were kept at their default values for each crop throughout the season. The combined effect of the parameters was a rather close correspondence between simulated canopy photosynthesis and fluorescence at both peaks. The effects of irradiance, carboxylation capacity, chlorophyll concentration and leaf area were combined, but due to different planting dates, the covariance between the irradiance and the other parameters was different for each crop. Despite these differences, a strong positive correlation between simulated fluorescence of both peaks and photosynthesis was observed.

3.6.2 Monte Carlo tests

Global sensitivity analysis (GSA) allowed quantification of the relative importance of each input parameter to model outputs, and allowed exploration of the interactions between factors. GSA techniques can help to set safe default values for less influential parameters. This greatly simplifies model calibration as the most influential parameters may be targeted for data acquisition and refinement (Saltelli *et al.* 1999).

In variance-based GSA methods the output variance is decomposed to the sum of contributions of each individual input parameter and the interactions (coupling terms) between different parameters. Based on the work of Sobol' (Sobol' 2001) the variance-based sensitivity measures are represented as follows:

$$1 = \sum_i S_i + \sum_i \sum_{j>i} S_{ij} + , \cdots , + S_{12,\ldots,k}, \qquad (3.8)$$

In this equation, S_i, S_{ij},…,$S_{12,\ldots,k}$ are the so-called ***Sobol's global sensitivity indices***.

The ***first order sensitivity index*** S_i measures and quantifies the sensitivity of model response Y to the parameter X_i (without interaction terms), whereas, S_{ij},…,$S_{12,\ldots,k}$ are the sensitivity measures for the higher order terms (interaction terms).

The ***total effect*** **sensitivity index** ***STi*** measures the whole effect of the variable X_i, i.e. the first order effect as well as its coupling terms with the other input variables.

Both first order (S_i) and total effect (STi) are often shown together as they provide complementary information, i.e., the individual and total (with interactions) impact.

Here, the GSA method of Saltelli *et al.* (2010) was used. Within each variable, 2000 samples were run according to Sobol'. Results were expressed as normalized First order and Total order Sobol's sensitivity indices.

In defining the parameter space, atmospheric and soil variables were kept fixed. It was assumed that weather information was invariable over an area and also was known, e.g., as derived from Sentinel-3. The influence of soil is marginal for closed canopies.

Vegetation height was also kept fixed. The reason is that the geometry of the vegetation in the SCOPE model can be linearly scaled (leaf width, canopy height, measurement height) without affecting the results. Only the ratios of leaf width to canopy height, and measurement height to canopy height matter. Leaf inclination was kept to 'spherical'. The ranges are listed in Table 3.4. Apart from these state variables, the variables which were kept fixed are listed in Table 3.5.

The following outputs were selected:

1. Spectral output:
    a. **Reflectance** (as a quality check);
    b. **Fluorescence** (650-850 nm range).

2. Fluxes:
    a. **Total fluorescence emitted at the top (Fluortot):** Hemispherically and spectrally integrated ChF at the top [W m^{-2}]. This variable is the integral of the fluorescence broadband signal.
    b. **Fluorescence yield (Fluoryield):** Fluortot / aPAR_energy units [W W^{-1}] and aPAR is the total absorbed PAR by leaves. Fluorescence yield is calculated as the balance of hemispherically integrated incoming and outgoing fluxes of PAR above and below the canopy.
    c. **Net photosynthesis of canopy** (Actot) [µmol m-2 s-1]: Although this is not a fluorescence variable, this flux is relevant for this study. It is comparable to 'Gross Primary Production' (GPP) that is derived from flux towers.

Table 3.4. The proposed SCOPE input variable space to run the GSA.

Leaf parameters	min	max	
Cab	0.1	80	Chlorophyll ab content
Cdm	0.001	0.03	Dry matter content
Cw	0.001	0.05	Leaf water equivalent layer
Cs	0.001	0.2	Senescent material fraction
N	1	2.5	Leaf thickness parameters
Leaf_Biochemical (MD12)			
Vcmo	0	200	Maximum carboxylation capacity (at optimum temperature)
m	2	20	Ball-Berry stomatal conductance parameter
kV	0	0.8	Extinction coefficient for Vcmo in the vertical (maximum at the top). 0 for uniform Vcmo
Rdparam	0	0.03	Respiration = Rdparam*Vcmo
Tyear	8	20	Mean annual temperature
beta	0	1	Fraction of photons partitioned to PSII (0.507 for C3, 0.4 for C4; Yin & Struik 2012; Yin *et al.* 2006)
kNPQs	0	10	Rate constant of sustained thermal dissipation (Porcar-Castell 2011)
qLs	0	1.0	Fraction of functional reaction centres (Porcar-Castell 2011)
stressfactor	0	1	Optional input: stress factor to reduce Vcmo (for example soil moisture, leaf age). Default value = 1.
Canopy			
LAI	0.1	7	Leaf area index
hc	1.0		Vegetation height
leafwidth	0.01	0.1	Leaf width
LIDFa, LIDFb	spherical		Leaf inclination
Angles			
tts	0	50	Solar zenith angle
tto	0	10	Observation zenith angle
psi	0	90	Azimuthal difference between solar and observation angle

Table 3.5. SCOPE fixed values.

Leaf_Biochemical	
C3 species	
F quantum yield efficiency	0.02

Weather conditions	
Incoming shortwave radiation	600
Air temperature	20
Atmospheric vapour pressure	15
CO_2 concentration in the air	380
Incoming longwave radiation	300
Air pressure	970
Wind speed	2
O_2 concentration in the air	209
Measurement height of meteorological data	10

Soil parameters	
Soil resistance for evaporation	500
Volumetric soil moisture content	0.25
Broadband soil reflectance in the thermal range	0.06
Volumetric heat capacity of the soil	1180
Specific mass of the soil	1800
Heat conductivity of the soil	1.55

Aerodynamic	
Drag coefficient of the isolated tree	0.35
Fitting parameters	20.6
Roughness layer correction	0.2
Drag coefficient for soil	0.01

Leaf parameters	
Broadband thermal reflectance	0.01
Broadband thermal transmittance	0.01

3.6.2.1 Results

Global sensitivity analysis according to the method of Saltelli *et al.* (2010) enabled identification of the driving and non-driving variables. Based on Sobol's Total sensitivity index (***STi)*** results were:

Driving variables for Reflectance + Fluorescence: Leaf area index, Chlorophyll content, Fraction of functional reaction centres, Rate constant of sustained thermal dissipation, Maximum carboxylation capacity, Ball-Berry stomatal conductance parameter, Solar zenith angle, Dry matter content, Leaf water content, Leaf thickness, Senescent material fraction.

>> Less important variables: Extinction coefficient for Vcmo, Leaf width, Azimuth difference, Observation zenith angle.

The variables that have not been mentioned may be considered as intermediate variables, which showed some impact but not enough to be considered as drivers. Given that this analysis was in part undertaken to identify non-driving variables that could be kept fixed in order to simplify model usage with FLEX data (fluorescence and reflectance data), it was concluded that the variables which could safely be kept fixed are:

> Extinction coefficient for Vcmo, Leaf width, Azimuth difference, Observation zenith angle. These variables hardly influence fluorescence and reflectance variation.

Driving variables for Fluorescence only: Main ones were Fraction of functional reaction centres, and the Rate constant of sustained thermal dissipation. Other driving variables were Chlorophyll content, LAI, Ball-Berry parameter, Dry matter content, Fraction of photons partitioned to PSII, Maximum carboxylation capacity, and the Stress factor to reduce Vcmo.

>> Less important variables: Extinction coefficient for Vcmo, Leaf width, Azimuth difference, Observation zenith angle, Leaf thickness, Leaf water content, Mean annual temperature, Respiration, Senescent material fraction. Therefore, if only fluorescence is of interest, more variables could be kept fixed.

Driving variables for Photosynthesis: For net photosynthesis of the canopy (i.e., equivalent to "GPP" from flux towers), driving variables were: Maximal carboxylation capacity, Ball-Berry stomatal conductance parameter, Fraction of functional reaction centres, Mean annual temperature, Respiration, Rate constant of sustained thermal dissipation, Leaf area index, Stress factor to reduce Vcmo, and Chlorophyll content.

Finally, when it comes to comparing the results of local and global sensitivity studies, it is recommended to follow first the guidelines of the GSA. The two types of sensitivity analyses are complementary. Global sensitivity analysis provides information about the relative importance based on the broad variable space. The non-driving variables can be safely set to default values in any situation. For subsequent refinement the guidelines of local sensitivity testing are useful, as they would be applicable to certain situations, such as according to plant functional types.

3.7 Error quantification for output variables versus uncertainties in input data

The next step was to quantify errors for each output variable versus the uncertainty in input data, and to evaluate the accuracy needed in each of the model inputs to provide a given error in each output variable. Additionally, potential correlations between parameters are discussed, on the basis of relationships reported previously in the literature.

Taking the results of both sensitivity analyses, it was possible to suggest two categories of driving parameters: core driving parameters which should absolutely be taken as variable when using the model, and secondary driving parameters which could be kept constant in a first approach. Core driving parameters considered here were:

- Leaf chlorophyll content (Cab);
- Maximum carboxylation capacity (Vcmo) and Ball-Berry parameter (m);
- Beta, KNPQs, qLs, and stressfactor for the MD12 biochemical model;
- Leaf area index (LAI);
- incoming shortwave radiation (*Rin*);
- Air temperature (Ta);
- Atmospheric vapour pressure (*ea*). This parameter is optional, affecting only C3 species in one case in the sensitivity analysis.

This reduces the number of model parameters to 10 (not including *ea*) when using the MD12 biochemical module. However, it should be recognized that effects of individual parameters can

each be more or less important, depending on many conditions (plant metabolism, choice of biochemical module, local vs global analysis, etc.).

The number of free parameters may be further reduced if potential correlations between them are taken into account. Variables can co-vary depending on PFTs, climate zones, temporal scales, etc. Here, two principal co-variations are identified: (i) between Vcmo and Cab, and (ii) between kNPQs and qLs. Vcmo may be described as a function of leaf nitrogen content, fraction of nitrogen in the carboxylating enzyme Rubisco, and catalytic turnover rate at reference temperature (Friend 1995, 1991). Nitrogen also is a major constituent of chlorophyll which in turn is a component of pigment protein complexes active in photosynthesis. With respect to the sustained heat dissipation constant (kNPQs) and the fraction of functional photosystem II reaction centers (qLs), these appear tightly anti-correlated, as evidenced in a study of *Pinus sylvestris* which showed a decrease in qLs associated with the onset of a high level of sustained non-photochemical quenching in winter (Porcar-Castell 2011). Short term changes appear less correlated.

In addition, correlation can occur between Cab and LAI during growth or senescence (Lausch *et al.* 2013; Daumard *et al.* 2012; Houborg & Boegh 2008; Curran & Milton 1983), but the covariance may exhibit different patterns according to conditions (species, phenology, stress, etc.) and should be used on a case by case basis.

Other potential correlations may exist between the other parameters. Incoming radiation (*Rin*) is obviously tightly linked to solar zenith angle (tts) through a cosine law. Depending on the climate and time scale, correlation may be found between radiation (*Rin*), air temperature (Ta), and vapour pressure (*ea*). Also, over the long term, canopy biophysical parameters are linked to PFT, and to climate variables.

For error analysis, secondary driving parameters were kept fixed according to values from the sensitivity analyses and listed in Tables 3.6 and 3.7. Leaf angle distribution was taken as spheroidal. Errors were estimated by computing the partial derivative with respect to the input, and were expressed in output unit versus input unit. When input is dimensionless, error output is expressed as percent variation of the input. Tables 3.8 and 3.9 present the computation of output errors versus input uncertainties for the core driving parameters, for the two vegetation types (C3 and C4).

Table 3.6. Input parameter values and ranges for C3 crop in a temperate climate (Cf).

Input parameters for C3 crop in a temperate climate (Cf)					
	Description	unit	mean ± range min : max	Effects on F or A	Source / ref
Cab	Leaf chlorophyll a+b content	µg cm-2	60 ± 30	high on F745 only	estimated from N data from Reich *et al.* 1998
Cdm	Dry matter content	g cm-2	0.001 : 0.03	medium	default
Cw	Leaf water equivalent layer	cm	0.001 : 0.05	0	default
Cs	Senescent material fraction	-	0.001 : 0.2	high	default
N	Leaf structure (thickness) parameter	-	1 : 2.5		default
Vcmo	Maximum carboxylation capacity (at optimum temperature)	µmol m-2 s-1	70 ± 26		leaf gas exchange
m	Ball-Berry stomatal conductance parameter	-	7.5 ± 4	0	from Ci/Ca
LAI	Leaf Area Index	m m-2	3.6 ± 2.3		Asner *et al.* 2003
LIDFa	Leaf inclination	-	-1 : 1		default
Rin	Broadband incoming shortwave radiation (0.4-2.5 um)	W m-2	350 ± 120		climate data
Ta	Air temperature	°C	19 ± 4		climate data
Rli	Broadband incoming longwave radiation (2.5-50 um)	W m-2	360 ± 18	0	climate data
p	Air pressure	hPa	970 ± 150	0	default
ea	Atmospheric vapour pressure	hPa	Rh=0.6 ± .14	0	climate data
u	Wind speed at height z	m s-1	± 5	0	default
Ca	Atmospheric CO_2 concentration	ppm	380 ± 15	0	default
tts	Solar Zenith Angle	deg	0 : 50	low	
beta	Fraction of photons partitioned to PSII	-	0 : 1		default
kNPQs	Rate constant of sustained thermal dissipation	-	5		arbitrary
qLs	Fraction of functional reaction centres	-	0.8		close to default

Table 3.7. Input parameter values and ranges for C4 vegetation in a tropical climate (Aw).

Input parameters for C4 vegetation in a tropical climate with one dry season (Aw)				
	Description	unit	mean	Source / ref
Cab	Leaf chlorophyll a+b content	µg cm-2	31 ± 10	from Vcmo, following Hobourgh *et al.* 2013
Cdm	Dry matter content	g cm-2	0.001 : 0.03	default
Cw	Leaf water equivalent layer	cm	0.001 : 0.05	default
Cs	Senescent material fraction	-	0.001 : 0.2	default
N	Leaf structure (thickness) parameter	-	1 : 2.5	default
Vcmo	Maximum carboxylation capacity (at optimum temperature)	µmol m-2 s-1	39 ± 10	Collatz *et al.* 1992
m	Ball-Berry stomatal conductance parameter	-	5.2 ± 4	from Ci/Ca and Lloyd and Farquhar 1994
LAI	Leaf Area Index	m m-2	3.6 ± 2.1	Asner *et al.* 2003
LIDFa	Leaf inclination	-	-1 : 1	default
Rin	Broadband incoming shortwave radiation (0.4-2.5 um)	W m-2	650 ± 65	climate data
Ta	Air temperature	°C	23 ± 1.7	climate data
Rli	Broadband incoming longwave radiation (2.5-50 um)	W m^{-2}	380 ± 17	climate data
p	Air pressure	hPa	970 ± 150	default
ea	Atmospheric vapour pressure	hPa	rh=0.68 ± 0.15	climate data
u	Wind speed at height z	m s^{-1}	± 5	default
Ca	Atmospheric CO_2 concentration	ppm	380 ± 15	default
tts	Solar Zenith Angle	deg	0 : 50	
beta	Fraction of photons partitioned to PSII	-	0 : 1	default
kNPQs	Rate constant of sustained thermal dissipation	-	5	arbitrary
qLs	Fraction of functional reaction centres	-	0.8	close to default (1)

Table 3.8. Output errors *vs* input uncertainties for C3 crop (temperate climate).

Output errors versus input uncertainties for C3 crop (temperate climate)						
Parameter	**Description**	**Central value**	**Units**	**F687 sensitivity** W m^{-2} sr^{-1} μm^{-1}	**F760 sensitivity** W m^{-2} sr^{-1} μm^{-1}	**A sensitivity** $\mu mol\ m^{-2}$ s^{-1}
	Leaf biophysical parameters					
Cab	Chlorophyll ab content	60	$\mu g\ cm^{-2}$	-0.002	0.001	-0.012
	Leaf biochemical parameters					
Vcmo	Maximum carboxylation capacity at optimal temperature	70	$\mu mol\ m^{-2}$ s^{-1}	0.015	0.004	0.2
m	Ball-Berry stomatal conductance parameter	7.5	%	0.0012	0.0003	0.01
	Biochemical parameters of the MD12 model					
beta	Fraction of photons partitioned to PSII	0.507	%	-0.02	-0.05	0.15
kNPQs	Rate constant of sustained thermal dissipation	0	%	-0.001	-0.0002	-0.013
qLs	Fraction of functional reaction centers	1	%	-0.05	-0.014	0.04
stressfactor	Optional parameter to reduce Vcmo. default=1.	1	%	0.01	0.0025	0.082
	Canopy structure					
LAI	Leaf area index	3.6	$m^2\ m^{-2}$	0.058	0.018	1.7
	Meteo					
Rin	Broadband incoming shortwave radiation (0.4-2.5 um)	360	W m^{-2}	0.002	0.001	0.02
Ta	Air temperature	19	°C	-0.04	-0.01	-0.14
ea	Atmospheric vapour pressure	13	hPa	0.06	0.016	0.5

Table 3.9. Output errors *vs* input uncertainties for C4 crop (tropical climate with dry season).

Output errors versus input uncertainties for C4 crop (tropical climate with dry season)						
Parameter	**Description**	**Central value**	**Units**	**F687 sensitivity** W m^{-2} sr^{-1} μm^{-1}	**F760 sensitivity** W m^{-2} sr^{-1} μm^{-1}	**A sensitivity** $\mu mol\ m^{-2}$ s^{-1}
	Leaf biophysical parameters					
Cab	Chlorophyll ab content	31	$\mu g\ cm^{-2}$	-0.017	0.008	-0.055
	Leaf biochemical parameters					
Vcmo	Maximum carboxylation capacity at optimal temperature	39	$\mu mol\ m^{-2}$ s^{-1}	0.06	0.011	0.65
m	Ball-Berry stomatal conductance parameter	5.2	%	0.006	0.00014	0.0005
	Biochemical parameters of the Magnani Model					
beta	fraction of photons partitioned to PSII	0.4	%	-0.058	-0.013	0.46
kNPQs	rate constant of sustained thermal dissipation	0	%	-0.0065	-0.0015	-0.037
qLs	fraction of functional reaction centers	1	%	-0.19	-0.042	0.20
stressfactor	optional parameter to reduce Vcmax. default=1.	1	%	0.004	0.001	0.004
	Canopy structure					
LAI	Leaf area index	3.6	$m^2\ m^{-2}$	0.16	0.041	3.35
	Meteo					
Rin	broadband incoming shortwave radiation (0.4-2.5 um)	650	W m^{-2}	0.0048	0.0017	0.034
Ta	air temperature	23	°C	-0.092	-0.021	1.73
ea	atmospheric vapour pressure	19	hPa	0.014	0.003	0.05

3.8 Conclusions

A consolidated model relating chlorophyll fluorescence and photosynthesis was presented here, consisting of the MD12 leaf biochemical module, Fluspect optical leaf module, and the SCOPE canopy radiative transfer model. SCOPE v1.53 has been updated significantly, including the preparation of new user documentation. It has been further integrated into a new automated GUI called A-SCOPE which facilitates data input, processing, plotting, outputs, and export. The consolidated model has been verified and validated for internal consistency and performance. It has undergone a preliminary field validation which indicates it is able to simulate photosynthesis as would be measured by the eddy-covariance technique (tower-based), and also fluorescence especially of the far-red peak. Further examinations will be needed to draw firm conclusions on its representation of the red fluorescence peak (O_2-B band).

Local and global sensitivity tests have been conducted which have identified driving and non-driving variables, thus identifying parameters that could be kept fixed in order to simplify and quicken model operation with FLEX fluorescence data. It may be possible to work with only 10 or 11 input parameters for a very simplified version of the model in certain circumstances, not taking into consideration parameter co-variation which could further reduce the number of core driving variables depending on the situation. Error quantification was computed for each output variable versus the uncertainty in input data, giving an indication of the accuracy needed in each of the inputs of the consolidated model to provide a given error in each output variable.

4. Algorithm development based on models

4.1 Introduction

The main objective of this task was to develop a Level-2 prototype algorithm deriving measures of photosynthesis (represented by GPP or eventually any other relevant parameter) from the observations to be obtained from the FLEX/S3 tandem mission. The models produced so far in the Photosynthesis Study are complex and may not be readily amenable to describing the wide variability of biomes, ecosystems, species, and environmental conditions that impact fluorescence-photosynthesis relationships. That is why a combined approach – mixing model uses and experimental data in various conditions – was favoured here. This task undertook to define and evaluate algorithms based on:

- inversion of the forward model developed in the study;
- statistical models;
- simple F-GPP relationships;
- health or stress indicators.

Results have been integrated toward the development of a prototype algorithm to estimate photosynthesis and/or vegetation state from FLEX/S3 observations.

4.2 Model inversion

The main objective of this component was to define and evaluate an algorithm to predict photosynthesis from FLEX/S3 observations based on inversion of the forward consolidated model. Two different approaches were used:

1. An inversion approach based on a minimization function and a simulated database (as prepared from the PARCS study),
2. A hybrid approach based on coupling a simulated database (from SCOPE) to a statistical regression model.

4.2.1 Cost function minimization

A direct inversion approach was pursued in which SCOPE output was propagated through the atmosphere, sampled in the bands of the sensors of Sentinel-3 and FLEX (S3/FLEX), and noise was added. Although direct model inversion may not be the best *operational* approach, it is useful in demonstrating the technical feasibility of retrieving net photosynthesis of the canopy (NPC) from all S3/FLEX data: the OLCI, SLSTR, and FLORIS sensors. A limitation was that both the database generation and the retrieval were carried out with the same model. The retrieval was applied to a limited number of cases (31).

The database used for the retrieval was built for the FLEX PARCS study. The database generation was repeated with the consolidated version of the model. The database consisted of 31 simulations where nine parameters were varied one by one. In addition, 13 different

atmospheric conditions were simulated (by varying the visibility, altitude, vapour, etc., in MODTRAN), and two solar zenith angles were used.

The database was constructed in three steps:

1. SCOPE was applied to 31 combinations of input parameters.
2. The output of SCOPE was propagated through the atmosphere.
3. TOA radiances were sampled in the sensor bands, and noise was added to the data.

The retrieval was carried out by minimizing the quadratic difference between forward simulated and 'true' sensor data in the database. The retrieval was carried out in two steps for computational efficiency:

1. A 'SCOPE-light' model (discussed below) was run repeatedly, starting with initial parameter values, until the cost function was minimized. To update the parameters after each run, the automatic Matlab function 'lsqnonlin' was used. The following parameters were optimized: Cab, Cdm, Cw, N, Cs, LAI, LIDFa, LIDFb, and two parameters characterizing the magnitude of the two fluorescence peaks (Table 4.1). TOC fluorescence spectrum retrieved this way was used in step 2.
2. The physiological parameter Vcmo was then retrieved from the full SCOPE model by minimizing the quadratic difference between the simulated fluorescence spectrum and the fluorescence spectrum as retrieved in the previous step. Other influential parameters – qLs, kNPQs, beta, and stomatal parameter *m* – were maintained at their default values.

SCOPE_light. Figure 4.1 flowcharts how the algorithm resolved the ten parameters of SCOPE_light and the two fluorescence parameters by means of an optimization loop. SCOPE_light consisted of only the optical radiative transfer module (RTMo) combined with FLUSPECT, which is used to provide leaf reflectance and transmittance. The fluorescence matrices of FLUSPECT were not used. Instead, fluorescence was modelled as just two linearly scaled spectral end members, corresponding to the PSI and PSII fluorescence spectra from Franck *et al.* (2002). After propagation of the surface reflectance factors and the fluorescence terms through the atmosphere and the spectral sampling by the sensors, the TOA radiance spectrum was compared to the 'measured' spectrum from the database.

In Figure 4.1 the termination of the loop is not indicated, but of course stopping conditions were used to establish the final solution of the model inversion. The default stopping criteria in the function 'lsqnonlin' were used, which included the change of the cost function with respect to the previous iteration, the change of the parameters with respect to the previous iteration, and the number of iterations, specified by tolerance settings.

To differentiate the performance in several sub-regions, spectral regions were defined as indicated in Table 4.2.

Table 4.1. Ranges of all 12 parameters varied in the optimization loop. The fluorescence weights *FI* and *FII* are multiplication factors applied to the spectral distribution functions found by Franck *et al.* (2002) for PSI and PSII, which are used here as spectral end members.

Parameter	Description	Min	Max
p_{LAI}	Transformed LAI	0	0.8
C_{ab}	Chlorophyll (µg/cm^2)	0	100
C_s	Brown pigment (-)	0	0.3
C_w	Water content (cm)	0	0.04
C_{dm}	Dry matter (g/cm^2)	0	0.05
N	Leaf mesophyll par. (-)	1	3
s	LIDFa+LIDFb	-1	1
d	LIDFa-LIDFb	-1	1
F_I	Fluorescence weight I	0	1000
F_{II}	Fluorescence weight II	0	1000
Vcmo	Max. carboxylation capacity	1	200

The cost function that was minimized during the feedback loop was:

$$C = \sum_{i=1}^{187}\left(\frac{L_i^{WBS} - L_i^{DB}}{N_i^{WBS}}\right)^2 + \sum_{j=1}^{288}\left(\frac{L_j^{NBS} - L_j^{DB}}{N_j^{NBS}}\right)^2 + \sum_{k=1}^{21}\left(\frac{L_k^{OLCI} - L_k^{DB}}{N_k^{OLCI}}\right)^2 + \sum_{l=1}^{6}\left(\frac{L_l^{SLSTR} - L_l^{DB}}{N_l^{SLSTR}}\right)^2 \quad (4.1)$$

which constitutes a sum of squared differences normalized for noise over all sensors (502 bands). Note that the 3 thermal bands of the SLSTR sensor are ignored in this process, since SCOPE_light is unable to simulate surface temperatures and thermal radiances (contrary to the full SCOPE).

Table 4.2. Definition of regions for which the retrieval was evaluated.

Region	Start (nm)	End (nm)
O_2-B1	686.65	688.40
O_2-B2	688.40	691.95
O_2-B3	691.95	696.95
O_2-A1	759.45	762.10
O_2-A2	762.10	767.00

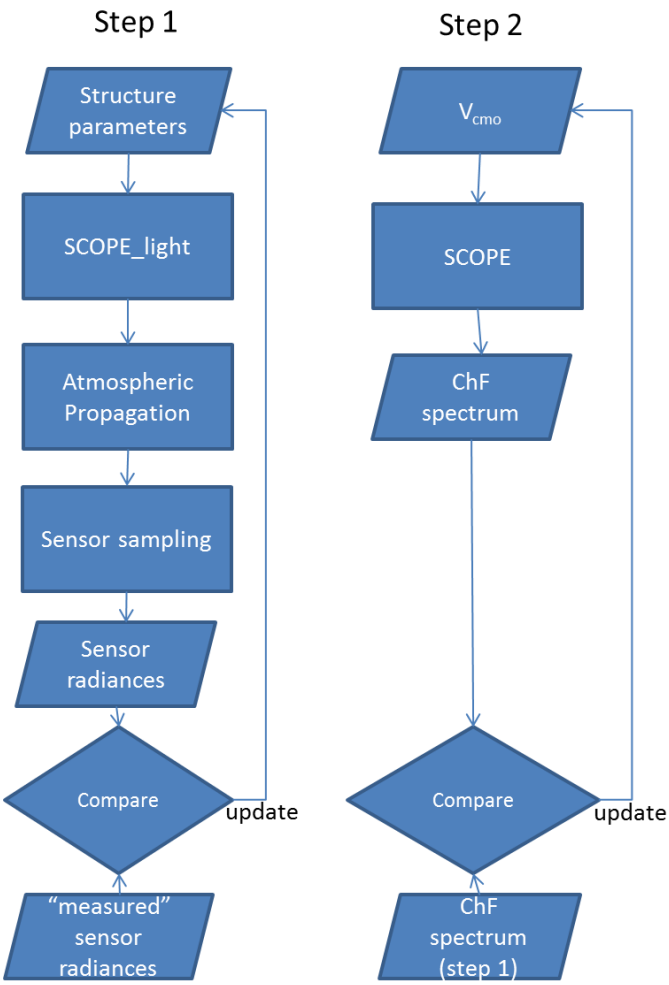

Figure 4.1. Optimization loop for the retrieval of fluorescence and biophysical parameters.

4.2.1.1 Results

The RSME of the retrieved fluorescence was about 10% of the fluorescence. In most cases, accurate retrievals were still possible even if the wrong atmosphere or wrong soil background was chosen. However, in the case of LAI=0.5, fluorescence could not be retrieved when using the wrong soil background. Figure 4.2 shows the efficacy of retrieved fluorescence and net canopy photosynthesis (NPC) for the 31 cases. However, the fluorescence of C4 vegetation was very high, and the retrieval algorithm did not succeed in retrieving these accurately, with the highest error in the O_2-A bands (far-red fluorescence).

Net canopy photosynthesis was also very high for C4 vegetation. The retrieval algorithm resolved neither the photosynthetic capacity nor the NPC, even when the photosynthetic pathway was known. Further investigation of this case is needed.

All parameters – except for LIDFb – could be accurately retrieved from the simulated (noisy) TOA radiances. In the case of completely erectophile leaf orientation, structural parameter (Cab, Cdm and N) could not be retrieved accurately.

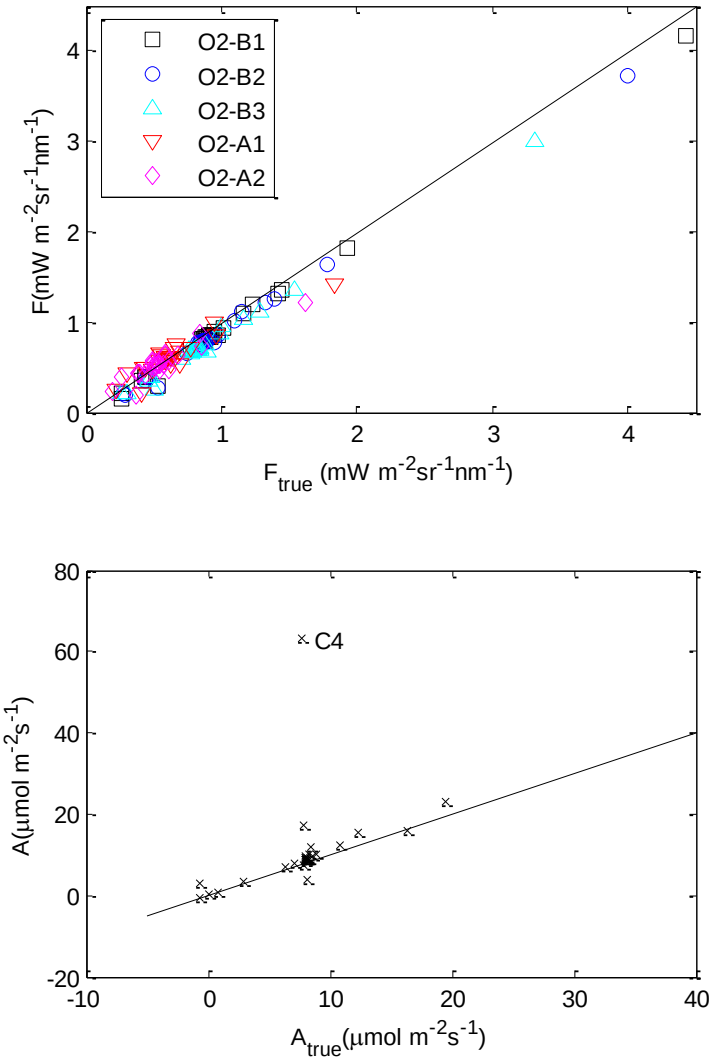

Figure 4.2. Retrieved fluorescence in different bands versus the simulated TOA true fluorescence in these bands (top), and retrieved total canopy photosynthesis versus the simulated values in the database (bottom).

4.2.2 Hybrid approach

The cost function minimization approach can have certain disadvantages: it tends to be time-consuming; it requires independent study to choose among the many available cost functions; it does not necessarily lead to the best performance (Verrelst *et al.* 2013); and although it is

possible to calculate NPC back from the input variables, a more direct inversion from fluorescence to NPC may in practice appear to be more robust.

Linking NPC with other data (e.g., fluorescence, reflectance, biophysical variables) may be viewed essentially as a multi-input regression problem, in this case suited to nonlinear nonparametric methods as they allow adaptive fitting. Optimization occurs automatically during the training phase, avoiding the time demands of manual fine tuning. Moreover, some nonparametric methods in the field of machine learning (i.e., Gaussian processes regression) possess additional useful features such as insight in relevant bands, and delivery of uncertainty intervals along with the per-pixel estimates (Verrelst *et al*. 2012).

The approach here can be considered as a hybrid method, since the machine learning algorithm was presented with training data generated by a radiative transfer model, i.e., SCOPE. Simulations from SCOPE were entered into a nonparametric Gaussian processes regression (GPR) based on a large number of simulations (1967). The predictive power of input data was assessed in estimating variable NPC. By doing so, regression strategies were evaluated such as: performance of reflectance, biophysical variables, and fluorescence data (F685, F740 and full fluorescence profile).

Input variables that were used to generate SCOPE simulations are listed in Table 4.3. These were chosen based on the sensitivity analyses (Section 3.6). One sensitive variable, solar zenith angle, was kept fixed because ranging it tends to break down the robustness of the regression models. Other variables were kept fixed. Simulations were generated for C3 and C4 species.

Table 4.3. LUT ranging variables with its minimum, maximum, and number of samples.

Variable	Min	Max	# samples
Chlorophyll content (*Cab*)	1	80	20
Water content (*Cw*)	0.001	0.03	5
Dry matter content (*Cdm*)	0.001	0.03	5
Leaf area index (*LAI*)	0.1	7	20
Maximum carboxylation capacity (Vcmo)	1	200	5
Ball-Berry stomatal parameter (*m*)	2	20	5
Respiration (*Rdparam*)	0.01	0.03	5

The ranging variables proposed here produce a large set of possible combinations (1250000). Such large datasets can lead to computation limitations in running the regression algorithm. Thus, a random subset of samples was chosen.

In choosing the fluorescence band features to use in the regression model for NPC, first one band was analyzed, then more information was added:

1. A band in the top of the second emission peak: 740 nm;
2. A band in the top of the first emission peak: 685 nm;
3. The full broadband fluorescence profile: 650-850 nm at 1 nm.

Top of canopy reflectance was also introduced, as were the biophysical variables LAI, Chl, and *f*APAR which are expected to be retrieved by FLORIS or in synergy with OLCI.

Samples were split into training (70%) and validation (30%) datasets. The training dataset was used to develop a model and the validation dataset for validating the trained model.

For the regression algorithm, various linear and nonlinear nonparametric regression algorithms were tested (further information on these algorithms is contained in Rivera *et al.* 2014). Algorithms within the family of kernel-based machine learning generally performed strongest.

4.2.2.1 Results

Results are summarized in Table 4.4. The inclusion of fluorescence data resulted in substantive improvement in algorithm performance for the estimation of net photosynthesis of the canopy. Strong relationships can be obtained using only the second emission peak F740, but the most information is contained within the first emission peak F685. The error threshold of 10% was already satisfied with the first emission band in C3 plants. Results could be subsequently improved by including more bands, the whole fluorescence profile, and additional biophysical variables, optimally yielding R^2 of 0.95. Neither reflectance data nor solely biophysical variables (Chl, LAI, *f*APAR) led to meaningful relationships with net photosynthesis of the canopy. With C4 plants, the full fluorescence profile was needed to meet the error threshold.

Table 4.4. Overview of analyzed strategies and validation results using the SCOPE v1.53 consolidated model, with the MD12 biochemical model, and C3 & C4 species.

Retrieval strategy for NPC:	**Validation :**		
C3 species	**R^2 adj, RMSE, NRMSE %**		
No fluorescence info: Reflectance (500-800 nm at 1 nm)	0.13	19.3	22.5%
No fluorescence info: only Chl, LAI, *f*APAR	0.15	19.1	22.3%
Only one fluorescence band: second peak (740 nm)	0.75	10.5	12.2%
Only one fluorescence band: first peak (685 nm)	0.87	7.6	8.8%
Two fluorescence bands: 2 peaks (685, 740 nm)	0.90	6.4	7.4%
The full fluorescence profile (641-850 nm at 1 nm)	0.94	5.1	5.9%
The full fluorescence profile (641-850 nm at 1 nm) + Chl, LAI, *f*APAR	0.95	4.8	5.6%
C4 species (fluorescence results only)			
Only one fluorescence band: second peak (740 nm)	0.78	10.6	15.9
Only one fluorescence band: first peak (685 nm)	0.86	8.4	12.6
Two fluorescence bands: 2 peaks (685, 740 nm)	0.88	7.7	11.6
The full fluorescence profile	0.99	2.3	3.4
The full fluorescence profile + Chl, LAI, *f*APAR	0.99	1.95	2.9

Here, regression models were trained and validated on simulated data only. A necessary next step is to apply the models to real data. In addition, the regression models will need to be more generally applicable to different geometries (viewing and solar angles).

4.3 Statistical algorithm based on model and/or observations

The main objective of this workpackage was to define statistical models linking remote observations including fluorescence to photosynthetic products. Simple parametric models were set up that use fluorescence in the two bands and reflectance indices as input variables.

Testing was done using a study database generated from the SCOPE (v1.53) model. The impact of each significant parameter on the relationship between photosynthesis and fluorescence was studied on the one hand, and the relationship between photosynthesis and optical observations on the other hand. Initially, data acquired by different groups in previous campaigns were to be used (Section 2.3), however, that data did not span a sufficiently large number of cases linking fluorescence to photosynthesis, especially at canopy level. Since it was shown in Chapter 3 that simulated outputs from the SCOPE model compared well with experimental data, that approach used here was considered acceptable.

The database used here was defined on the basis of the most relevant parameters for fluorescence and photosynthesis (Chapter 3, Sections 3.6 & 3.7). This database was split into sub-databases for C3 and C4 vegetation, and each sub-database was further split into two equally sized databases – one used for training and the other for testing the model.

Leaf-level data were not included in this test of statistical algorithms but were incorporated in an evaluation of long term sustained non-photochemical quenching using fluorescence-based indices (Section 4.5, “Simplified algorithms based on health or stress indicators”).

In many experimental situations, a high linear correlation has been reported between gross primary production (GPP) and far-red fluorescence (Guanter *et al.* 2012; Berry *et al.* 2013; Frankenberg *et al.* 2011b; Rossini *et al.* 2010). Here, this relationship was considered as a reasonable starting point to define more sophisticated statistical algorithms. As a first step, the relationship between GPP and F760 was analyzed, to identify the main drivers of the relationship. Then photosynthetic variables (GPP, LUE, APARChl) were expressed in terms of parametric models depending on remote optical variables, and the best models and optical variable combinations for describing photosynthesis were evaluated.

4.3.1 Results

The F760-GPP relationship was far from linear when the whole set of relevant parameters was used; this was true also for F687-GPP (Figure 4.3). Some linear structures were observed in scatter diagrams indicating that correction procedures could be useful for linearizing the relationship.

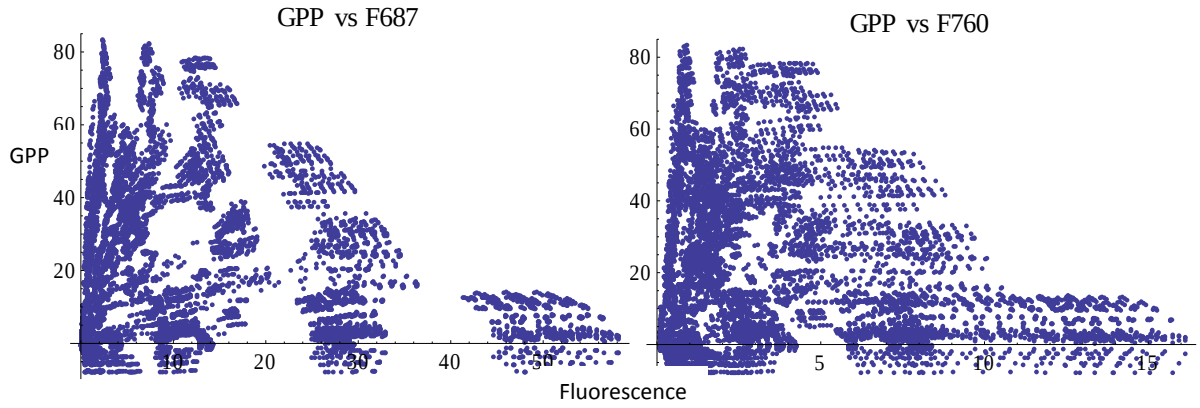

Figure 4.3. GPP-F relationship over the whole database for red (left) and far-red (right) fluorescence.

As a next step, to evaluate the individual effect of each parameter on the relationship, input parameters were changed one at a time and the corresponding relationship between GPP and F760 was plotted.

The fractional functional reaction centers parameter, qLs, had a strong impact on fluorescence: fluorescence greatly increased when qLs decreased, while GPP decreased at the same time. To our knowledge, observed long-term changes in qLs are associated with an increase in kNPQs (Porcar-Castell 2011; Porcar-Castell *et al.* 2008a; Porcar-Castell *et al.* 2008b), so effects of qLs must be evaluated with corresponding changes in kNPQs.

Maximum carboxylation capacity (Vcmo) and leaf area index (LAI) had a significant effect on both fluorescence and GPP. As this effect was almost proportionally equal on GPP and F760, it did not change the linear relationship between them, except for Vcmo at highest F760 and GPP values. Cover type (i.e., leaf angle distribution classified as erectophile, planophile, or spheroidal) was the main factor of change in the slope of the linear F-GPP relationship. Leaf chlorophyll content (Cab) also had an effect on the slope, but less than cover type. Finally, the Ball-Berry parameter and the sun zenith angle had little impact on the F-GPP relationship.

In view of the observed characteristics of the GPP-F760 relationship, we proposed to add into the statistical relationship remote observations that are representative of the most influential parameters:

- Vcmo, which can be represented by fluorescence;
- LAI, cover type, and Cab, which can be represented by a selection of reflectance indexes.

Here, the following remote indexes were investigated:

- Fluorescence radiances in the two oxygen bands, F687 (O_2-B) and F760 (O_2-A), as representative of the red (690 nm) and far-red (740 nm) chlorophyll fluorescence peaks. F760 has been empirically correlated to GPP (Guanter *et al.* 2014; Berry *et al.* 2013; Frankenberg *et al.* 2011b; Rossini *et al.* 2010). Far-red fluorescence F760 is enriched PSI fluorescence, while variable PSII fluorescence contributes to both peaks (Agati *et al.* 2000; Genty *et al.* 1990). Furthermore, red fluorescence is impacted by both leaf

chlorophyll content (Pedrós *et al.* 2010; Gitelson *et al.* 1999; Gitelson *et al.* 1998) and canopy structure (Daumard *et al.* 2012; Fournier *et al.* 2012);

- The Normalized Difference Vegetation Index (NDVI), which is widely used in the remote sensing community and is linked to Cab, LAI and cover type (Malenovský *et al.* 2009; Glenn *et al.* 2008);
- The Modified Canopy Adjusted Ratio Index 2 (MCARI2), as a predictor of green LAI (Haboudane *et al.* 2004);
- The MERIS Terrestrial Chlorophyll Index (MTCI) (Dash & Curran 2007) for its link to chlorophyll content.

Five models of different degrees of complexity were tested: polynomials of degrees up to 3, and rational function of polynomial of degrees up to 2. On the basis of the RMSE values given in Table 4.5, it was possible to select – for each photosynthetic product and each number of independent variables – the best performing model (highlighted in red). We can note that RMSE were lower for C3 plants compared to C4 plants. The reason for this difference is unknown at this time.

Table 4.5. Root Mean Squared Error (RMSE) on the predicted response of the best GPP, LUE and APARChl models, according to the different combinations of input variables. Model type is indicated in parenthesis. The table highlights the best performing models for each photosynthetic product and each number of independent variables.

	GPP		LUE x 1000		APARChl	
	C3	**C4**	**C3**	**C4**	**C3**	**C4**
1 variable						
F687	11.52 (r2)	18.40 (r2)	8.09 (r2)	8.80 (r2)	286.6 (r2)	349.6 (4)
NDVI1	11.44 (r2)	11.85 (p3)	8.55 (r2)	8.51 (p3)	98.29 (r2)	99.10 (r2)
2 variables						
F687, F760	8.84 (r2)	17.91 (r2)	4.59 (r2)	8.11 (r2)	285.0 (4)	339.8 (r2)
F760, NDVI	11.35 (p3)	10.40 (r2)	8.45 (p3)	8.37 (p3)	73.52 (p3)	52.23 (p3)
MTCI, NDVI	11.32 (r2)	11.52 (r2)	8.43 (r2)	8.51 (p3)	87.92 (r2)	91.42 (p3)
MCARI2, NDVI	10.59 (r2)	10.65 (r2)	7.93 (r2)	8.50 (p3)	43.15 (r2)	43.63 (r2)
3 variables						
F687, F760, MTCI	3.46 (r2)	10.40 (r2)	1.84 (r2)	7.14 (r2)	194.0 (r2)	173.5 (r2)
F687, F760, NDVI	6.21 (p3)	10.18 (p3)	4.10 (r2)	7.61 (p3)	58.1 (p3)	37.35 (p3)
F760, MCARI2, NDVI	8.96 (p3)	10.08 (r2)	6.78 (r2)	8.24 (p3)	36.04 (r2)	25.22 (r2)
MTCI, MCARI2, NDVI	10.53 (p3)	10.57 (r2)	7.84 (p3)	8.37 (p3)	28.64 (p3)	29.31 (p3)
4 variables						
F687, F760, MTCI, MCARI2	2.17 (r2)	9.07 (r2)	1.43 (r2)	7.34 (p3)	23.53 (r2)	24.45 (r2)
F687, F760, MTCI, NDVI	2.29 (r2)	9.10 (p3)	1.59 (r2)	7.12 (r2)	29.53 (p3)	26.93 (p3)
F687, F760, MCARI2, NDVI	2.22 (p3)	8.98 (p3)	1.60 (r2)	6.74 (p3)	15.79 (r2)	13.96 (p3)
F760, MTCI, MCARI2, NDVI	4.59 (p3)	9.99 (p3)	3.40 (p3)	7.75 (p3)	22.77 (r2)	16.59 (r2)
5 variables						
F687, F760, MTCI, MCARI2, NDVI	1.94 (r2)	8.27 (p3)	1.36 (r2)	6.43 (p3)	9.52 (p3)	9.84 (p3)

Good predictions were obtained for all photosynthetic products for C3 plants, but only GPP and APARChl could be predicted for C4 plants. The analysis was conducted for unstressed vegetation.

It was found that both fluorescence bands were required for predicting GPP and LUE, while reflectance indices alone gave the best results for predicting APARChl.

In the case of one-variable models, F760 surprisingly was found to be non-predictive for any products, regardless the plant type (C3, C4). This is in contrast with the previously reported high correlation between far-red fluorescence and GPP deduced from experimental data (Guanter *et al.* 2012; Berry *et al.* 2013; Frankenberg *et al.* 2011b; Rossini *et al.* 2010). But it was consistent with the better retrieval of Net Photosynthesis of Canopy (NPC) obtained by Gaussian processes regression with F685 nm band compared with the F740 nm band (see Section 4.2.2).

The following conclusion can be drawn about the link between photosynthetic products and remote observations that can be obtained by the FLORIS/OLCI instruments combination:

1. Simple regression models (polynomial and rational) that use only simple optical data in a low number of channels was able to predict photosynthetic products (GPP, LUE, APARChl) for C3 plants in a non-stressed case (qLs=1. and kNPQs=0.) with high performance.
2. In the case of C4 plants, only APARChl could be predicted with high accuracy – performance was rather low for GPP, and poor for LUE.
3. Both fluorescence bands were needed to predict GPP and LUE. This means that the two fluorescence bands do not carry the same information.
4. Reflectance data alone were able to predict APARChl with high performance.

Although the models tested in this study were simple and used a limited number of variables, they proved their efficacy to predict photosynthetic products such as GPP, LUE and APARChl, at least in the case of C3 plants in the absence of severe stress.

However, the models were trained and validated with simulated data only. Their robustness against noise, or the case of real data were not evaluated. Nonetheless, given the simplicity of these models, it gives confidence in the possibility to link remote data including fluorescence to photosynthetic products in a more general case if more sophisticated models are used.

It is recommended here to carry on the validation work on the SCOPE model with true experimental data and to test the regression models on experimental data on one hand, and simulated data that have been consolidated against real data, on the other hand.

4.4 Algorithms based on simple F-GPP relationships – leaf-level considerations

This section considers linkages between fluorescence and photosynthesis at the leaf level, which are instructive in helping to understand basic physiological influences on the dynamics of canopy level relationships between fluorescence and GPP. This discussion incorporates information gleaned from active analytical techniques, which have been helpful in deriving an understanding of such fundamental processes.

Earlier studies (Magnani *et al.* 2009) and the quantitative analysis carried out in the Photosynthesis Study (see Chapter 2) have suggested the existence of a general, quasi-linear relationship between fluorescence radiance and electron transport rate (and – to a lesser extent – net photosynthesis) under short-term changes in environmental conditions (e.g., CO_2, temperature, light). This would appear to support recent suggestion (Guanter *et al.* 2014) of a linear link between vegetation GPP and SIF. Other studies, however, have suggested a more nuanced picture under field, stressful conditions, in particular for natural vegetation not relieved by irrigation or fertilization. Severe temperature (Porcar-Castell 2011; Öquist & Huner 2003) and drought stress (Fernández-Marín *et al.* 2011; Baraldi *et al.* 2008) are known to result in sustained non-photochemical quenching (NPQs), through the overnight retention of de-epoxidated zeaxanthin, as well as in a reduction in the fraction of active reaction centres (qLs). Other reports (e.g., Chen & Cheng 2003; Lu & Zhang 2000; Verhoeven *et al.* 1997) have also suggested zeaxanthin retention and sustained non-photochemical quenching as a protection mechanism against excess light under conditions of low nutrient availability, which typically reduces the photosynthetic efficiency of the leaf and therefore the potential for photochemical dissipation of absorbed light.

A decline in chlorophyll content is also commonly reported under conditions of nutrient stress, in parallel with changes in nitrogen content and photosynthetic potential. The significance of such coordinated changes under conditions of nutrient stress (which, in contrast with freezing temperatures and drought affect most natural vegetation) have not been duly considered in previous modelling studies of the relationship between fluorescence radiance and photosynthesis.

Here, these effects were first assessed through a review of the literature. The implications of the observed patterns were then explored through the application of the biochemical_MD12.m routine in the SCOPE v1.53 model, so as to analyze key issues related to the fluorescence-photosynthesis relationship without the confounding effects of canopy-scale structure and energy transfer.

The literature search targeted papers reporting concurrent changes in chlorophyll modulated fluorescence, maximum electron transport rates and leaf biochemistry (chlorophyll, nitrogen and xanthophyll content, on a leaf area basis) in response to fertilization and changes in nutrient availability. The dataset was integrated with additional papers reporting changes in response to changes in growth irradiance and other stresses (ozone, elevated CO_2), as well as inter-specific and provenance comparisons. In total, 23 publications were included in the database, accounting for a total of 43 species encompassing C3 and C4 photosynthesis and a range of plant functional types (grasses, crops, deciduous and evergreen broadleaf trees, coniferous trees).

For the modelling analysis, the mutual relationships between biochemical and functional parameters that resulted from re-analysis of the literature were implemented in the biochemical_MD12.m routine of SCOPE v1.53, for both C3 and C4 species.

4.4.1 Results

4.4.1.1 Literature review

Results of the literature review are shown in Figures 4.4 and 4.5. The dark-adapted yield (Fv/Fm) declined in association with low chlorophyll contents (Fig. 4.4A) from its typical value of 0.83 under unstressed conditions to values as low as 0.64 under nutrient stress; this would correspond to an increase in the rate constant kNPQs from 0 to 1.31 x 10^9, corresponding to a value of NPQ_S of 1.87. The relationship could be captured by a non-quadratic hyperbolic function, which was used in the modelling analysis. The relationship between sustained photoprotection and chlorophyll depletion would appear to apply to a wider variety of long-term stress, as exemplified in Figure 4.5.

A general positive association was also observed between chlorophyll content and maximum electron transport rates (Jmax), although with a poorer fit (R^2 = 0.39); chlorophyll is not directly involved in the determination of Jmax, but the observed relationship emerges from the association of both traits with leaf nitrogen content. Despite the lack of a direct causal link, the linear relationship presented in Fig. 4.4B was applied in Scenarios 3 and 4 in the current study.

A general positive association was indicated between leaf chlorophyll and nitrogen contents across species and conditions (Fig. 4.4C); the remote sensing of leaf chlorophyll has indeed been proposed as a possible tool to estimate its nitrogen content, although the relationship appears to be variable between species.

Data for the relationship with total xanthophyll content are not presented here. The analysis will be further refined as part of future studies.

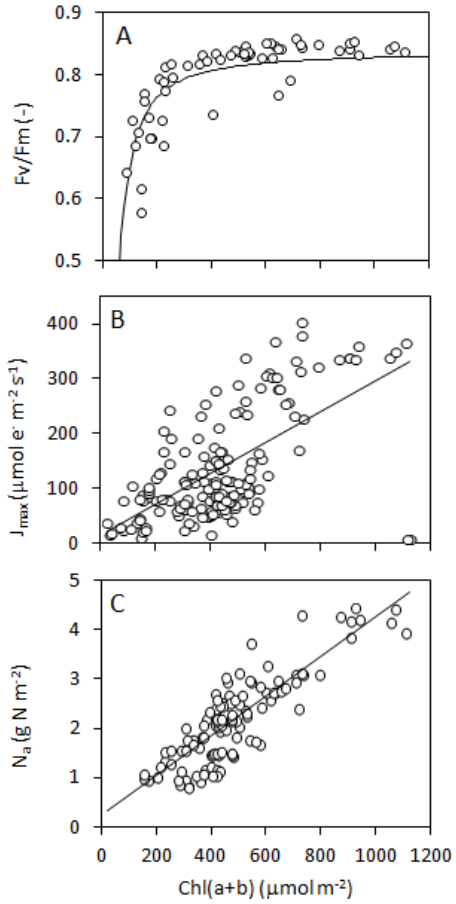

Figure 4.4. Relationship between leaf photochemical properties (F_v/F_m, maximum photochemical yield; Jmax, maximum electron transport rate) and leaf chlorophyll content (Chl(a+b)), from a review of available datasets. Also presented is the relationship between chlorophyll and nitrogen content (N_a).

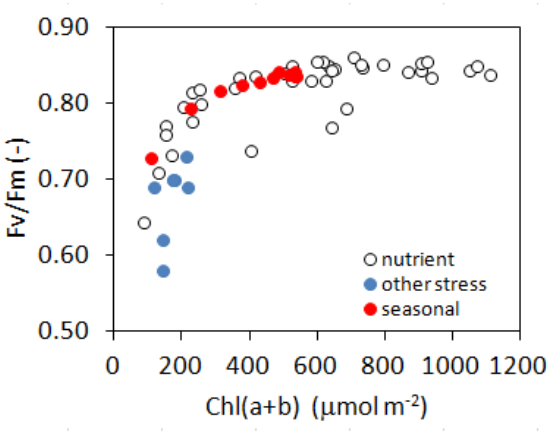

Figure 4.5. Relationship between leaf maximum photochemical yield (F_v/F_m) and chlorophyll content (Chl(a+b)), showing the different sources of variability in the two traits.

4.4.1.2 Modelling analysis

The association between fluorescence radiance and net photosynthesis under different scenarios was explored for both high- and low-light conditions. As already discussed (Magnani *et al.* 2014), high-light conditions appear to be best suited for the remote sensing of photosynthetic rates, as both electron transport and fluorescence radiance are insensitive to stomatal limitations under light-limited conditions. The analysis therefore primarily focused on simulations assuming saturating light (1000-1300 µmol m^{-2} s^{-1}). Under such conditions, the effects of chlorophyll content are mainly related to the re-absorption of fluorescence radiance in the leaf, since both photosynthesis and fluorescence yields are already saturated by light and therefore insensitive to changes in leaf absorbance.

Assuming a constant value for Jmax and kNPQs (Scenario 1; left panel in Figure 4.6), increasing levels of chlorophyll result therefore in higher fluorescence radiances, without any changes in photosynthesis. The variability within each series (different colours; corresponding to one level of chlorophyll content) is largely the result of stomatal changes, while the effects of changes in irradiance are almost negligible under these light-saturated conditions (vertically stacked lines).

On the contrary, if we assume Jmax to change without a parallel increase in chlorophyll content (Scenario 2; center panel in Fig.4.6), both net photosynthesis and fluorescence radiance are predicted to change almost in parallel, resulting in a coherent, quasi-linear relationship that is also largely consistent between C3 and C4 species (not shown).

Based on the co-variation observed in the literature re-analysis, chlorophyll contents and Jmax values would be expected to co-vary, both in response to fertility and between species. The expected relationship at leaf level showed the joint effects of chlorophyll content (lower fluorescence radiance at high chlorophyll contents, as a result of re-absorption) and of the parallel increase in Jmax (and maximum carboxylation rate: higher levels of both photosynthesis and fluorescence radiance) (Fig. 4.6, right panel). The relationship between fluorescence radiance and photosynthesis is clearly variable, depending on the level of chlorophyll considered; for each level, however, the relationship was predicted to be largely the same for C3 and C4 species (not shown).

Only after correcting the data for chlorophyll re-absorption would the curves collapse onto a single relationship (corresponding to Scenario #2 in Fig. 4.6), which appears to be largely insensitive to changes in (saturating) light, stomatal closure and fertility. The application of a simple empirical model (at leaf and canopy level), as was recently suggested (Guanter *et al.* 2014; Lee *et al.* 2013), would clearly require a preliminary correction for fluorescence re-absorption, or a variable calibration depending on the chlorophyll level considered. In both cases, an ancillary estimate of leaf chlorophyll content would be required.

Under low-light conditions (100-400 µmol m^{-2} s^{-1}; data not shown), the relationship is often dominated by the parallel effects of irradiance on both fluorescence and photosynthesis. Under light-limited conditions, stomatal closure has an effect on photosynthesis only in C3 species, as a result of photorespiration, but no effect on fluorescence radiance.

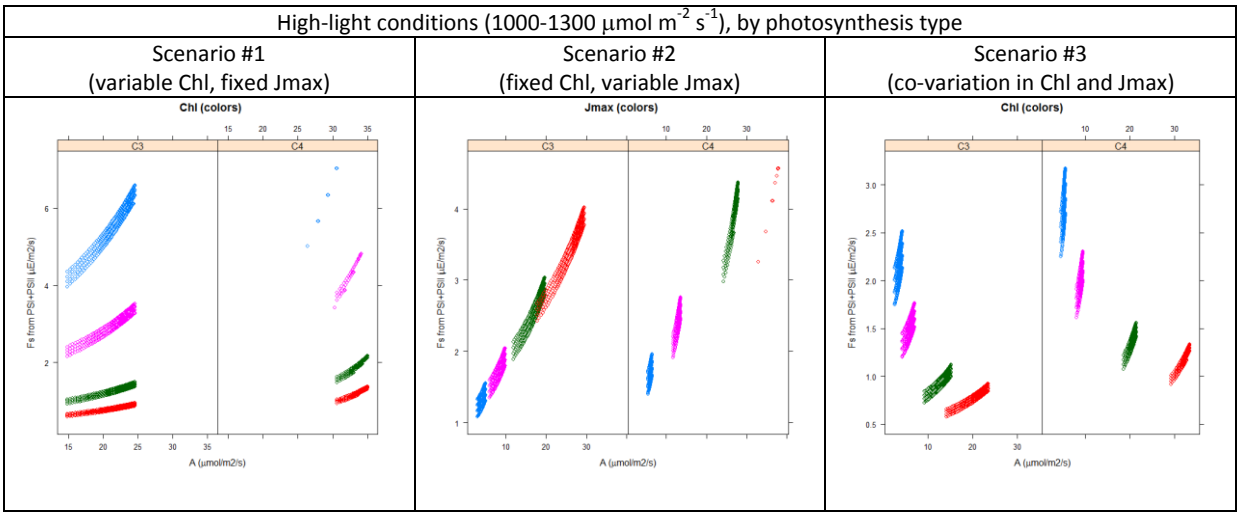

Figure 4.6. Model predictions of leaf-level relationships between photosynthesis and fluorescence radiance under high-light (1000-1300 µmol m-2 s-1) conditions and variable levels of stomatal closure, under three scenarios of Chl and Jmax co-variation; panels refer to C3 and C4 species, colours to variable levels of Chl or Jmax, from lowest (blue) to highest (red).

Also under light-limiting conditions, the predicted response appears to be highly sensitive to leaf chlorophyll content. In this case, the effect will be two-fold, since increasing chlorophyll will result in: (i) greater light absorption, with a positive effect on both photosynthesis and fluorescence radiance, but also (ii) greater fluorescence re-absorption, resulting in lower values of fluorescence radiance. As already discussed for high-light conditions, no single empirical relationship should be expected, unless data are preliminarily corrected for fluorescence re-absorption within the leaf (and canopy).

Under an operational perspective, the complete lack of sensitivity of fluorescence radiance to stomatal limitations under low-light conditions suggests the need for measurements of solar-induced fluorescence under light-saturated conditions (which could occur at irradiances above 300-500 µE m^{-2} s^{-1}, depending on leaf conditions, but at higher light levels at canopy level, because of average leaf orientation and shading), with important implications for planned overpass times.

It should be noted that the effects of changes in sustained non-photochemical quenching (NPQs), as reported in the literature as a result of nutrient limitations (as well as drought and low temperatures), should not be a matter of concern for the proposed FLEX mission, as they only affect the relationship under low-light conditions, which are unsuitable for reliable measurements.

On the contrary, the effects of photodamage (qLs < 1) as a result of cold or dry conditions would affect also the relationship between photosynthesis and fluorescence radiance also under high-light conditions. Their detection and representation will require additional measurements and modelling efforts, and will be the subject of future studies.

The following conclusions may be drawn from this investigation:

1. A re-analysis of available literature data clearly demonstrated an important feature, namely a widespread association between leaf chlorophyll content and photosynthetic potentials, which is commonly neglected in predictions of the relationship between fluorescence radiance and photosynthesis.
2. As a result, a single consistent relationship between fluorescence and photosynthesis can only be expected after correcting the signal for re-absorption effects. Without such a model-based correction, the empirical relationship should be independently calibrated for set levels of chlorophyll content, based on results from process-based models.
3. The analysis confirmed the need to rely on measurements of fluorescence radiance under light-saturated conditions (which could occur at irradiances above 300-500 μmol m^{-2} s^{-1}, depending on leaf conditions, but at higher light levels at canopy level, because of average leaf orientation and shading), so as to capture also the effects of environmentally-induced stomatal closure on leaf photosynthesis and GPP; this could be achieved with a late-morning or near-midday satellite overpass, but the appropriate timing will largely depend on latitudinal and seasonal changes in irradiance.

Finally, this evaluation demonstrated the insensitivity of the results to sustained photoprotection, as the latter only influences the relationship under light-limiting conditions. Further studies are needed to assess the role of photodamage under severe stress conditions.

4.5 Simplified algorithms based on health or stress indicators

The objective of this part of the study was to incorporate the use of health or stress indices based on fluorescence measurements into the proposed algorithm of the FLEX/S3 tandem mission. Inputs to this exercise came from two sources: (i) the research reported in Chapter 5 of this report ("Fluorescence as an indicator of vegetation health and stress resilience"), and (ii) a dynamic study based on the long-term PC11 data of Porcar-Castell (2011) (Section 2.3) to assess the ability of fluorescence-based indicators to monitor changes in sustained reduced photosynthesis capacity. The PC11 data enabled estimation of sustained and reversible components of photochemical (PQ) and non-photochemical (NPQ) quenching. Two parameters derived from leaf chlorophyll fluorescence were defined and estimated: the rate constant of sustained non-photochemical quenching (kNPQs) and the fraction of functional reaction centers (qLs).

4.5.1 Results

In the first component (based on Chapter 5), three types of stress were analyzed: water stress, nitrogen deficiency, and temperature stress. The latter was further refined to cold stress and heat stress. Changes in fluorescence were identifiable in response to these stresses, and trends were noted for both passive or active measurement methods, strengthening the confidence that fluorescence changes were not caused by any artifact (canopy structure effect, inaccurate retrieval method, etc.) linked to the passive method. The use of both fluorescence peaks was especially valuable in identifying stress effects, and to a limited degree in discriminating among

the different stresses (although fluorescence is not suggested *per se* as a means of identifying types of stress, but only the manifestation of stress effects). It should be noted that changes in fluorescence can overlap, therefore analysis should incorporate external data such as temperature, precipitation, vegetation type, etc. Focussing on passive measurements of canopies, it was evident that a stress discrimination using characterization of SIF in the two fluorescence bands might be feasible in some cases, although the limited number of studies available prevents the assessment of error margins.

In the second component, which used the PC11 long-term dataset, it was found that a large amount of sustained NPQ was accumulated during winter, associated with a decreased fraction of functional reaction centers. The seasonal relationship between kNPQs and qLs showed an annual cycle with a high level of functional centers (qLs) and low values of kNPQs in summer, and low qLs and high kNPQs in winter (Fig. 4.7). The transition phase in spring was characterized by a rapid decrease of kNPQs, in a process that has been reported to be regulated by air temperature (Porcar-Castell 2011). On the other hand, the transition of qLs from winter to summer values was slower and took place later in the season.

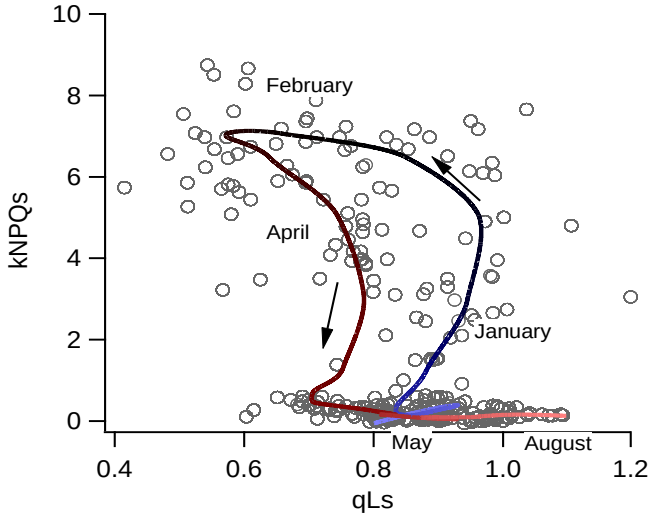

Figure 4.7. Relationship between sustained non-photochemical quenching (kNPQs) and fraction of functional reaction centres (qLs) during one seasonal cycle from 15 August 2008 (blue part of the curve) to 15 August 2009 (red part of curve).

In an attempt to derive an algorithm that could detect changes in sustained non-photochemical quenching from space, the SCOPE model (v1.53) was used to simulate the time course of vegetation optical parameters during one seasonal cycle using the PC11 dataset. Other parameters were obtained from PC11 and the SMEAR II database (e.g., Porcar-Castell 2011), or estimated from consistency analyses (performed in Chapter 3).

A high variation of both fluorescence fluxes in the O_2-B (F687) and O_2-A bands (F760) was observed over the course of the year. A fast and high transition in the apparent fluorescence yield was observed during spring, starting in the middle of April and culminating in the middle of May. This change in fluorescence was associated with a change in the fluorescence emission ratio F687/F760: during the same period of time, F687/F760 increased from approximately 2.3 to almost 3.10 (Fig. 4.8). The yearly time course of GPP showed a severe reduction in winter because of the very low light level during that period.

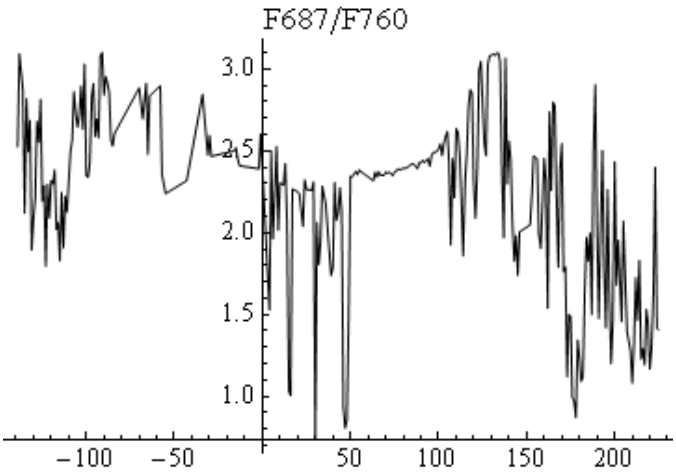

Figure 4.8. Yearly changes in fluorescence emission ratio in a canopy experiencing a severe winter stress, computed with the SCOPE model.

In the time period corresponding to the spring recovery, from the beginning of March to mid-July, and considering clear sky days (as would be the case for FLEX measurements), results showed that F687/F760 correlated fairly well with qLs, ΔGPP and ΔLUE (Table 4.6). This indicates that changes in the fluorescence emission ratio F687/F760 can be regarded as a potential index for detection of changes in GPP induced by sustained NPQ during the spring transition in evergreen needle leaf vegetation. However, these results must be taken with care, as many factors can be involved in the correlation. It should be noted that these results were based solely on a single set of experimental data. Further work, both experimental and theoretical, is needed to account for the different factors that link canopy fluorescence and photosynthetic response to sustained components of NPQ.

Table 4.6. Coefficients of determination between fluorescence parameters (F687, F760, F687/F760) and vegetation parameters computed with SCOPE. The highest correlation is obtained between fluorescence emission ratio F687/F760 and qLs, ΔGPP and ΔLUE.

	kNPQs	qLs	GPP	ΔGPP	LUE	ΔLUE
F687	-0.00548	0.14260	-0.01148	0.41302	-0.00394	0.14758
F760	0.03882	0.07075	0.01986	0.34222	0.01503	0.08083
F687/F760	0.13386	**0.62480**	0.03145	**0.65558**	-0.01994	**0.48572**

To summarize, it was was found that different stress situations – temperature stress, water stress, nitrogen deficiency – have different impacts on the two emission peaks of fluorescence. A stress discrimination using characterization of SIF in the two fluorescence bands might be feasible, although the limited amount of available data prevented assessment of error margins.

In the second part, where leaf level quenching analysis was up-scaled to infer fluorescence annual pattern of canopy fluorescence and reflectance using the SCOPE model, it was shown that fluorescence emission ratio F687/F760 could detect photosynthetic impairment that occurs during the cold season, and which is characterized by sustained quenching mechanisms.

4.6 Strategies integration and development of a prototype algorithm

The objective of this component was to consolidate results from Sections 4.2 to 4.4 of this chapter and Sections 5.2 to 5.3 of the following Chapter 5 dealing with stress effects, for the purpose of deriving one or more relatively simple prototype algorithms for: (i) photosynthetic products retrieval, and (ii) stress indices. Such algorithms would be available for further testing following the PS Study and as candidate functions or indices for use with FLEX.

4.6.1 Prototype algorithm for photosynthesis retrieval

In this study, three different algorithms for photosynthesis retrieval were assessed:

- model inversion through cost function minimization (CFM) (Section 4.2.1);
- statistical modelling using Gaussian processes regression (GPR) (Section 4.2.2);
- statistical modelling using polynomial and rational functions (PRF) (Section 4.3).

Table 4.7 summarizes the comparative analysis of these different retrieval approaches. They proved to be able to retrieve canopy photosynthesis (NPC), which was simulated with the SCOPE v1.53 model, using only optical data, and eventually biophysical parameters that can be retrieved from optical data. At the same time, they showed that both red and far-red fluorescence peaks were needed for the retrieval.

Cost function minimization, in its current state, can retrieve photosynthesis directly from TOA radiances. However, its performance was not better than the two statistical algorithms (GPR and PRF), and it has been proven to be operational only on a limited database built around a single central standard point. Therefore, at this time, we propose to focus the algorithm development on statistical algorithms.

The two statistical approaches GPR and PRF gave highly accurate results for retrieval of canopy photosynthesis in the case of C3 plants, with a high coefficient of determination (≥ 0.95) and a low RMSE (≤ 5 μmoles m^{-2} s^{-1}), although PRF makes use of more simple mathematical functions. With C4 plants, GPR was superior. These results, obtained with different methods and from slightly different input data (fluorescence plus biophysical parameters *vs* fluorescence plus a set of reflectance indices), gave a high confidence in the possibility of photosynthesis retrieval from remote sensing data, including fluorescence. At this time, there is no information on their

performance in the case of stress. Also, algorithms were tested with the same model as the one that generated the training database, which is a drawback.

Therefore, we recommend the further development of the prototype algorithm:

- to evaluate GPR and PRF simultaneously on the same database, with different case studies, including C3 and C4, all well as various values of stressfactor, kNPQs and qLs for stress simulations;
- to test the robustness of the algorithm by adding noise or uncertainties to input data, by using different model formulations between training and test databases, and by using experimental data.

4.6.2 Indices-based algorithms

Three types of stress – high temperature, water and nitrogen deficiency – were studied in the meta-analysis carried out in Section 5.3. Results from that analysis can serve as a preliminary basis for a strategy that aims to develop health or stress indicators with fluorescence data.

Many different experimental, instrumental or measurement conditions were encountered in the meta-analysis. Under such circumstances it is advantageous to normalize fluorescence values in some way. In this case, fluorescence under stress was compared to controls. The different types of stress might then be characterized by different regions of a bi-dimensional fluorescence parameter space, when fluorescence is expressed relative to the control situation.

Once normalized, red and far-red fluorescence define a point in a bi-dimensional space with coordinates (FR/FR_C, FFR/FFR_C; where FR is the red fluorescence peak, FFR is the far-red fluorescence peak, and c is the control). Starting from the control, stress induction defines a direction that is characteristic of the type of stress, namely temperature (T), water stress (W), or nitrogen deficiency (N) (Figure 4.9).

It is then possible to define two types of fluorescence indicators (FI):

- the stress intensity index is defined as the distance between the point with coordinates (FR/FR_C, FFR/FFR_C) and the control having coordinates (1,1)

- the stress type index is defined by three numbers related to the angles (e.g. the cosine of the angle) between the (C,X) line (where C is the position of control and X the position of the measured point with coordinates (FR/FR_C, FFR/FFR_C)).

In this approach, it was implicitly assumed that the stress develops from the control following a straight line on average.

Table 4.7. Comparative analysis of the retrieval algorithms for Net Photosynthesis of Canopy (NPC) assessment. Algorithm performances for retrieval of net photosynthesis of canopy (NPC) are given in terms of coefficient of determination (R^2), root mean squared error (RMSE) and RMSE normalized to the total variation range of NPC (NRMSE).

Algorithm	Cost function minimization (CFM)	Gaussian processes regression (GPR)	Polynomials and rational functions (PRF)
Database			
Number of samples	31	1967	1296
Sampling method	One at a time around a standard case	Tiled sampling	Tiled sampling
Training/test database	n.a.	70/30	50/50
Varied parameters	Cab, Cw, Cdm, Cs, Vcmo, m, LAI, LIDFa, LIDFb	Cab, Cw, Cdm, LAI, Vcmo, m, Rdparam	Cab, LAI, Vcmo, m, LIDF, SZA
C metabolism	C3, C4 (one case)	C3	C3, C4
Fixed core driving parameters	beta, kNPQs, qLs, stressfactor, Rin	beta, kNPQs, qLs, stressfactor, Rin,Ta	qLs, kNPQs, stressfactor, Rin, Ta
Retrieval			
Input variables	TOA radiances from all FLORIS, OLCI and SLSTR bands	- Full F broadband spectrum - Option: Cab, LAI, fAPAR	F687, F760, NDVI, MCARI2, MTCI
Retrieved variables	LAI, Cab, Cs, Cw, Cdm, N, LIDFa, LIDFb, FI, FII, Vcmo NPC is computed from the retrieved model parameters	NPC	NPC, LUE, APARChl
Errors on NPC for best model in the category			
MD12 - C3			
R^2	0.81	0.95	0.99
RMSE (μmoles m^{-2} s^{-1})	2.5	4.8	1.94
NRMSE	12 %	5.6 %	2.8 %
MD12 - C4			
R^2	failed	0.99	0.85
RMSE (μmoles m^{-2} s^{-1})	failed	1.95	8.29
NRMSE	failed	2.9 %	11.4 %

The mathematical formulation of these indices can be given as:

- **Stress intensity**, or **Stress Intensity Fluorescence Index (SIFI)**:

$$SIFI = \sqrt{\left(\frac{FR}{FR_C} - 1\right)^2 + \left(\frac{FFR}{FFR_C} - 1\right)^2} \tag{4.2}$$

Stress type index is expressed as the cosine of the angle between the direction of the measured point, starting from control, and the direction of the stress.

It is then possible to define the **Temperature Stress Fluorescence Index (TSFI)**, as:

$$TSFI = \frac{\left(\frac{FR}{FR_C} - 1\right)\left(T_{FR} - 1\right) + \left(\frac{FFR}{FFR_C} - 1\right)\left(T_{FFR} - 1\right)}{\sqrt{\left(\frac{FR}{FR_C} - 1\right)^2 + \left(\frac{FFR}{FFR_C} - 1\right)^2}\sqrt{\left(T_{FR} - 1\right)^2 + \left(T_{FFR} - 1\right)^2}} = \frac{1.41 - 0.74\frac{FR}{FR_C} - 0.67\frac{FFR}{FFR_C}}{\sqrt{\left(\frac{FR}{FR_C} - 1\right)^2 + \left(\frac{FFR}{FFR_C} - 1\right)^2}} \tag{4.3}$$

by taking the coordinates of the T point from the results of the meta-analysis (see Figure 4.9).

Similarly, we can define:

- the **Water Stress Fluorescence Index (WSFI)**:

$$WSFI = \frac{0.885 + 0.109\frac{FR}{FR_C} - 0.994\frac{FFR}{FFR_C}}{\sqrt{\left(\frac{FR}{FR_C} - 1\right)^2 + \left(\frac{FFR}{FFR_C} - 1\right)^2}} \tag{4.4}$$

- and the **Nitrogen Stress Fluorescence Index (NSFI)**:

$$NSFI = \frac{-0.754 + 0.975\frac{FR}{FR_C} - 0.222\frac{FFR}{FFR_C}}{\sqrt{\left(\frac{FR}{FR_C} - 1\right)^2 + \left(\frac{FFR}{FFR_C} - 1\right)^2}} \tag{4.5}$$

(Preliminary indications are that simplified versions of the indices may also be possible, and that aspect needs to be investigated more fully.)

It should be stated that TSFI, WSFI and NSFI do not measure the intensity of the stress, but are rather quality factors that indicate the closest type of stress among the three ones that have been characterized.

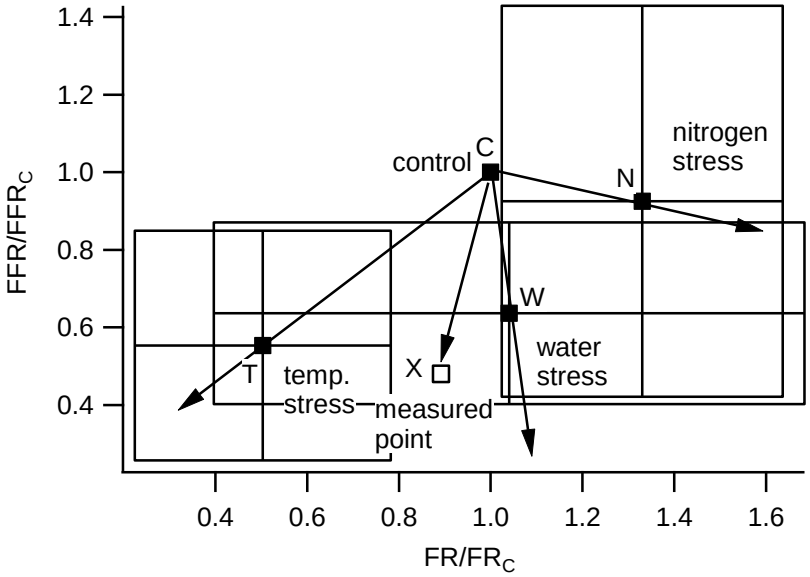

Figure 4.9. Representation of vegetation stresses in the parameter space defined by red (FR) and far-red (FFR) fluorescence radiances normalized by control values. Positions of the stress situations T, W and N are the mean fluorescence values deduced from the basic statistics analysis of Section 5.3 for high temperature, water and nitrogen stresses, respectively. Rectangles around the mean positions denote standard deviations.

4.7 Conclusions

A comparative analysis of algorithms was performed, with the aim to eventually retrieve photosynthetic products from fluorescence data acquired with the FLORIS instrument and from complementary data provided by Sentinel 3.

Results from three retrieval algorithms were analyzed and compared. The two statistical algorithms – Gaussian processes regression (or GPR) and polynomial & rational functions fitting (or PRF) – gave highly accurate results for retrieval of canopy photosynthesis in the case of C3 plants, acceptable results with C4 plants using PRF, and excellent results with C4 using GPR.

Retrieval by cost function minimization was not superior to the two statistical methods, although the possibility to retrieve canopy parameters directly from space seems attractive.

On the basis of the retrieval results, no strong evidence can be brought forward to select between GPR and PRF methods. Both warrant further investigation to test the robustness of the retrievals, preferably with real data such as that recently made available from the *HyPlant* airborne sensor.

Besides retrieval algorithms, several novel fluorescence-based stress indicators have been proposed to assess stress intensity as well as stress quality in relation with water, temperature, and nitrogen stress. Further investigations and evaluations of these new stress indicators should be undertaken. These indicators are in addition to simple indices already shown to be effective for identification of stress, most notably the ratio of red to far-red fluorescence (reviewed in more detail in Chapter 5).

5. Fluorescence as an indicator of vegetation health and stress resilience

5.1 Introduction

The main goals of this task were to: (i) evaluate the usage of steady-state F as an indicator of a few important stresses, namely, water deficit, temperature extremes, and nitrogen deficiency; and (ii) to recommend how SIF data from the FLEX mission could be utilized in the detection of stress effects. The major activities were to develop:

- a database of publications dealing with stress responses of steady-state F to the three kinds of stress;
- an analysis of the literature to determine the potential for use of the novel F signal;
- an evaluation of knowledge gaps;
- a conceptual framework for FLEX operations to use SIF in stress detection.

There are many stresses that can inflict a cascade of structural, functional, and performance effects in vegetation. Photosynthesis is the most sensitive physiological process in plants, a target for direct and indirect effects of stress. Adverse impacts to photosynthesis can arise from damage to critical cell or organelle membranes, denaturation of photosynthetic proteins or enzymes, impaired chloroplast function, destruction of chlorophyll or other pigments, blocked uptake or transport of water or other nutrients, buildup of toxic substances, and damage to protective mechanisms (Hasanuzzaman *et al.* 2013; Nishiyama *et al.* 2011; Takahashi & Badger 2011; Treshow & Anderson 1989; Levitt 1980). These effects often are discernible from steady-state chlorophyll fluorescence.

If CF can provide an early warning of physiological strain, it might be possible to trigger the execution of remedial tactics before visible (possibly irreversible) damage develops. This capability would be especially useful with perennial food systems such as fruit orchards and other long-term plantations. How frequently these measurements would need to be conducted will depend on the anticipated rate of change in physiological condition and the objectives of management in a specific situation (i.e., how valuable the crop is, and how critical the intervention would be).

It must also be recognized, however, that whilst SIF may be diagnostic for the existence of stress, it usually would not be expected on its own diagnose the specific stress (e.g., drought, salinity, pest etc.), given that different stresses can produce a similar result. Hence, there will be a need for a strong foundation of ancillary information to provide the full context for such understanding – this is the way that fluorescence has always been used most effectively.

5.2 Database of stress responses

As a first step, a literature review was conducted to identify papers that addressed the quantitative link between stress and steady-state fluorescence, including SIF. From this analysis it was then possible to identify not only general patterns of stress-related F signals but proceed to the identification of major knowledge gaps.

Literature from various platforms (Web of Science, EBSCO, GoogleScholar) was collected on the topics of passive and active CF signals recorded under conditions of water stress, temperature stress, and nitrogen stress.

Relevant information on fluorescence retrieval and experimental procedures were extracted from this selection of literature and compiled into a database[1] (Literature on Fluorescence and Stress; LiFS), which is accessible online (http://www.fz-juelich.de/ibg/ibg-2/lifs) (Figure 5.1). The database is currently hosted at the Institute of Bio- and Geosciences at Forschungszentrum Jülich (which is one of the PS Study partners). It is a web platform that allows any of the papers to be downloaded as PDF documents.

The database also contains an Excel spreadsheet summarizing for each reference the key attributes of the study according to plant species, plant functional type (herb, grass, broadleaf deciduous tree/shrub, broadleaf evergreen tree/shrub, needleleaf evergreen tree), plant age, scale (cell, leaf, plant, canopy), stress factor, stress intensity, period of stress, indicators of stress, time/timing of measurements, number of repetitions, method(s) used, CF-signal type (active, passive), CF spectrum or lines, key variables addressed (CF and other physiological variables), key message(s), relevant figure(s) & table(s), units of CF measurement, irradiance, growth conditions, maximum PAR, maximum/mean temperature, relative humidity, CO_2 concentration, specific details from figures, and various derived CF quantities & ratios.

Altogether, over 120 experimental case studies were considered, of which 65 papers pertained to the stresses of interest. Major attributes of the collection are summarized in Table 5.1.

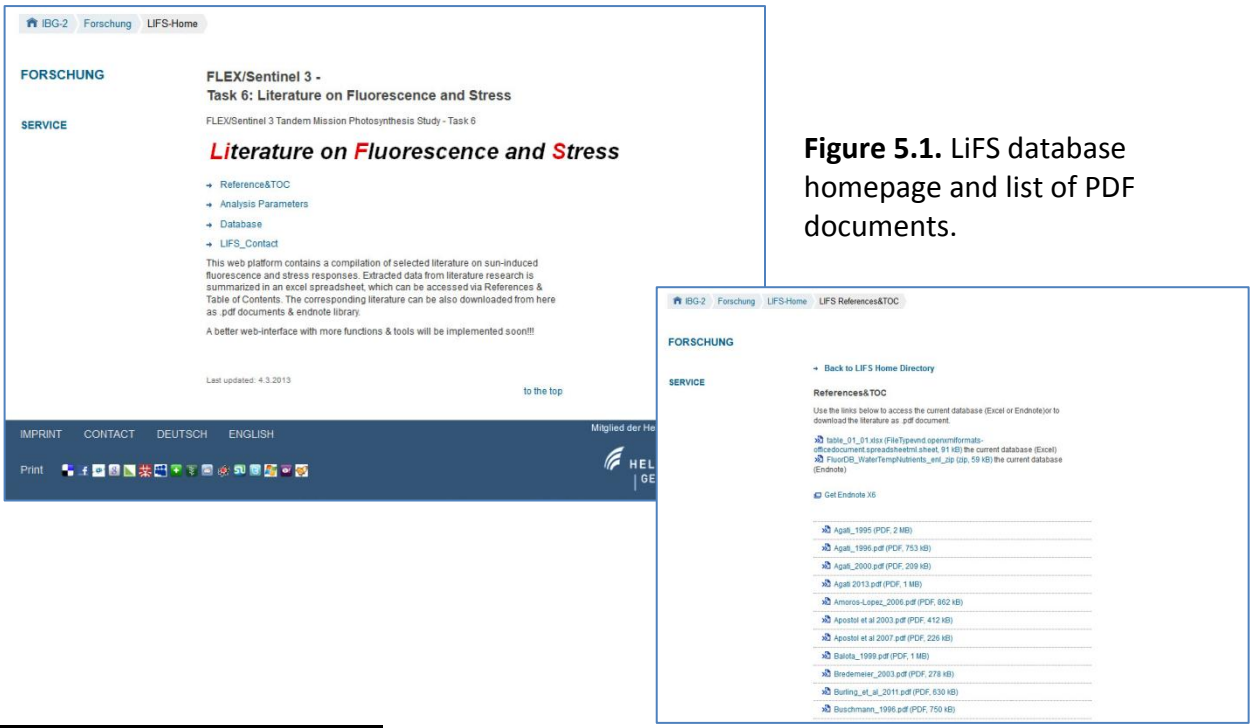

Figure 5.1. LiFS database homepage and list of PDF documents.

[1] Username: ibg-2_lifs
Password: sentinel3

5.3 Analysis of the literature

The analysis included data obtained using passive and/or active techniques of CF acquisition to produce the steady-state CF (Table 5.1). Passive techniques rely solely on ambient sunlight, whereas active instruments use artificial light to stimulate the F emission or to deliver a pulsed signal that allows steady-state CF to be discriminated from extraneous outdoor light. It is not yet certain as to how truly comparable the CF signal derived from these two approaches might be, and this is one of the uncertainties that can be at least partially answered in this type of review.

The value of this kind of evaluation is that it can help to choose useful indicators of stress for remote sensing and appropriate ancillary technologies (passive or active) for use during the FLEX mission to help validate and interpret fluorescence retrievals at leaf or canopy levels.

The steady-state CF features most often reported – hence the main focus of this analysis – are the red & far-red spectral peak amplitudes and the ratio of the red to far-red F peaks.

The potential of the fluorescence signal was assessed by evaluating the data in the papers in two ways: (i) simple evaluation of the data averages and medians; and (ii) a random-effects meta-analysis. Since the latter method was considered to be a more robust statistical approach it will be emphasized here. Results of the random-effects meta-analysis reported here have also been submitted to the journal *Remote Sensing of Environment* (Ač *et al.* 2014).

Table 5.1. Basic characteristics of reviewed papers dealing with remote application of passive or active measurements of steady-state CF, associated to environmental stresses. Note: numbers not in brackets indicate total number of papers that include biotic stresses.

Number of species 50			
Number of cases (papers) 124 (69)			
Stress factors			
Water	Temperature	Nutrients	Others
49 (34)	16 (10)	52 (21)	7 (4)
Scale			
Leaf		Canopy	
97		28	
Method used			
Passive		Active	
35		106	
Environment			
Indoor		Outdoor	
59		75	
Plant functional types			
Grass+herb	Trees+shrub evergreen	Trees+shrub deciduous	
76	19	23	

5.3.1 Statistical approach

Since the published trials were performed independently, differences in methodological approaches (e.g., different measurement devices and protocols) tend to have a non-systematic impact on final results. To standardize the fluorescence measurements expressed often in different physical units or even in relative scale, the standardized mean difference (*d*) between treated (stressed) and control (unstressed) experiments was computed as a summary statistic for the meta-analysis. It was computed as:

$$d = \frac{\overline{F_{s1}} - \overline{F_{s2}}}{\sqrt{\frac{s_1^2(n_1 - 1) + s_2^2(n_2 - 1)}{n_1 + n_2 - 2}}} \qquad (5.1)$$

where $\overline{F_{s1}}$ is the mean steady-state chlorophyll fluorescence (F_s or SIF) of n_1 observations of stressed plants with the standard deviation σ_1^2, and $\overline{F_{s2}}$ is a mean steady-state chlorophyll fluorescence of n_2 observations of unstressed (control) plants with the standard deviation σ_2^2.

The random-effects model used here is one of two popular statistical models for meta-analysis (the other being the fixed-effect model). The random-effects approach is suited to situations where different approaches are used. A detailed description and also logical differences between fixed-effect and random-effects meta-analysis models can be found in Borenstein *et al.* (2009).

Not all collected and reviewed scientific papers provided information about the standard deviation of the steady-state CF measurements as required for the statistical meta-analysis, but even studies publishing just mean steady-state values contain a valuable indication about stress effects. Therefore, an additional basic analysis was performed without taking into account variability within and between experiments. These statistical outputs are considered as an additional and supportive measure of stress indication for cases where the comprehensive meta-analysis cannot be properly applied due to a small number of input studies.

While examining the input studies we encountered different measurement units and detection methods for fluorescence. Differences were also found in the spectral position and width of measured spectral bands, in excitation wavelengths, and in CF extraction methods. To perform a simple comparison among all studies while accounting for the considerable differences due to varying units and experimental set-ups, the extracted F_S and SIF values were transformed into a stress to control (S/C) ratio. If the S/C ratio is lower than one, then the stress factor is causing a decrease in CF, while a ratio higher than one indicates an CF increase due to the stress exposure. The ratio equal (or close) to one indicates no change in steady-state CF due to stress. To provide a consistent comparison, the ratio of red to far-red CF was transformed into the S/C ratio too. Finally, revealing the non-Gaussian distribution of the collected data, a non-parametric statistical Mann-Whitney U-test (Mann & Whitney 1947) was applied. It is important to note that the S/C steady-state CF ratio does not account for the size of experimental datasets and their variability, nor for a varying number of input studies clustered

into the leaf-active, leaf-passive, canopy-active, and canopy-passive groups. Therefore, S/C results should be considered only as an interpretive support of lesser confidence for cases where the random-effects meta-analysis encountered too small a number of input studies (i.e., only two or three studies).

5.3.2 Results

Results of the random-effects meta-analysis indicated that:

1. Water stress was, in general, associated with a decline in steady-state red and far-red fluorescence signal intensity measured at the leaf and canopy level;
2. Chilling, for which only studies with active measurements at the leaf level were available, significantly increased the red and far-red fluorescence;
3. Heat stress produced a less convincing decrease in red and far-red fluorescence, notably in canopies measured passively;
4. The clearest indicator of temperature stress was the ratio of red to far-red fluorescence, which declined significantly and consistently, even when combining chilling and heat stress results;
5. The ratio of red to far-red fluorescence was also the clearest indicator of nitrogen deficiency, increasing with deficiency upon analysis of 36 studies.

These findings indicate that acquisition of both red and far-red chlorophyll fluorescence signals with future airborne or spaceborne sensors will be beneficial for timely detection of plant stress events. In addition to the value of the individual bands, the stress indicating character of the red to far-red ratio suggests that the red and far-red fluorescence measurements are complementary rather than redundant and should, therefore, be collected simultaneously.

A decline in steady-state CF under water stress might be attributed at least in part to photoprotective processes (e.g., non-photochemical quenching) that are triggered under conditions of water stress and which tend to lower fluorescence (Flexas *et al.* 2002; Medrano *et al.* 2002).

Temperature stress events can affect various plant physiological metrics such as chlorophyll content, chloroplast thylakoid membrane integrity, functioning of Photosystems I and II, stimulation of protective dissipative processes, and overall photosynthetic rates – with complex effects on steady-state CF (Hasanuzzaman *et al.* 2013; Larcher 1994).

Nitrogen insufficiency can produce myriad physiological dysfunctions because of the many vital roles of this macronutrient, and it is the most common limitation to growth after water stress. Nitrogen is an important constituent of chlorophyll, structural proteins, enzymes (including the main photosynthetic enzyme Rubisco), nucleotides, plant hormones, and vitamins (Kozlowski & Pallardy 1997; Marschner 1986). Deficiency frequently produces reduction in chlorophyll content as a result of reduced manufacture and increased breakdown. Below certain chlorophyll thresholds, there is less reabsorption of emitted fluorescence within foliar tissues, thus higher CF amplitudes – especially in the red band – detected by sensors. This explains why

N deficiency often can produce an increase in the red to far-red CF ratio. However, because the roles of N are varied and complex, sometimes it is difficult to discern a clear relationship between leaf N content and chlorophyll content (Homolová *et al.* 2013).

Given the intricacies of temperature and nitrogen pressures on vegetation, it is indeed encouraging that the ratio of red to far-red fluorescence appears very promising as an indicator.

5.3.3 Knowledge gaps

An analysis of information gaps was conducted for the three categories of stress (water deficit, temperature extremes, nitrogen insufficiency) that were considered. First-order priorities across all three stresses were:

- temporal resolution required for reliable detectability by SIF;
- influence of canopy structural complexity on SIF;
- detectability across plant functional types;
- influence of environmental spatial heterogeneity;
- impact of combined stressors on SIF.

Other gaps are of first-order priority for at least one of the three stresses, or of second-order priority for at least two stresses:

- consistency of red and far-red SIF changes for all three stresses;
- consistency of active and passive data for the three stresses, especially temperature extremes and N-deficiency;
- consistency of SIF changes at leaf and canopy levels for the three stresses, especially temperature extremes and N-deficiency;
- influence of chlorophyll content for the three stresses, especially N-deficiency;
- effects of nitrogen deficiency – over the short and long term.

To help address the information needs with respect to water deficit, temperature stress, and nitrogen deficiency, the gap analysis suggests that future work should seek to:

- better link active to passive F features using systematically coordinated experiments;
- utilize both natural & managed vegetation systems, and test different compositional complexities with incorporation of manipulative treatments in the simpler systems;
- utilize a global network of long-term research sites;
- explore tolerances and temporal dynamics (e.g., seasonal) for stress development among species;
- decipher ecosystem-specific spatial and temporal aspects;
- investigate measurement errors and interferences;
- standardize experiment protocols and data processing;
- define sensors that can be used in the various spatial domains.

In addition to these needs, we can add other priorities that are generally recognized as being important in stress detection programs (Niinemets 2010; Mohammed *et al.* 2003):

- availability of early or pre-visual indicators of strain, which helps to pinpoint sites for in-depth ground or airborne assessments and possible intervention to mitigate damage;
- discrimination between acclimatory versus damaging strain, the former typically a positive response associated with stress resistance, resilience, and recovery.

These aspects, therefore, were priorities for the conceptual framework (Section 5.7).

5.4 Food crops and stress effects – SIF applications

A significant potential application of space-based SIF would be to provide indicators of natural and anthropogenic stresses on global food crops. Methods and tools useful for helping to ensure the safety, quality, and productivity of plant food species are needed at spatial scales relevant to strategic programs of monitoring, management, and enhancement. In particular, the capacity to assess the development and intensity of photosynthetic strain caused by biotic and abiotic stresses would provide a powerful analytical tool to support decisions and mitigation efforts. Especially helpful would be methods of early detection of stress effects, which could increase the window of opportunity for remedial actions or adjustments in strategic planning.

Supplementary to the activity on stress evaluations conducted in the preceding sections, we have included here an introduction to the effects of a broader range of stresses on steady-state or solar-induced fluorescence in food crop species.

Table 5.2 summarizes published findings of stress effects on food crops. It is evident that stress effects are manifested in a suite of steady-state fluorescence features that include both red & far-red emission signals and the full spectral emission profile, the latter allowing calculation of fluorescence attributes such as the spectral position of the peaks and the area under the emission curve. There is a richness of information from the full profile that facilitates inspection of stress effects. Even from this preliminary consideration of findings pertinent to food security issues, it was clear that usage of SIF in stress detection will require the information content of the entire SIF emission signature.

Aspects of food security which could be amenable to SIF application include:

- Early previsual identification of stress effects in food vegetation;
- Tracking the recovery of plant photosynthetic function following catastrophic events;
- Delimitation of compromised agricultural sites from biotic and abiotic stresses;
- Identification of optimal growing & management strategies for food crops;
- Performance appraisal of vegetation bred for stress resistance.

Where there is a reduction in photosynthetic competence (which can include reduced photosynthetic rate), it is not uncommon to see a decrease in the amplitude of steady-state fluorescence in the red or far-red emission bands, such as occurs following the imposition of

water stress (Section 5.3.2; Ač *et al.* 2014). Or under certain nutrient deficiencies, e.g., nitrogen, there can be an increase or decrease of SIF, depending on the particular circumstances and degree of advancement of the stress. Losses of chlorophyll may be manifested as an increase in the amplitude of the red emission as discussed earlier, owing to a tendency for measurably lowered reabsorption of emitted fluorescence when chlorophyll declines beyond a certain level (Buschmann & Lichtenthaler 1998). Changes in chlorophyll may also be manifested as shifts in the wavelength position of peak emissions. It is therefore possible that by analyzing fluorescence responses over time that a progression of change could be followed to identify early and advancing signs of photosynthetic stress. The benefit of an early warning system is that it can be used to trigger the execution of remedial tactics to mitigate against catastrophic losses in productivity. This capability could be especially useful with perennial staple crops, which increasingly are the focus of international strategies for food security (Batello *et al.* 2014).

SIF offers a tool for tracking plant responses to catastrophic events, including both human-induced and natural disasters. Events such as volcanic eruptions, ice storms, pollutant spikes, fast-spreading pest outbreaks, fire damage, industrial plant accidents, and other unanticipated pressures confront the Earth's vegetation with toxins, light-blocking substances, physical assault to tissues, and depletion of site quality. Field studies of chlorophyll fluorescence have proven the technique to be not only a sensitive barometer of such effects but also a means to track the presence and depth of recovery (Zarco-Tejada *et al.* 2012; Methy *et al.* 1994; Theisen *et al.* 1994). Such information could help to prioritize sites for intensive intervention and to forecast future inventories and shortages in vulnerable regions of the world.

Whether as a result of a catastrophic event or due to gradual intensification of sub-optimal growing conditions, it is important to identify compromised agricultural or horticultural sites that may require ameliorative or rehabilitative action. The capacity to identify physiological strain in lands currently under (or being considered for) production improves the feasibility and cost-effectiveness of planning exercises. For example, grasslands being considered for pasture or conversion to croplands could harbour nutrient shortages or toxicities that alter SIF emission amplitude. Responsiveness of grassland steady-state fluorescence has already been documented (Ač *et al.* 2012; Fournier *et al.* 2012).

In situations where there is an apparent locus of physiological assault upon vegetation, knowledge of the actual spatial breadth and distribution of the problem is often lacking. An example would be an industrial plant that emits damaging chemicals into the atmosphere which reaches nearby and possibly more distant vegetation. A physiologically-based indicator such as SIF would be helpful in delineating the spatial scale of the impacts to existing vegetation in the vicinity, and potentially in generating a strain-gradient from the source outward. Again, this information could serve to plan current and future land usage and manage existing plantings. In a related way, it has been shown that fluorescence-linked reflectance indices in the far-red bands reveal information about sites contaminated with substances such as the explosive TNT, which persists as residuals of past geopolitical conflicts or industrial activities (Naumann *et al.* 2010).

Identification of effective production strategies is a key priority of all food producing regions. Optimization of yields at affordable cost and with minimal damage to soil and water resources is one of the great challenges of today's food production systems. In North America, for example, the balanced use of fertilizer – notably nitrogen – has been a worry for farmers who have ready access to fertilizers but who face criticisms over excessive inputs to groundwater sources and consequent overloading of drinking water, wetlands, and other water bodies. Groups such as NASA's Goddard research teams have been using remotely sensed chlorophyll fluorescence as a signature of nitrogen fertilizer effects in crops, e.g., maize (Corp *et al.* 2009, 2006; Middleton *et al.* 2008).

Finally, efforts continue around the globe with respect to crop improvement – whether through conventional breeding, biotechnological genetic enhancement, or screening of naturally stress-resistant lines. These efforts have been underway for many decades with all of the major crop species of the world, including wetland crops like rice. Fluorescence is being used successfully to identify performance advantages (Burling *et al.* 2011a; Ennajeh *et al.* 2009). Major stresses currently being targeted for improved resistance include drought, heat, salinity, and pests – all of which have been shown to be amenable to fluorescence analysis, including passively acquired steady-state fluorescence.

Given its potential utility, retrievals of the full fluorescence emission could have tangible benefits in supporting food security issues through identification of stress-induced strain in food crop species. It is recommended, therefore, that this subject receive further comprehensive investigation in future study activities.

Table 5.2. Applications of steady-state chlorophyll fluorescence in food plants. Note: Fs denotes steady-state fluorescence that is a combination of red and far-red emission bands.

Stress or aspect	Fluorescence feature affected	Reference
acid rain	F690, F736, F740	Krajicek & Vrbova 1994
cadmium toxicity	F685, F730, F735, ratio, shifts in peak position	Mishra & Gopal 2005
cadmium toxicity	F690/F735 ratio	Cherif *et al.* 2011
cadmium toxicity	F685, F735, F685/F735 ratio	Da Silva *et al.* 2012
cadmium, copper toxicity	F690, F710, F740, F690/F740 ratio, peak position (blue or red shifts)	Kancheva *et al.* 2007
chilling	F685/F735, F685/F730 ratio	Agati *et al.* 2000, 1996, 1995
chilling	F690/F730 ratio	Di Paola *et al.* 1992
chilling	F690/F730 ratio	Lipucci di Paola *et al.* 1992
chlorosis	F685/F730 ratio	Agati *et al.* 1996
chlorosis	F690, F735, F690/F735 ratio	Babani *et al.* 1996
gamma irradiation, pollution	F690, F735, F690/F735 ratio	Jovanic & Dramicanin 2003
heavy metals	F685, F735	Gouveia-Neto *et al.* 2012
herbicide damage	F690, F760	Carter *et al.* 2004
herbicide damage	F688, F760, F688/F760 ratio	Liu *et al.* 2013
herbicide damage	F687, F760	Meroni & Colombo 2006
herbicide damage	Fs, F760	Moya *et al.* 2004
high light intensity	Fs	Weis & Berry 1987
leaf rust disease	F687	Burling *et al.* 2011a
leaf rust disease, powdery mildew, nitrogen deficiency	F689/F737 ratio	Burling *et al.* 2011b
mutagenic damage	F685/F735 ratio, area under spectral curve, peak positions	Srivastava & Pandey 2012
nickel stress	F680/F730 ratio	Gopal *et al.* 2002
nitrogen deficiency	F690/F730 ratio	Bredemeier & Schmidhalter 2003
nitrogen deficiency	F685, F685/F740 ratio	Campbell *et al.* 2008
nitrogen deficiency	F690, F760, F690/F760 ratio	Kebabian *et al.* 1999
nitrogen deficiency, powdery mildew, leaf rust	F690 & F730 heterogeneity (std deviation)	Kuckenberg *et al.* 2009
nitrogen deficiency, water deficit	Fs	Suarez & Berni 2012, Suarez *et al.* 2008
nitrogen status	F680, F688, F740, F760	Middleton *et al.* 2008
nitrogen status	various red to far-red ratios	Theisen 2002
nitrogen status	F690/F730 ratio	Thoren & Schmidhalter 2009
nitrogen status	e.g. F690/F740 ratio	Tremblay *et al.* 2012
nitrogen, chlorophyll	various red & far-red ratios	Corp *et al.* 2006, 2003
nuclear (ionizing) radiation	F740, F690/F740 ratio, area under emission curve	Jovanic *et al.* 2012
nutrient deficiency	peak positions, red & far-red bandwidth, F690/F730 ratio	Subhash & Mohanan 1997
nutrient deficiency, ultraviolet	F690/F730 ratio, peak positions, area under emission curve	Subhash 1995
physical damage	F680	DeEll & Toivonen 2003

potassium deficiency	F690, F740	Chappelle *et al.* 1984
potassium deficiency	F690/F735 ratio	Diomande *et al.* 1998
stripe rust disease	F688, F760, F688/F760 ratio	Zhang *et al.* 2007
water deficit	Fs	Araus *et al.* 2010
water deficit	F685, F760	Daumard *et al.* 2010
water deficit	Fs	Ennajeh *et al.* 2009
water deficit	Fs	Gu *et al.* 2012a,b
water deficit	various ratios	Leufen *et al.* 2013
water deficit	Fs	Medrano *et al.* 2002
water deficit	F760	Perez-Priego *et al.* 2005
water deficit	Fs, F760	Rascher *et al.* 2009
water deficit	F747, F762, F780	Zarco-Tejada *et al.* 2012
water deficit	F757, F760	Zarco-Tejada *et al.* 2009
water deficit (irrigation)	Fs, various far-red peaks	Zarco-Tejada *et al.* 2013b
water deficit, heat, heavy metals, high light etc.	F685, F735, F685/F735 ratio	Gouveia-Neto *et al.* 2011
water deficit, nitrogen deficiency	F760	Panigada *et al.* 2010
water deficit, nutrient deficiency	Fs	Flexas *et al.* 2002, 1999
water deficit, nutrient gradients	F763	Zarco-Tejada *et al.* 2013a
water deficit; heat	F690/F735 ratio	Balota & Lichtenthaler 1999

5.5 Photosynthesis modelling – application to stress detection

The Photosynthesis Study has resulted in the development and implementation of a process-based consolidated model linking vegetation fluorescence to photosynthesis at the leaf-to-canopy level. This model includes modules for the biochemical level, an optical module that addresses radiative transfer within the leaf, and a canopy RT model. SCOPE v1.53 and its automated GUI version A-SCOPE v1.53 are the main outputs, with supporting activities including local & global sensitivity analyses, error analysis, and preliminary model validation. Potential complementarities between the model and stress detection are also possible, for example, in the application of the model as a tool in stress detection using a ratio of actual to potential photosynthesis rate as an indicator of vegetation stress; or alternatively, various stress scenarios could be simulated with the model to help formulate expectations from spaceborne platforms. Further, stress detection data could be applicable for parameterization of SCOPE inputs, for example, in setting values and limits for parameters such as the fraction of open reaction centres and/or rate constants for sustained thermal dissipation. These aspects warrant further consideration beyond the current study.

At present, the SCOPE model has certain restrictions that may affect its immediate usage in stress detection. One potential drawback is that it is a one-dimensional vertical model (assumes horizontal homogeneity) and is thus not suited to canopies with significant shadows or soil fractions – such as is often present in agricultural row plantings or open tree canopies. Certain other restrictions of SCOPE (i.e., that it is instantaneous, and is diagnostic rather than

prognostic) should not pose significant issues in view of the anticipated availability of repeated measurements from FLEX, which would build its own history for vegetation scenes for the purpose of tracking the development of strain.

The modelling tasks also included development of a Level-2 prototype algorithm to derive measures of photosynthesis (represented by GPP or other relevant parameters). The objective was to investigate simplified approaches as an adjunct to the multi-parameter full SCOPE model.

We can suggest priorities for future developments and applications of SCOPE and related algorithms in stress detection. These include:

- investigation into the use of the ratio of actual to potential photosynthesis rate as an indicator of photosynthetic strain;
- simulation of stress scenarios with the model;
- adaptation of SCOPE modules to address effects of canopy structure and complexity, i.e., moving beyond the 1-D vertical aspect of the model;
- adaptation of SCOPE as a dynamic vegetation model which could serve more of a prognostic function for stress evaluation;
- further testing & improvement of SCOPE for retrievals in the red band (O_2-B);
- incorporation of additional stress-related features such as PRI, non-photochemical quenching, and improved energy partitioning between PSI and PSII under stress;
- evaluation of the most feasible options for providing SIF-GPP products from FLEX;
- further development of simplified algorithms for retrieval of physiological effects;
- investigation of synergies between FLEX and other sensors for calibration & validation activities, and continued model improvements.

5.6 Limitations & challenges

Aside from sources of error arising from satellite data capture, atmospheric corrections, and retrieval algorithms for SIF, the variety of stresses and their sometimes confounding effects on SIF introduce potential sources of error and variability that must be considered for interpretation of SIF signals. Otherwise, such factors can contribute errors in interpretation and alter the efficacy of applications. Interpretation of SIF data should be undertaken recognizing there are interacting effects of normal photosynthetic adjustments, pigment content & function, actions & interference of various fluorophores, species structure & function, and stresses. Furthermore, it is important to improve our understanding of the interplay of stress with features such as site characteristics, vegetation composition & structure, and diurnal & seasonal patterns of photosynthetic function.

In general, sources of variability and error may be categorized as arising from vegetation factors, environmental factors (including stresses), and instrumental or data processing factors (Figure 5.2). In studies of SIF, clearly it is more practical to control instrumental or data processing methods than vegetation and environmental factors, necessitating the availability of adequate supporting and ground-truthing information to assist investigations.

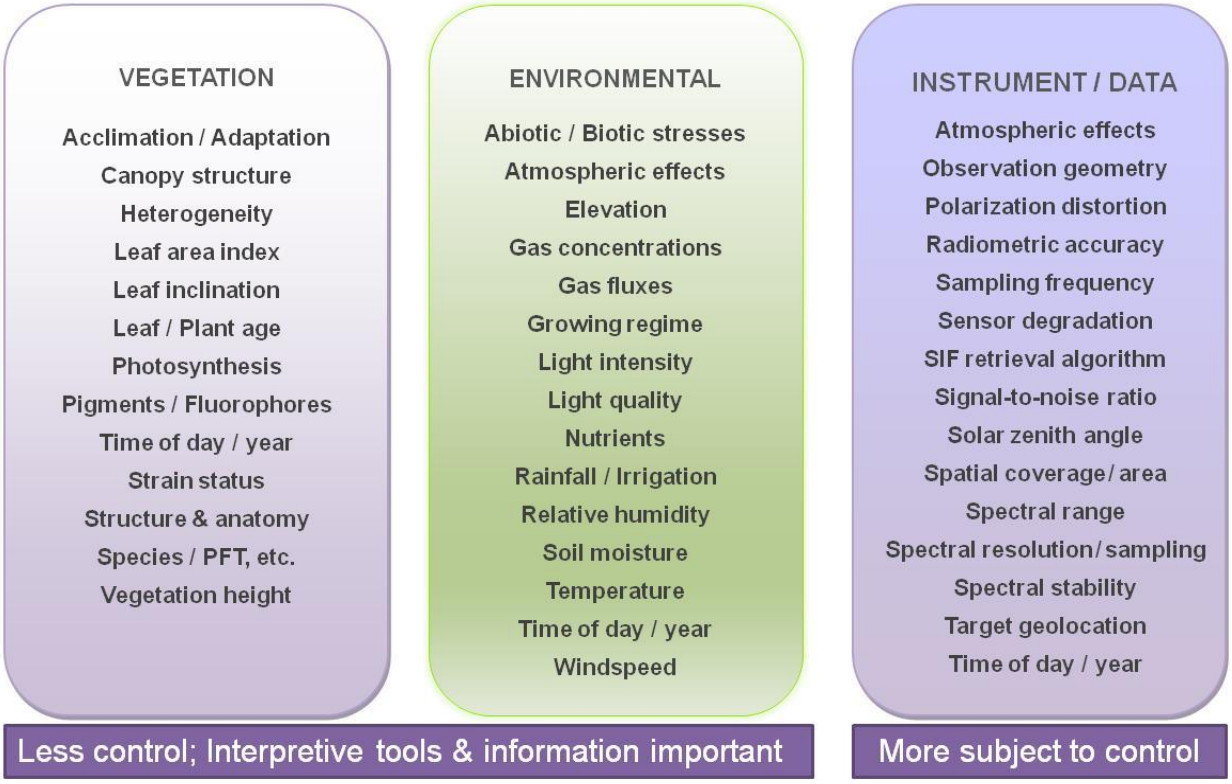

Figure 5.2. Sources of variability and error in SIF measurements and interpretation.

5.7 Conceptual framework

This section advances the discussion of SIF as an indicator of physiological health and strain in terrestrial vegetation by suggesting elements necessary to address knowledge gaps within the context of a conceptual framework for SIF in stress detection. Major components of the framework are:

- identification of overall goal & target applications;
- prioritization of vegetation sites for analysis;
- identification of likely stresses, timeframes, sources of error;
- selection of SIF indicators;
- supporting measures (calibration, validation, interpretation).

In addition, there are considerations with respect to the types of expertise required and overall recommendations for studies and actions in the coming years.

Addressing the types of needs identified in the gap analysis will help to provide the scientific information to set scientific objectives and effective studies for FLEX deployment. To put the different components into perspective, it is helpful to develop a conceptual framework for how SIF could be applied during FLEX deployment. Such a framework is suggested in Figure 5.3. It

then can become evident how experiments fit into the framework leading up to and during FLEX deployment.

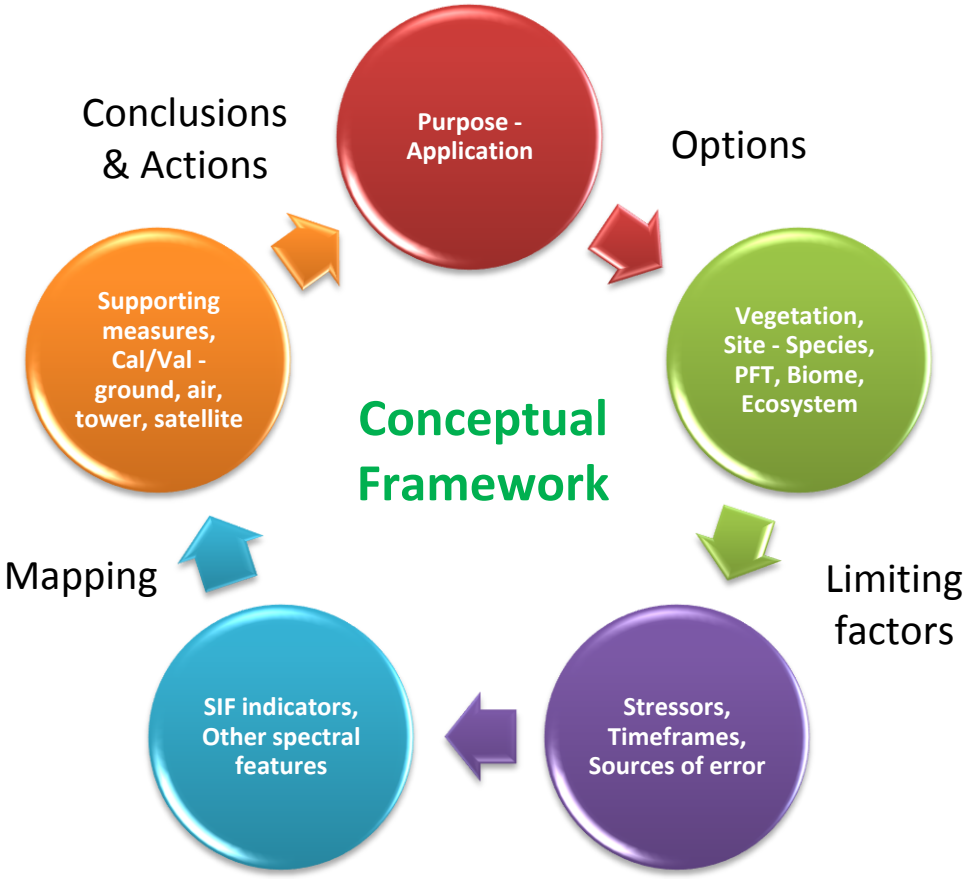

Figure 5.3. Conceptual framework for the use of SIF in stress detection.

5.7.1 Identification of overall goal & target applications

These could include, for example, food or feed production & quality, forest health & productivity, wetland health, condition of ecologically sensitive biomes, reclamation status of priority sites, coastal zone monitoring, or early identification of insect & disease problems. Goals & objectives should be set in consultation with policymakers and resource managers in order to ensure relevance and consistency with management priorities.

Key requirements include:

- identification of user communities & networks – e.g., government agencies at national/regional/local levels, resource managers, applications scientists, research networks, large-scale private users;
- identification of specific goals & objectives for the short, medium, and long term;
- articulation of information flow pathways among FLEX information providers and user communities;
- analysis of available sources of information, historical trends, emerging issues, geopolitical factors;
- identification of key contacts for communication.

5.7.2 Prioritization of vegetation sites for analysis

The type of application will have implications for the choice of spatial dimensions, species types & composition, geographic locations, seasonality of the vegetation targets, and other aspects. For significant natural ecosystems or established artificial populations, there may be permanent or long-term plots for which a substantial history of information already exists and for which a suite of measures is ongoing at various spatial and temporal scales. Given that FLEX will provide spatial resolution of 300 m, the applicability to common management or monitoring landscapes must be evaluated. For example, production farms in Canada average roughly 315 ha[2] in size, which would occupy about 35 pixels of FLEX imagery. In Europe, where average farm size is only 12 ha[3], it would represent < 2 pixels. For forests, Canada has a network of national research forests which serve as living laboratories and which have monitored vegetation composition, silvicultural treatments, forest health, provenance trials, climate change, etc., with long-term data sets going back as far as 1933.[4] Those forests occupy 9,000 to 10,000 hectares, which would translate to 1,000 to 1,111 pixels from FLEX. In Europe, there is an extensive network of long-term forest plots (e.g., Pretzsch *et al.* 2014) of various sizes. However, there is currently no extensive international ground-based network that continuously measures fluorescence (Berry *et al.* 2013).

[2] Statistics Canada, 2011 Census of Agriculture.
[3] European Commission, Agriculture and Rural Development, 2013 data.
[4] Natural Resources Canada.

Key requirements for site prioritization include:

- relevance to the goals & objectives;
- suitability of spatial dimensions (e.g., farm/field, plot, stand, landscape, region);
- decision on the level & functional aspects of the vegetation system (e.g., species, phenological type, plant functional type, landscape, ecosystem, biome);
- compliance with project aims re: amount of canopy homogeneity/heterogeneity, other vegetation factors, and environmental factors;
- accessibility of sites for validation activities;
- availability of supporting data useful to interpretation of SIF retrievals & indices;
- availability & relevance of existing long-term plot networks and data sets;
- permanence and projected longevity of the site.

In the choice of vegetation systems, it must be decided at what level of complexity and functionality the work should be done – for example, at the level of species, phenological type, plant functional type, landscape, ecosystem, or biome. The **biome** concept categorizes large-scale ecological variations, typically by their predominant vegetation within the context of temperature and rainfall conditions. There are various naming/categorization systems – one example identifies 14 terrestrial biomes: **Tundra**, **Taiga** (including boreal coniferous forests), **Desert**, **Savanna**, **Grassland** (1.Temperate grassland; 2.Tropical savanna and grassland), **Chaparral**, **Forest** (1.Temperate forest; 2.Tropical deciduous forest), **Rainforest** (1.Temperate forest and rainforest; 2.Tropical rainforest), **Scrub forest** (1.Tropical scrub forest; 2.Temperate scrub forest), **Mountains** (either without vegetation or covered by low, tundra-like vegetation), and **Ice Cap** (Myers *et al.* 2014). But since biomes can be complex assemblages of species, the concept potentially introduces many sources of variation and error. Within a biome there could be myriad ecosystems ranging in size from very tiny (unidentifiable in a FLEX pixel) to very large.

Another concept is that of **plant functional type**, which defines groups by a variety of optical, morphological, and physiological parameters – for example, needleleaf evergreen tree, needleleaf deciduous tree, broadleaf evergreen tree, broadleaf deciduous tree, tropical seasonal tree, evergreen shrub, deciduous shrub, arctic deciduous shrub, C3 grass, C4 grass, arctic grass, or crop (Bonan *et al.* 2002). Landscapes may be viewed as patches of PFTs. Phenological types are rather similar to PFTs as they refer to specific traits.

There are advantages to working initially with relatively homogeneous targets (e.g., of a single species, PFT/landscape, or phenological type) in order to reduce confounding effects from combinations of species, age groups, canopy architectures, and site profiles. Such targets could be used for the establishment of baseline SIF responses over time, and can be the foundation of manipulative treatments for which effects may be more readily discriminated than with heterogeneous systems. Targets that are horizontally homogeneous could further be the subjects of photosynthetic modelling with a 1-D vertical model such as SCOPE. But it should be noted that even “homogeneous” targets are likely to have inherent complexity.

5.7.3 Identification of likely stresses, timeframes, sources of error

It is necessary to anticipate what the potential stresses are in a given situation. This information makes it possible to set hypotheses for deliberate study and choose appropriate ancillary activities rather than to simply monitor sites with no underpinning strategy.

Combined / multiple stressors

In this study, we chose to focus on the stresses of water deficit, temperature extremes, and nitrogen insufficiency. The gap analysis identified a need for future consideration of other stressors. Figure 5.4 depicts the diversity of stresses that can confront vegetation – these can act singly, in combination, or in sequential manner to affect SIF amplitudes. For example, water deficit can arise as a primary effect of drought, or as a consequence of other stresses that affect availability or transport of water within plant tissues (Figure 5.5). By the time early evidence of water deficit is manifested as a change in SIF, potentially there could be other more advanced symptoms of strain from other stresses. These types of complexities require further study.

Requirements for stress definition include:

- understanding of the biome(s), PFTs, and biogeoclimatic character of the area;
- consideration of past meteorological and other environmental records;
- statistics from existing regional or local vegetation monitoring programs (e.g., agricultural agencies, forest & land management organizations, ecological & natural heritage networks);
- publications & reports of stress events from researchers studying the area;
- consideration of resource management activities, proximal site activities, silvicultural treatments, etc. being planned for the future, in order to anticipate the likelihood of certain stresses arising;
- awareness of the potential for combined or sequential stresses that tend to develop in association with each other;
- awareness of stresses developing in distant locales which could spread to target areas;
- consideration of likely timeframes for stress/strain development, given the nature & seasonality of the stress, vegetation, site, and environment, in order that measurement repeat cycles will be appropriately utilized in capturing the information needed to draw conclusions;
- understanding of the sources of error that could confound meaningful conclusions, and designing appropriate mitigation approaches.

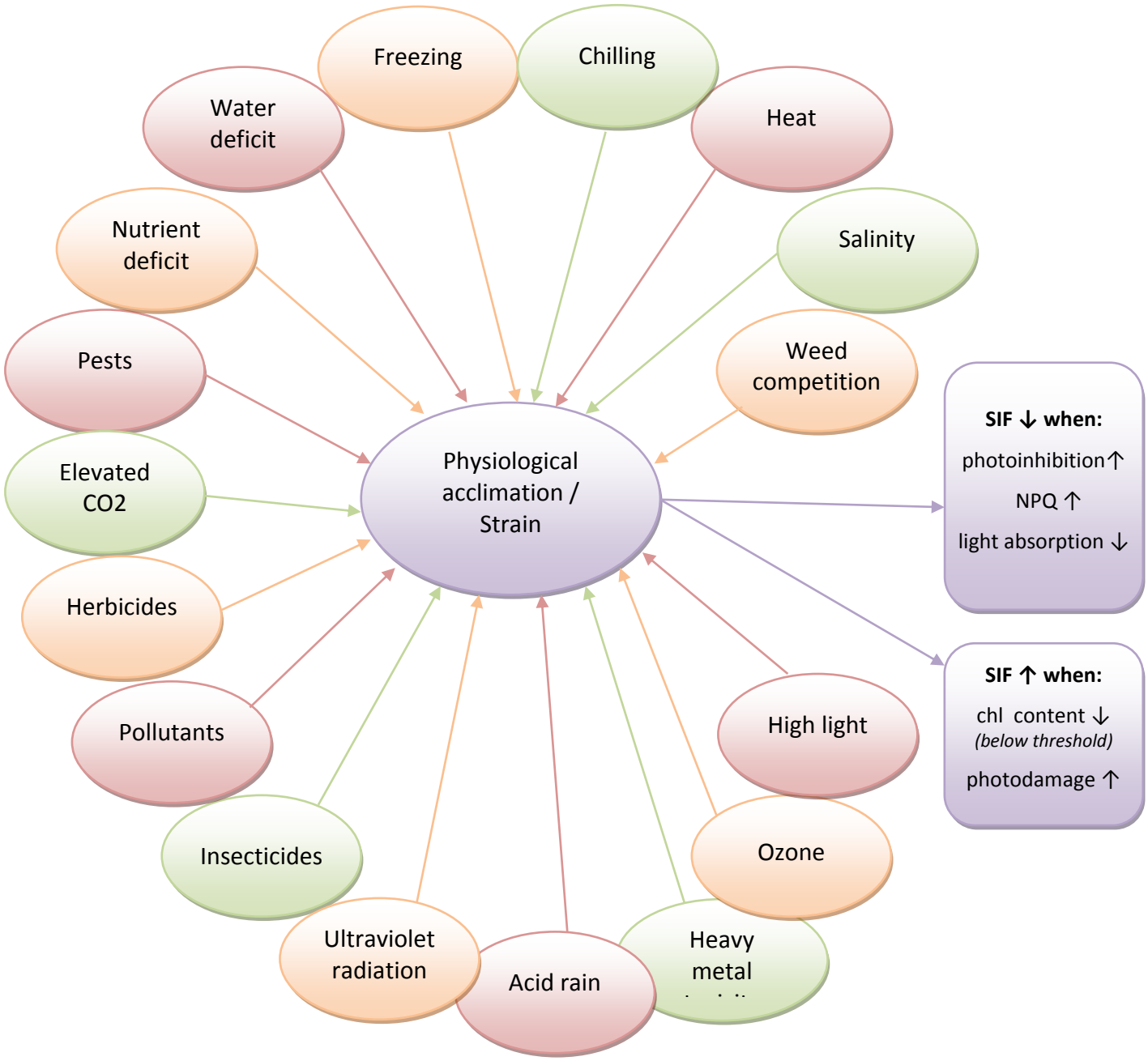

Figure 5.4. A simplified scheme of possible stress effects on SIF. Stresses act singly or in concert to trigger acclimatory responses and/or physiological strain in plant tissues. The result can be an increase or decrease in SIF depending on the net effects of absorption of incident light, chlorophyll content changes, photochemistry, non-photochemical quenching, photodamage, and light reabsorption in foliage and canopies. Example: Decreased chlorophyll content below certain thresholds can result in lower CF reabsorption in foliage and increased SIF emission (especially red); a similar effect might arise from decline in LAI from foliar loss, reducing canopy reabsorption of SIF.

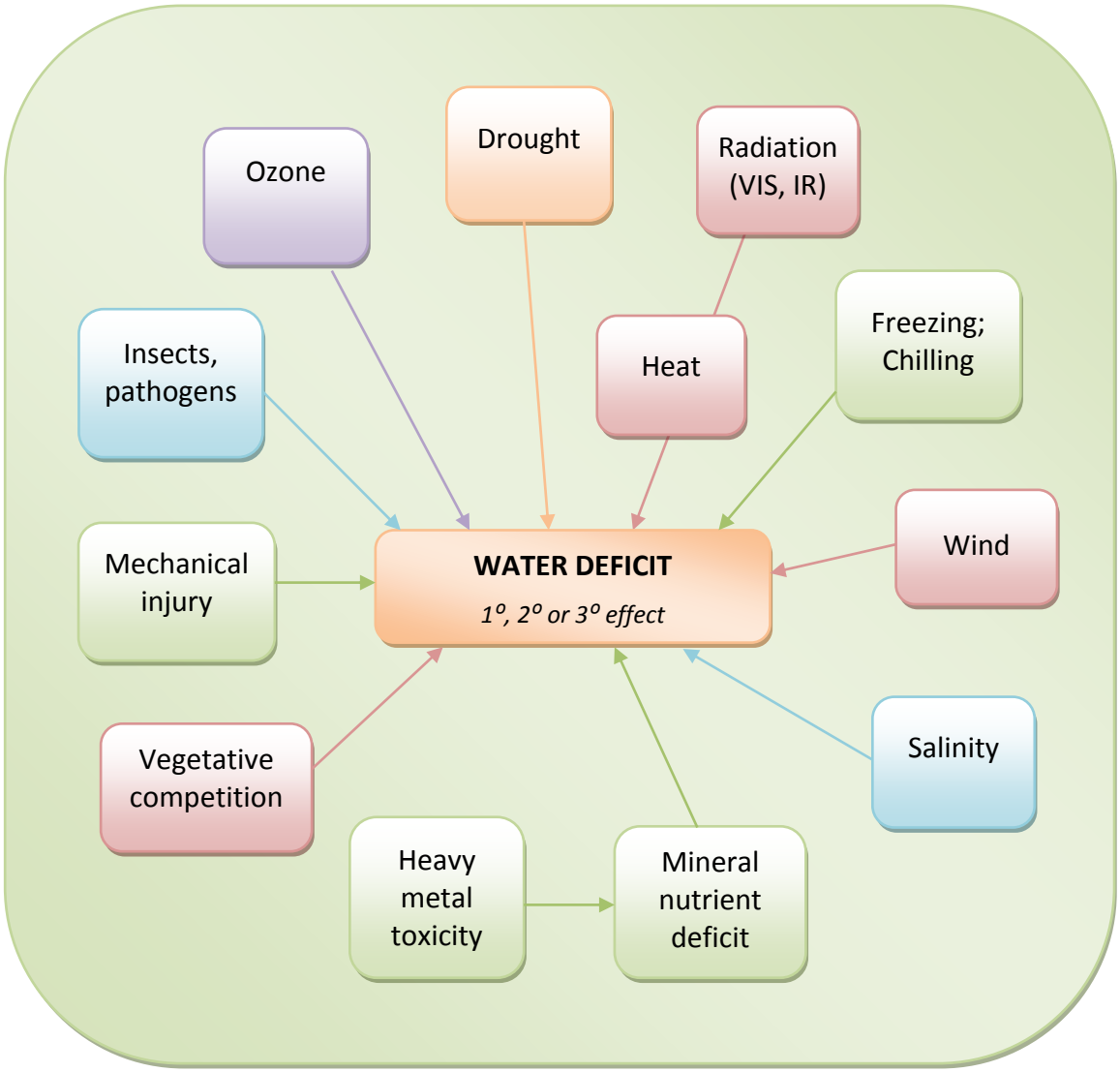

Figure 5.5. Causes of water deficit in plant tissues. Water deficit may be a primary stressor or it can arise as a result of other stresses. Modified from Levitt (1980).

5.7.4 Selection of SIF indicators

It will be necessary to target SIF features likely to be responsive to the stress(es) anticipated in a given situation. Features such as the amplitude of red and/or far-red emission peak, spectral position of the peak, ratio of peaks, area under the emission curve, normalized SIF yield, and statistical variability of SIF features might be useful singly or in combination, depending on the particular types of situations. Here, several stress indices have been postulated based on the results of the statistical analyses of literature data. The benefit of the full spectral emission offers considerable advantages in choosing several potential response features in order to provide some degree of redundancy and checks in the campaigns, not to mention the possibility of analyses by technologies as yet unknown.

Selection of SIF indicators will require:

- a more complete understanding of the responses of SIF emission features to various types of stresses;
- consideration of which features change over the short *vs*. the longer term, and how these might be manifested over the measurement repeat cycle;
- consideration of how to distinguish acclimatory reactions from strain responses leading to damage;
- appreciation of SIF features that reflect acclimation/adaptive responses *vs*. evidence of pre-visual or advanced damage;
- anticipation of the variability/sources of error that could be induced by vegetation, environment, measurement protocols, and data processing schemes;
- consideration of other spectral emission features (e.g., PRI, emission from pigments/fluorophores other than chlorophyll, other indicators of non-photochemical quenching) which have complementary and interpretive value in combination with SIF.

5.7.5 Supporting measures – calibration, validation, and interpretation

Ultimately, it is necessary to be able to draw meaningful interpretations and conclusions from remotely acquired SIF data from space. An effective strategy will help to ensure that FLEX data and its derived products will be useful and any applications will have a high likelihood of success. Pivotal to this effort is the articulation of an appropriate suite of tools that can be used at the different spatial scales in order to provide interpretive strength to FLEX measurements.

Challenges for validation of space-based SIF data are mainly owing to the difficulty of relating such remote information back to canopy and leaf-level physiology. For example, Nichol *et al.* (2012) refer to the 'canopy conundrum' of relating leaf-scale properties to those of the whole ecosystem taking into account complex 3-D canopy structure. There is the element of coarse resolution and within-pixel heterogeneity from current satellites – a problem which would be greatly alleviated with FLEX's relatively high spatial and spectral resolution.

According to Berry *et al.* (2013), the categories of validation strategy are: (i) assessment of the SIF signal itself (i.e., its absolute accuracy; consistency of spatio-temporal pattern); (ii) evaluation of the causal relationships between retrieved SIF and environmental variables or

ecosystem properties; and (iii) quantification of factors influencing and potentially disturbing SIF retrievals (e.g., atmospheric absorption & scattering, surface anisotropy, applied methods, and instrumentation).

Requirements for this stage include:

- definition of validation error metrics and goal/threshold accuracies for the different products delivered by the FLEX mission;
- definition of cal/val strategies for basic vegetation fluorescence products: prime target areas, super sites, statistical sampling procedures, measurement protocols, etc.;
- definition of FLEX Level 2 & Level 3 products and a validation plan for each product;
- understanding and linking of leaf and TOC fluorescence measurements ;
- definition of common protocols and state-of-the-art instruments to be used for estimation of SIF in the context of calibration and validation activities.

Tools, technologies, and methods have been reviewed by Lee *et al.* (2010) and Malenovský *et al.* (2009) and include:

- leaf- and canopy active CF sensors;
- airborne spectrometers – including on unmanned aerial vehicles, passive hyperspectral sensors [such as HyPlant (Rascher *et al.* 2013)], active sensors [such as CALSIF, now under development in France (Goulas *et al.* 2014)], or other laser or LED instruments;
- stationary and mobile tower- or crane-based technologies (including eddy-covariance and tower-mounted sensors) for spectrometry or physiology at the canopy level;
- leaf-based biochemical technologies for analysis of pigments, antioxidants, stress proteins, macro/micronutrient analysis, etc.;
- leaf ultrastructural microscopy for analysis of anatomical features;
- additional stress-based indicators (e.g., for gas exchange, water status, stress-induced volatile emissions, electrical conductivity, genetic markers);
- assessments of whole-plant performance (e.g., growth & development, productivity, grain/fruit quality).

Interpretation is facilitated in vegetative systems which are already being monitored regularly for productivity, health, and function as indicated above -- with long-term monitoring plot networks. Physiological automated monitoring is facilitated by existing eddy-covariance flux tower networks, primarily **FLUXNET** (Baldocchi *et al.* 2001), which coordinates regional and global analysis of observations from micrometeorological tower sites in Europe, the Americas, Asia, and the Oceania region of the Pacific. The flux tower sites measure exchanges of carbon dioxide, water vapour, and energy between terrestrial ecosystems and the atmosphere. Other networks include the Total Carbon Column Observing Network (**TTCON**), an international network of ground-based Fourier Transform Spectrometers measuring solar spectra in the NIR (Wunch *et al.* 2011); the National Ecosystem Observatory Network (**NEON**), a proposed U.S. continental-scale long-term research platform for discovering and understanding the impacts of climate change, land-use change, and invasive species on ecology (Keller *et al.* 2008); and

SpecNet, a network of sites and scientists using optical sampling to enhance remote sensing capabilities for biospheric monitoring (Meroni *et al.* 2011).

5.7.6 Expertise relevant to SIF

Inevitably, the successful exploitation of SIF in research and applications – assuming that the technology platforms are in place – comes down to the decisions and actions of visionary planners & policymakers, skilled researchers, applications experts, and a host of technical support professionals. Diverse and complementary kinds of scientific expertise are required for SIF research & development and applications. A cross-section of expertise will be required in mounting projects and it would be valuable to create a database of experts who can be invited to participate on project teams. It has been noted that, in addition to the problem of sustained funding for large complex studies, there is an ongoing need for professional teams with complementary expertise – especially for the study of complex biomes such as forests (Nichol *et al.* 2012).

Recently, approximately 100 individuals attended the *5th International Workshop on Remote Sensing of Vegetation Fluorescence* in Paris (22-24 April 2014). That workshop brought together a community of professionals interested in passive remote sensing of SIF which included not only fluorescence experts, modellers, remote sensing experts, and instrument developers – but also a bevy of atmospheric scientists, space engineers, and national science policymakers. The community of interested fluorescence parties is substantially larger when one takes into account the hundreds of researchers who use leaf-based (mainly active) techniques in plant ecophysiology, horticulture, agriculture, and forestry.

It should also be recognized that there are complementarities between terrestrial and aquatic SIF that have not yet been explored in much detail. These form a natural avenue for progress through a mission such as FLEX which is envisaged to provide coastal SIF data. Furthermore, experiences and approaches from the aquatic SIF community may be instructive for eventual FLEX data applications and calibration/validation efforts (e.g., Gower & King 2012).

Besides the diversity of scientific/technical/professional expertise beneficial to FLEX deployment for SIF retrievals and usage, there are some overriding capabilities that should be emphasized:

- Ability to effectively formulate & test hypotheses. It will be important to resist the temptation to simply amass data from FLEX without having clear objectives and plans in mind. The novel technology will make it relatively easy to collect years of spatially and spectrally explicit data for generation of maps. However, there must be an emphasis on interpretation – and that requires posing clear questions at the start and designing a thoughtful strategy to answer those questions and come to conclusions.

- Capability in problem solving & troubleshooting. To yield meaningful, applicable results from FLEX, investigators should be able to foresee and tackle the assorted challenges that attend multi-scale, multi-temporal, and multifaceted investigations. For example, FLEX will produce data that needs to be ground-truthed (wherever feasible) and

interpreted using an integrated system of tools and techniques that can involve an array of airborne, tower-based, and ground-level sensors. Making such campaigns work in situations that are often less than ideal requires people who can adapt equipment setups, respond to changing measurement windows, arrange workarounds, and capitalize on opportunities. In field work, there will always be equipment malfunctions, potential incompatibilities among platforms, and constraints on time & resources. Creative problem solvers frequently represent the difference between a failed and a successful campaign.

- Facility in shifting between generalist and specialized fields. SIF from remote platforms engages a diverse array of specialties and capabilities as discussed, and will need to be communicated effectively to both technical and non-technical audiences. This has traditionally been a challenge with chlorophyll fluorescence because of the complexity of the underlying photobiology & photochemical aspects, the terminology, and the range of technology platforms. This situation intensifies with the addition of fluorescence modelling, signal retrieval approaches, atmospheric corrections, spectral nuances, statistical methods, calibration & validation, vegetation systems, and stress physiology. Some members of the fluorescence community are beginning to express a degree of confusion with the various technical streams. This was evident, for example, at the Fluorescence Workshop in Paris where some advised the need for straightforward communications on SIF that could be grasped by all.

- Versatility in a field that needs individuals who can find order and connectivity among streams, who can transfer knowledge, and who can relate to potential users with less specialized expertise in fluorescence science. At the same time – given that the novel science of SIF can be an attractive subject to the media because of its visual appeal and therefore always runs the potential risk of being oversold – there can be a tendency to oversimplify and over-promise. An ability to effectively represent the balance of all aspects is invaluable. This also is key to integrating different kinds of expertise when assembling project teams and in the delivery of useful, non-superficial information to funding agencies.

5.7.7 Recommendations

This task overall has identified fluorescence indicators useful for detection of water deficit, temperature stresses, and nitrogen deficit. It has further identified information gaps as well as various factors that must be considered in order to correctly utilize SIF in the detection of stress effects. To support planning for the FLEX mission, we suggest a number of actions and studies relevant to stress applications. These suggested initiatives are summarized in Table 5.3 and encompass the timeframe leading up to deployment and into the mission.

Table 5.3. Actions and studies recommended to facilitate SIF usage and applications in stress detection.

Topic	Before FLEX mission	During FLEX mission
Purpose / Application		
user identification	identify user communities & networks in government, resource management, and science who can help to establish priorities for FLEX applications; establish specific contact individuals or agencies	maintain a feedback process to share findings, discuss implications, and adjust approaches where possible to achieve agreed-upon objectives
goals & objectives	identify goals and objectives for the short, medium, and long term, using inputs from user communities and considering a variety of data, emerging trends, anticipated future stresses	implement strategies necessary to meet the agreed-upon objectives, refining strategies as appropriate
types of applications	review the full range of applications, and the types of SIF indicators used; perform comprehensive investigation of options for SIF applications to production of food, feed, fodder, and fuel	set objectives for study that target a small number of key stresses which are manifested in at least two SIF features
information flow pathways	develop a multi-technique communications plan with users that will operate during the FLEX mission – incorporating a variety of tools	implement the communication strategy, and identify & fix areas that need improvement
Prioritization of Vegetation Sites		
vegetation management	identify areas of natural and managed vegetation (including existing and planned networks) which may be used for studying SIF behaviour and which may be amenable to manipulative treatments at spatial scales relevant to FLEX	emphasize analysis efforts for those sites which are already a part of existing networks or which are planned to receive intensive ground/remote assessment
canopy structural complexity	define likely limits of canopy structural complexity for remote SIF assessment, taking into account vegetation composition (e.g., species, PFTs, ecosystems, biomes, phenologies) and site attributes	test the degree to which apparently 'homogeneous' sites express variability in SIF, and apparently 'heterogeneous' sites express similar SIF
site & environmental complexity	determine the extent to which site and environmental heterogeneity influence SIF acquisitions, and suggest limits for such heterogeneity within a scene	stratify measurement targets to allow meaningful conclusions

SCOPE application	test the photosynthesis outputs of the model in different types of canopy vegetation composition & structure; recommend site & vegetation types	utilize the model within the confines of vegetation restrictions on optimal sites, degree of canopy complexity, etc.
Stresses / Timeframes / Sources of Error		
combined stressors	determine which combinations of stresses could generate spectral results that facilitate or preclude interpretive efforts; identify the circumstances (e.g., sites, vegetation systems, times of year, environmental conditions) in which such effects occur	focus the most intensive ground-based or airborne interpretive efforts where combined stresses are likely to occur, in order to provide sufficient explanatory power
major stresses	review the known temporal patterns of major stresses in sites of concern and suggest how these patterns may be reasonably tracked by the repeated measurement cycle of FLEX	target those stresses for long-term tracking which develop gradually, and evaluate whether an early alarm system is possible using FLEX retrievals
sources of error – vegetation factors	review variability & errors arising from factors such as plant/foliar age, species, pigments & fluorophores, LAI, etc.; review mitigation strategies	employ and test best practices to mitigate errors
sources of error – environmental factors	review variability & errors arising from factors such as abiotic/biotic stresses, atmospheric effects, light, moisture, temperature, nutrients, and growing regimes; review mitigation strategies	employ and test best practices to mitigate errors
sources of error – instrument/data	review variability & errors arising from factors such as measurement geometry/anisotropy, signal-to-noise ratio, retrieval algorithms; review mitigation strategies	employ and test best practices to mitigate errors
SIF Indicators / Other Spectral Features		
SCOPE – improvement of stress-related inputs	improve stress content information of model by representing features such as PRI, NPQ, PSI/PSII partitioning	utilize key SIF and non-SIF features of the full emission for photosynthetic tracking and model inputs
SCOPE – increased versatility	test SIF retrievals in the red (O_2-B) band for different canopies, incorporating module improvements as indicated (e.g., for leaf radiative transfer)	apply methods that produce reliable retrievals in the red band
algorithm development	improve simplified algorithms for F-GPP or other physiological features in different types of canopies	compare space-based retrievals using a small number of algorithms against ground-based and airborne data

types of indicators	identify SIF features in addition to the red and far-red bands that could be used to indicate stress-induced strain, including early and late indicators, and looking at consistency of responses at leaf and canopy levels	test a few key SIF and non-SIF features of the full emission for photosynthetic tracking and model inputs
universality of indicators	test whether there are SIF indicators that are effective across different vegetation systems, e.g., species, PFTs, biomes, ecosystems	apply identified universal indicators to derive spatial maps of vegetation health & stress status
clarification of N-deficit effects on SIF	develop hypotheses to explain the differential effects of nitrogen deficit on SIF, and use controlled experiments with C3 and C4 species at leaf and canopy levels to test how these effects may be discriminated	determine the confidence level with which space-based retrievals are able to discriminate the differential effects of N-deficit
acclimation versus damaging strain	distinguish the physiological manifestations of acclimatory/adaptive responses versus damaging strain for various stresses in the context of SIF & other spectral features; identify threshold values where feasible; hypothesize which stages should be amenable to detection by SIF and other spectral features from FLEX	test hypotheses to distinguish acclimatory/adaptive responses from damaging strain
Supporting Measures / Cal-Val		
strategy for calibration / validation	develop an integrated strategy for calibration / validation for FLEX products – identifying error metrics, goal/threshold accuracies, leaf to canopy linkages, protocols & methodologies	implement the elements of the strategy, incorporating sensor and ancillary technologies for data capture at relevant biological and spatial scales
complementary & supporting technologies	determine potential synergies between FLEX and other sensors which could be used at different spatial scales (ground, tower, airborne, other satellites); evaluate data already acquired from the FLEX demonstration sensor HyPlant to link airborne maps of fluorescence to vegetation structure & function and other ground parameters; determine if and how active sensors may be used in comparisons and interpretations of SIF data	use complementary sensors and technologies to help interpret FLEX retrievals

6. Overall Conclusions & Recommendations

The Photosynthesis Study developed and tested an integrated 1-D vertical model linking steady-state fluorescence and photosynthesis. SCOPE v1.53 – an advancement of the original model published by Van der Tol *et al.* (2009b) – is comprised of modules that represent biochemical processes at the leaf level and radiative transfer at the leaf & canopy levels. SCOPE was updated here to improve its constituent modules, modularity and operational performance. Further, the usability of the consolidated model was facilitated through the novel creation of A-SCOPE, a Graphic User Interface customized for SCOPE v1.53 which facilitates data input, storage, graphics, and output management.

A promising leaf biochemical module, MD12, was selected for the consolidated SCOPE platform. MD12 was the culmination of developments over several years, and it was contributed for the study and further optimized by F. Magnani and his team at the University of Bologna. In validation testing, MD12 demonstrated superior performance in comparison to other leaf-level physiological models in goodness-of-fit tests with photosynthesis. Also, since versatility was considered a distinct advantage for the overall SCOPE platform, additional leaf modules – TB12 and TB12-drought, which require fewer parameters – were also included in the software package as alternatives to MD12.

The consolidated model has undergone sensitivity and validation testing. In general, it performs well, being able to simulate both canopy diurnal photosynthesis as well as the shape of the fluorescence emission. The model successfully simulates steady-state fluorescence, especially in the O_2-A band. However, preliminary indications are that it may be overestimating fluorescence in the O_2-B band – further investigation is required.

SCOPE is a complex model that necessitates significant run times. However, sensitivity analyses identified 10 to 12 core driving parameters that could suffice in most routine operations, and other parameters which could safely be kept fixed (i.e., set to default values), thus increasing computational speed. Consideration of co-varying parameters can further streamline model operation, but in other circumstances, the richness of SCOPE's full complement of parameters may offer advantages in addressing diverse terrestrial vegetation canopies.

Algorithm development based on the model was also investigated, including the possibility to deduce relatively simple relationships between SIF and GPP or net canopy photosynthesis (NPC). Model inversion work indicated that inclusion of fluorescence data resulted in substantive improvement in algorithm performance for the estimation of NPC. The two types of statistical algorithms – Gaussian processes regression (or GPR) and polynomial & rational functions fitting (or PRF) – gave highly accurate results for retrieval of canopy photosynthesis in the case of C3 plants, while with C4 plants excellent results were obtained using GPR (lower success with PRF). PRF using only simple optical data in a low number of channels was able to predict photosynthetic products (GPP, LUE, APARChl) for C3 plants in a non-stressed case with high performance; for C4 plants, only APARChl could be predicted with high accuracy. Both fluorescence bands were needed to predict GPP and LUE using PRF, meaning that the two bands do not carry the same information. Using GPR, although relationships were obtained

using only the second emission peak F740, the most information apparently is contained within the first emission peak F685. An error threshold of 10% was already achievable with the F685 emission band in C3 species using GPR; including more bands, the whole fluorescence profile, and additional biophysical variables optimally yielded R^2 of 0.95 in C3 plants. In C4 plants, GPR required the full fluorescence profile to meet the error threshold. Neither reflectance data nor solely biophysical variables (Chl, LAI, *f*APAR) led to meaningful relationships with NPC. However, it is prudent to take chlorophyll content into account due to its effects on light absorption (which influences photosynthesis and fluorescence radiance positively) and reabsorption (which decreases fluorescence emission).

Although the models tested in this study were simple and used a limited number of variables, they proved their efficacy to predict photosynthetic products, at least in the absence of severe stress. Further investigations should be undertaken to test the robustness of the retrievals, preferentially with canopy SIF data such as that recently made available from the *HyPlant* airborne sensor, designed as an airborne prototype for FLORIS.

In the case of one-variable models, F760 surprisingly was found to be non-predictive for any products, regardless the plant type (C3, C4). This is in contrast with the previously reported high correlation between far-red fluorescence and GPP deduced from experimental data (Guanter *et al.* 2012; Berry *et al.* 2013; Frankenberg *et al.* 2011b; Rossini *et al.* 2010).

As a complementary stream of investigation, stress applications of steady-state fluorescence were evaluated, specifically in detecting physiological strain from water deficit, temperature extremes, and nitrogen deficiency. A random-effects meta-analysis identified clear benefits of the red and far-red fluorescence bands – and the ratio of the bands – for detection of stress-induced strain. Information gaps were considered, and these highlighted the need for better understanding of canopy structural complexity, environmental heterogeneity, stress interactions, and sources of error, among other factors.

Several novel fluorescence-based stress indicators have been proposed here to assess stress intensity as well as stress quality in relation with water, temperature, and nitrogen stress. Further investigations and evaluations of these new stress indicators should be undertaken. These indicators are in addition to simple indices already known to be effective for identification of stress, most notably the ratio of red to far-red fluorescence (particularly expressed as a ratio of stressed:control values). The importance of normalizing SIF features was evident. Here, control values were used in normalization; however, where control values are not available, another approach is to express fluorescence as a function of incident or absorbed PAR (Daumard *et al.* 2010; Rossini *et al.* 2010; Meroni *et al.* 2008). In addition, in the case of future FLEX data, the repeated measurements also create a change detection system whereby initial (baseline) readings can serve an additional normalization function. The photosynthesis model or its simplified formats – and F-GPP algorithms developed in this study – provide further options for stress indices based on ratios of actual to potential photosynthesis.

Finally, a conceptual framework was developed depicting key elements for the application of remote SIF for stress detection, and identifying priorities for further study. Aspects such as the

setting of goals and objectives for studies and monitoring programs, prioritization of vegetation sites for analysis, identification of stresses, selection of indicators, and the types of supporting measures have been addressed.

Significance for the FLEX mission

Outputs from the PS Study that are of key relevance to the FLEX/S3 mission include:

1. **model advances** – the availability now of a powerful consolidated model for linking canopy SIF and photosynthesis, making it possible to derive photosynthesis from FLEX fluorescence retrievals (upon conversion to top-of-canopy signals);
2. **model GUI for users** – development of the new A-SCOPE Graphic User Interface, greatly facilitating usage of the photosynthesis model and opening the door to a potentially broad range of users for FLEX-derived products;
3. **calibration/validation tool** – availability of the SCOPE v1.53 model for calibration and validation activities during mission deployment;
4. **processing advancements** – demonstration of streamlining options for the photosynthesis model, thereby making more feasible the execution of large-volume analyses to be triggered from FLEX data;
5. **support of FLORIS spectral strategy** – substantiation in the model inversion work of the inherent value of both fluorescence peaks and the full fluorescence profile for estimation of net photosynthesis of the canopy, thus conferring a singular advantage to the FLORIS sensor scheme to extract the complete emission profile;
6. **algorithms** – indications that simple regression models were able to predict photosynthetic products for C3 and C4 plants with high performance in a non-stressed case;
7. **stress applications** – development of novel stress indices, and confirmation of the benefits of using both red and far-red peaks for tracking strain induced by the stresses of water deficit, temperature extremes, and nitrogen insufficiency, which are all issues of contemporary concern in food production and management of significant vegetation systems worldwide;
8. **strategic approach** – depiction of a conceptual framework to support application of SIF to issues involving vegetation stresses and resource management.

Next steps

To build upon the findings of the Photosynthesis Study, the following further developments are recommended:

- **advanced model parameterization** – advances in parameterization within the model of strategic physiological variables such light energy distribution between the photosystems, quantification of photoprotective quenching, and photodamage;
- **comprehensive model testing** – evaluation of model performance under a broader range of field situations, including stress scenarios;

- **algorithm testing** – evaluation of the robustness of simple regression models found here to relate SIF and photosynthetic products;
- **expanded stress detection** – consideration of a wider range of stresses – including multiple-stress situations – for which SIF might serve as an indicator, and identification of additional features from the full spectral emission profile that could be used;
- **stress indices testing & validation** – prototype stress indices have been suggested by the study activities which merit further testing and validation under various conditions and with a range of species and functional types;
- **calibration & validation** – development of a thorough strategy for calibration and validation of SIF from FLEX so that accurate interpretations may be drawn in the various application areas;
- **analysis & mitigation of errors** – elucidation of sources of variability and potential errors arising from biological and environmental factors which may constrain interpretations of SIF behaviour in response to stress, and presentation of strategies to mitigate errors and misinterpretation.

A comprehensive suite of recommendations has been developed for actions and studies which would encompass the timeframe leading up to and during FLEX deployment (see Chapter 5). They serve to underscore the fact that SIF from space is truly a fresh and emerging arena for understanding real-time photosynthetic behaviour of land vegetation – a possibility not envisaged before the prospect of the FLEX mission. Even now, with intensifying efforts from researchers endeavouring to extract SIF data from non-optimized satellite platforms such as GOSAT, GOME-2, OCO-2, etc., it is evident that the FLEX mission is unique and advantageously positioned to fully exploit this fascinating signal. Ultimately, FLEX and its sensor FLORIS would be the vanguard for this new way to view the actual functioning of terrestrial vegetation from space.

7. References

Ač A, Malenovský Z, Olejníčková J, Gallé A, Rascher U, Mohammed G. 2014. Meta-analysis assessing potential of steady-state chlorophyll fluorescence for remote sensing detection of plant water, temperature and nitrogen stress. *Remote Sensing of Environment* (submitted).

Ač A, Malenovský Z, Urban O, Hanus J, Zitova M, Navratil M, Vrablova M, Olejníčková J, Spunda V, Marek M. 2012. Relation of chlorophyll fluorescence sensitive reflectance ratios to carbon flux measurements of Montanne grassland and Norway spruce forest ecosystems in the temperate zone. *Scientific World Journal 2012*, Article ID 705872, 13 pages, doi: 10.1100/2012/705872.

Adams III WW, Demmig-Adams B. 2004. Chlorophyll fluorescence as a tool to monitor plant response to the environment. In: Papageorgiou GC, Govindjee (eds.) *Chlorophyll a Fluorescence. A Signature of Photosynthesis*, pp. 583-604. Springer.

Adams WW, Demmig-Adams B, Verhoeven AS, Barker DH. 1995. 'Photoinhibition' during winter stress. Involvement of sustained xanthophyll cycle-dependent energy dissipation. *Australian Journal of Plant Physiology* **22** 261-276.

Agati G. 1998. Response of the in vivo chlorophyll fluorescence spectrum to environmental factors and laser excitation wavelength. *Pure & Applied Optics* **7** 797-807.

Agati G, Cerovic Z, Moya I. 2000. The effect of decreasing temperature up to chilling values on the in vivo F685/F735 chlorophyll fluorescence ratio in *Phaseolus vulgaris* and *Pisum sativum*: The role of the Photosystem I contribution to the 735 nm fluorescence band. *Photochemistry and Photobiology* **72** 75-84.

Agati G, Mazzinghi P, Fusi F, Ambrosini I. 1995. The F685/F730 chlorophyll fluorescence ratio as a tool in plant physiology: response to physiological and environmental factors. *Journal of Plant Physiology* **145** 228-238.

Agati G, Mazzinghi P, Lipucci di Paola M, Fusi F, Cecchi G. 1996. The F685/F730 chlorophyll fluorescence ratio as indicator of chilling stress in plants. *Journal of Plant Physiology* **148** 384-390.

Agati G, Palombi L, Lognoli D, Raimondi V, Toci G, Cecchi G. 2008. SIF and photosynthesis: peak ratio. ESA AO/1-5229 FLEX-DVM Midterm Presentation, Noordwijk, 5 May 2008.

Allen RG, Pereira LS, Raes D, Smith M. 1998. Crop evapotranspiration: Guidelines for computing crop requirements. Irrigation and Drainage Paper No. 56, FAO, Rome, Italy, 300 pp.

Alonso L, Gomez-Chova L, Vila-Frances J, Amoros-Lopez J, Guanter L, Calpe J, Moreno J. 2008. Improved Fraunhofer line discrimination method for vegetation fluorescence quantification. *IEEE Transactions in Geoscience and Remote Sensing* **5** 620-624.

Amthor JS, Baldocchi DD. 2001. Terrestrial higher plant respiration and net primary production. In: Roy J, Saugier B, Mooney HA (eds.) *Terrestrial Global Productivity*, pp. 33-59. Academic Press.

Ananyev G, Kolber ZS, Klimov D, Falkowski PG, Berry JA, Rascher U, Martin R, Osmond B. 2005. Remote sensing of heterogeneity in photosynthetic efficiency, electron transport and dissipation of excess light in *Populus deltoides* stands under ambient and elevated CO_2 concentrations, and in a tropical forest canopy, using a new laser-induced fluorescence transient device. *Global Change Biology* **11** 1195-1206.

Antal T, Rubin A. 2008. In vivo analysis of chlorophyll a fluorescence induction. *Photosynthesis Research* **96** 217-226.

Araus JL, Sanchez C, Cabrera-Bosquet L. 2010. Is heterosis in maize mediated through better water use? *New Phytologist* **187** 392-406.

Asner GP, Scurlock JM, Hicke J. 2003. Global synthesis of leaf area index observations: implications for ecological and remote sensing studies. *Global Ecology and Biogeography* **12** 191-205.

Babani F, Lichtenthaler HK. 1996. Light-induced and age-dependent development of chloroplasts in etiolated barley leaves as visualized by determination of photosynthetic pigments, CO_2 assimilation rates and different kinds of chlorophyll fluorescence ratios. *Journal of Plant Physiology* **148** 555-566.

Babani F, Lichtenthaler HK, Richter P. 1996. Changes of chlorophyll fluorescence signatures during greening of etiolated barley seedlings as measured with the CCD-OMA fluorometer. *Journal of Plant Physiology* **148** 471-477.

Baldocchi D, Falge E, Gu LH, Olson R, Hollinger D, Running S, Anthoni P, Bernhofer C, Davis K, Evans R, Fuentes J, Goldstein A, Katul G, Law B, Lee XH, Malhi Y, Meyers T, Munger W, Oechel W, Paw KT, Pilegaard K, Schmid HP, Valentini R, Verma S, Vesala T, Wilson K, Wofsy S. 2001. FLUXNET: A new tool to study the temporal and spatial variability of ecosystem-scale carbon dioxide, water vapor, and energy flux densities. *Bulletin of the American Meteorological Society* **82** 2415–2434.

Ball JT, Woodrow IE, Berry JA. 1987. A model predicting stomatal conductance and its contribution to the control of photosynthesis under different environmental conditions. In: Biggins I (ed.) *Progress in Photosynthesis Research, Vol. IV*, pp. 221–224. Martinus-Nijhoff Publishers.

Balota M, HK Lichtenthaler. 1999. Red chlorophyll fluorescence as an ecophysiological method to assess the behaviour of wheat genotypes under drought and heat. *Cereal Research Communications* **27** 179-187.

Baraldi R, Canaccini F, Cortes S, Magnani F, Rapparini F, Zamboni A, Raddi S. 2008. Role of xanthophyll cycle-mediated photoprotection in *Arbutus unedo* plants exposed to water stress during the Mediterranean summer. *Photosynthetica* **46** 378-386.

Batello C, Wade L, Cox S, Pogna N, Bozzini A, Choptiany J. (eds). 2014. Perennial Crops for Food Security, Proceedings of the FAO Expert Workshop, 28-30 August 2013, Rome, Italy. Food and Agriculture Organization of the United Nations. www.fao.org/3/a-i3495e.pdf

Berry JA, Frankenberg C, Wennberg P. 2013. Proc. New Methods for Measurements of Photosynthesis from Space, 26-31 August 2012, Keck Institute for Space Studies, Pasadena, CA. 72 p. www.kiss.caltech.edu/study/photosynthesis/2013KISS_flourescence_final_report.pdf.

Bonan GB, Levis S, Kergoat L, Oleson KW. 2002. Landscapes as patches of plant functional types: An integrating concept for climate and ecosystem models. *Global Biogeochemical Cycles* **16** 5-1 to 5-23.

Borenstein M, Hedges LV, Higgins JPT, Rothstein HR. 2009. *Introduction to Meta-Analysis*. Wiley.

Borisov BA, Bykov OD. 2008. Spectral changes in the fluorescence of chlorophyll during photosynthesis induction. *Optics and Spectroscopy* **104** 186-189.

Bredemeier C, Schmidhalter U. 2003. Non-contacting chlorophyll fluorescence sensing for site-specific nitrogen fertilization in wheat and maize. In: Stafford J, Werner A (eds.) *Precision Agriculture*, pp. 103-108. Wageningen Academic Publishers.

Burling K, Hunsche M, Noga G, Pfeifer L, Damerow L. 2011a. UV-induced fluorescence spectra and lifetime determination for detection of leaf rust (*Puccinia triticina*) in susceptible and resistant wheat (*Triticum aestivum*) cultivars. *Functional Plant Biology* **38** 337-345.

Burling K, Hunsche M, Noga G. 2011b. Use of blue-green and chlorophyll fluorescence measurements for differentiation between nitrogen deficiency and pathogen infection in winter wheat. *Journal of Plant Physiology* **168** 1641-1648.

Buschmann C. 1995. Variation of the quenching of chlorophyll fluorescence under different intensities of the actinic light in wildtype plants of tobacco and in an aurea mutant deficient of light harvesting-complex. *Journal of Plant Physiology* **145** 245-252.

Buschmann C, Lichtenthaler HK. 1998. Principles and characteristics of multi-colour fluorescence imaging of Plants. *Journal of Plant Physiology* **152** 297-314.

Campbell PKE, Middleton EM, Corp LA, Kim MS. 2008. Contribution of chlorophyll fluorescence to the apparent vegetation reflectance. *Science of the Total Environment* **404** 433-439.

Carter GA, Freedman A, Kebabian PL, Scott HE. 2004. Use of a prototype instrument to detect short-term changes in solar-excited leaf fluorescence. *International Journal of Remote Sensing* **25** 1779-1784.

Carter GA, Theisen AF, Mitchell RJ. 1990. Chlorophyll fluorescence measured using the Fraunhofer line-depth principle and relationship to photosynthetic rate in the field. *Plant Cell and Environment* **13** 79-83.

Cecchi G, Mazzinghi P, Pantani L, Valentini R, Tirelli D, De Angelis P. 1994. Remote sensing of chlorophyll a fluorescence of vegetation canopies: 1. Near and far field measurement techniques. *Remote Sensing of Environment* **47** 18-28.

Cerovic ZG, Goulas Y, Gorbunov M, Briantais J-M, Camenen L, Moya I. 1996. Fluorosensing of water stress in plants. Diurnal changes of the mean lifetime an yield of chlorophyll fluorescence, measured simultaneously and at distance with a ?-LIDAR and a modified PAM-fluorimeter, in maize, sugar beet and Kalanchoë. *Remote Sensing of Environment* **58** 311-321.

Chappelle EW, Wood Jr, FM, McMurtrey III, JE, Newcomb WW. 1984. Laser-induced fluorescence of green plants. 1: A technique for the remote detection of plant stress and species differentiation. *Applied Optics* **23** 134-138.

Chen LS, Cheng L. 2003. Both xanthophyll cycle-dependent thermal dissipation and the antioxidant system are up-regulated in grape (*Vitis labrusca* L. cv. Concord) leaves in response to N limitation. *Journal of Experimental Botany* **54** 2165-2175.

Cherif J, Derbel N, Nakkach M, Mediouni C, von Bergmann H, Jemal F, Lakhdar ZB. 2011. Detection of photosynthetic activity under cadmium stress by measurement of the red and far-red chlorophyll fluorescence. *International Journal of Remote Sensing* **32** 4233-4248.

Collatz GJ, Ball JT, Grivet C, Berry JA. 1991. Physiological and environmental regulation of stomatal conductance, photosynthesis and transpiration: a model that includes a laminar boundary layer. *Agricultural and Forest Meteorology* **54** 107-136.

Collatz GJ, Ribas-Carbo M, Berry JA. 1992. Coupled photosynthesis-stomatal conductance model for leaves of C_4 plants. *Australian Journal of Plant Physiology* **19** 519-538.

Corp LA, McMurtrey JE, Middleton EM, Mulchi CL, Chappelle EW, Daughtry CST. 2003. Fluorescence sensing systems: In vivo detection of biophysical variations in field corn due to nitrogen supply. *Remote Sensing of Environment* **86** 470-479.

Corp LA, Middleton EM, Entcheva Campbell PK, Huemmrich KF, Cheng Y-B, Daughtry CST. 2009. Remote sensing techniques to monitor nitrogen-driven carbon dynamics in field corn. In: Gao W, Jackson TJ (eds.) Proc. SPIE 7454, Remote Sensing and Modeling of Ecosystems for Sustainability VI, 5-6 August 2009, San Diego, California.

Corp LA, Middleton EM, McMurtrey JE, Campbell PKE, Butcher LM. 2006. Fluorescence sensing techniques for vegetation assessment. *Applied Optics* **45** 1023-1033.

Cowan I. 1977. Stomatal behaviour and environment. *Advances in Botanical Research* **4** 117-228.

Curran PJ, Milton EJ. 1983. The relationships between the chlorophyll concentration, LAI and reflectance of a simple vegetation canopy. *International Journal of Remote Sensing* **4** 247-255.

Damm A, Elbers J, Erler A, Gioli B, Hamdi K, Hutjes R, Kosvancova M, Meroni M, Miglietta F, Moersch A, Moreno J, Schickling A, Sonnenschein R, Udelhoven T, van der Linden S, Hostert P, Rascher U. 2010. Remote sensing of sun-induced fluorescence to improve modeling of diurnal courses of gross primary production (GPP). *Global Change Biology* **16** 171-186.

Da Silva AJ, do Nascimento CWA, da Silva Gouveia-Neto A, da Silva-Jr EA. 2012. LED-induced chlorophyll fluorescence spectral analysis for the early detection and monitoring of cadmium toxicity in maize plants. *Water Air Soil Pollution* **223** 3527-3533.

Dash J, Curran P.J. 2007. Evaluation of the MERIS terrestrial chlorophyll index (MTCI). *Advances in Space Research* **39** 100-104

Daumard F, Champagne S, Fournier A, Goulas Y, Ounis A, Hanocq JF, Moya I. 2010. A field platform for continuous measurement of canopy fluorescence. *IEEE Transactions in Geoscience and Remote Sensing* **48** 3358-3368.

Daumard F, Goulas Y, Champagne S, Fournier A, Ounis A, Olioso A, Moya I. 2012. Continuous monitoring of canopy level sun-induced chlorophyll fluorescence during the growth of a sorghum field. *IEEE Transactions on Geoscience and Remote Sensing* **50** 4292-4300.

Dayyoub A. 2011. Novel Techniques for the Remote Sensing of Photosynthetic Processes. PhD Thesis, University of Bologna.

DeEll JR, Toivonen PMA. 2003. Use of chlorophyll fluorescence in postharvest quality assessments of fruits and vegetables. In: DeEll JR, Toivonen PMA (eds.) *Practical Applications of Chlorophyll Fluorescence in Plant Biology*, pp. 203-242. Kluwer.

Demmig-Adams B, Moeller DL, Logan BA, Adams WW. 1998. Positive correlation between levels of retained zeaxanthin plus antheraxanthin and degree of photoinhibition in shade leaves of *Schefflera arboricola* (Hayata) Merrill. *Planta* **205** 367-374.

Di Paola ML, Mazzinghi P, Pardossi A, Vernieri P. 1992. Vegetation monitoring of chilling stress by chlorophyll fluorescence ratio. *EARSeL Advances in Remote Sensing* **1**(2 - II).

Diomande K, Ballo K, Konate A, Adjo VK, Soro A, Ebby N. 1998. Detection of potassium deficiency on palm oil tree (Elaeis guineensis (jack)) by laser induced fluorescence. United Nations Educational Scientific and Cultural Organization and International Atomic Energy Agency, The ABDUS Salam International Centre for Theoretical Physics, Trieste, Italy, IC/98/16. http://streaming.ictp.trieste.it/preprints/P/98/016.pdf

Ennajeh M, Vadel AM, Khemira H. 2009. Osmoregulation and osmoprotection in the leaf cells of two olive cultivars subjected to severe water deficit. *Acta Physiologiae Plantarum* **31** 711-721.

Evain S, Camenen L, Moya I. 2001. Three channels detector for remote sensing of chlorophyll fluorescence and reflectance from vegetation. In: Leroy M (ed.) 8th International Symposium: Physical Measurements and Signatures in Remote Sensing, 8-12 January 2001, Aussois, France, pp. 395-400.

Evain S, Flexas J, Moya I. 2004. A new instrument for passive remote sensing. 2. Measurement of leaf and canopy reflectance changes at 531 nm and their relationship with photosynthesis and chlorophyll fluorescence. *Remote Sensing of Environment* **91** 175-185.

Farquhar GD, Von Caemmerer SV, Berry JA. 1980. A biochemical model of photosynthetic CO_2 assimilation in leaves of C3 species. *Planta* **149** 78-90.

Fernandez-Jaramillo AA, Duarte-Galvan C, Contreras-Medina LM, Torres-Pacheco I, Romero-Troncoso RJ, Guevara-Gonzalez RG, Millan-Almaraz JR. 2012. Instrumentation in developing chlorophyll fluorescence biosensing: A review. *Sensors* **12** 11853-11869.

Fernández-Marín B, Míguez F, Becerril JM, Garcia-Plazaola JI. 2011. Dehydration-mediated activation of the xanthophyll cycle in darkness: is it related to desiccation tolerance? *Planta* **234** 579-588.

Flexas J, Briantais J-M, Cerovic ZG, Medrano H, Moya I. 2000. Steady-state and maximum chlorophyll fluorescence responses to water stress in grapevine leaves: a new remote sensing system. *Remote Sensing of Environment* **73** 283-297.

Flexas J, Escalona JM, Evain S, Gulias J, Moya I, Osmond CB, Medrano H. 2002. Steady-state chlorophyll fluorescence (Fs) measurements as a tool to follow variations of net CO_2 assimilation and stomatal conductance during water-stress in C_3 plants. *Physiologia Plantarum* **114** 231-240.

Flexas J, Escalona JM, Medrano H. 1999. Water stress induces different levels of photosynthesis and electron transport rate regulation in grapevines. *Plant Cell and Environment* **22** 39-48.

Fournier A, Daumard F, Champagne S, Ounis A, Goulas Y, Moya I. 2012. Effect of canopy structure on sun-induced chlorophyll fluorescence. *Journal of Photogrammetry and Remote Sensing* **68** 112-120.

Franck F, Juneau P, Popovic R. 2002. Resolution of the photosystem I and photosystem II contributions to chlorophyll fluorescence of intact leaves at room temperature. *Biochimica et Biophysica Acta (BBA)-Bioenergetics* **1556** 239-246.

Frankenberg C, Butz A, Toon GC. 2011a. Disentangling chlorophyll fluorescence from atmospheric scattering effects in O_2 A-band spectra of reflected sun-light. *Geophysical Research Letters* **38** L03801, doi:10.1029/2010GL045896, 2011.

Frankenberg C, Fisher JB, Worden J, Badgley G, Saatchi SS, Lee J-E, Toon GC, Butz A, Jung M, Kuze A, Yokota T. 2011b. New global observations of the terrestrial carbon cycle from GOSAT: Patterns of plant fluorescence with gross primary productivity. *Geophysical Research Letters* **38** L17706, doi:10.1029/2011GL048738.

Freedman A, Cavender-Bares J, Kebabian PL, Bhaskar R, Scott H, Bazzaz FA. 2002. Remote sensing of solar-excited plant fluorescence as a measure of photosynthetic rate. *Photosynthetica* **40** 127-132.

Friend AD. 1995. PGEN: an integrated model of leaf photosynthesis, transpiration and conductance. *Ecological Informatics* **77** 233-255.

Friend AD. 1991. Use of a model of photosynthesis and leaf microenvironment to predict optimal stomatal conductance and leaf nitrogen partitioning. *Plant, Cell and Environment* **14** 895-905.

Garcia-Camacho F, Sanchez-Miron A, Molina-Grima E, Camacho-Rubio F, Merchuck JC. 2012. A mechanistic model of photosynthesis in microalgae including photoacclimation dynamics. *Journal of Theoretical Biology* **304** 1-15.

Gastellu-Etchegorry JP, Demarez V, Pinel V, Zagolski F. 1995. Modeling radiative transfer in heterogeneous 3D vegetation canopies. pp. 38-49, *Satellite Remote Sensing*, International Society for Optics and Photonics.

Genty B, Wonders J, Baker N.R. 1990. Nonphotochemical quenching of F0 in leaves is emission wavelength dependent - consequences for quenching analysis and its interpretation. *Photosynthesis Research* **26** 133-139.

Gitelson A, Buschmann C, Lichtenthaler HK. 1999. The chlorophyll fluorescence ratio F735/F700 as an accurate measure of the chlorophyll content in plants. *Remote Sensing of Environment* **69** 296-302.

Gitelson AA, Buschmann C, Lichtenthaler HK. 1998. Leaf chlorophyll fluorescence corrected for re-absorption by means of absorption and reflectance measurements. *Journal of Plant Physiology* **152** 283-296.

Glenn EP, Huete AR, Nagler PL, Nelson SG. 2008. Relationship between remotely-sensed vegetation indices, canopy attributes and plant physiological processes: what vegetation indices can and cannot tell us about the landscape. *Sensors* **8** 2136-2160.

Gopal R, Mishra KB, Zeeshan M, Prasad SM, Joshi MM. 2002. Laser-induced chlorophyll fluorescence spectra of mung plants growing under nickel stress. *Current Science* **83** 880.

Goudriaan J. 1977. *Crop micrometeorology: a simulation study.* Simulation Monographs 683, Pudoc, Wageningen, The Netherlands.

Goulas Y, Ounis A, Daumard F, Baret F, Chelle M, Moya I. 2014. Assessment of canopy fluorescence yield with airborne passive and active measurements: the CALSIF project. 5th International Workshop on Remote Sensing of Vegetation Fluorescence, 22-24 April 2014, Paris, France.

Gouveia-Neto AS, Da Silva-Jr EA, Cunha PC, Oliveira-Filho RA, Silva LMH, Da Costa EB, Camara TJR, Willadino LG. 2011. Abiotic stress diagnosis via laser induced chlorophyll fluorescence analysis in plants for biofuel. In: Dos Santos Bernardes MA (ed.) *Biofuel Production – Recent Developments and Prospects,* pp. 3-22. InTech.

Gouveia-Neto AS, Da Silva-Jr EA, Da Silva AJ, Do Nascimento CWA. 2012. Heavy metal stress detection and monitoring via LED-induced chlorophyll fluorescence analysis of *Zea mays* L. seedlings aimed at polluted soil phytoremediation. In: Farkas DL, Nicolau DV, Leif RC (eds.) Proc. SPIE 8225, Imaging, Manipulation, and Analysis of Biomolecules, Cells, and Tissues X, 21 January 2012, San Francisco, CA.

Gower J, King S. 2012. Use of satellite images of chlorophyll fluorescence to monitor the spring bloom in coastal waters. *International Journal of Remote Sensing* **33** 7469-7481.

Gu J, Yin X, Stomph T-J, Wang H, Struik PC. 2012a. Physiological basis of genetic variation in leaf photosynthesis among rice (*Oryza sativa* L.) introgression lines under drought and well-watered conditions. *Journal of Experimental Botany* **63** 5137-5153.

Gu J, Yin X, Struik PC, Stomph TJ, Wang H. 2012b. Using chromosome introgression lines to map quantitative trait loci for photosynthesis parameters in rice (*Oryza sativa* L.) leaves under drought and well-water field conditions. *Journal of Experimental Botany* **63** 455-469.

Guanter L, Frankenberg C, Dudhia A, Lewis PE, Gomez-Dans J, Kuze A, Suto H, Grainger RG. 2012. Retrieval and global assessment of terrestrial chlorophyll fluorescence from GOSAT space measurements. *Remote Sensing of Environment* **121** 236-251.

Guanter L, Zhang Y, Jung M, Joiner J, Voigt M, Berry JA, Frankenberg C, Huete A, Zarco-Tejada PJ, Lee J.E, Moran MS, Ponce-Campos G, Beer C, Camps-Valls G, Buchmann N, Gianelle D, Klumpp K, Cescatti A, Baker JM, Griffis TJ. 2014. Global and time-resolved monitoring of crop photosynthesis with chlorophyll fluorescence. *Proceedings of the National Academy of Sciences, PNAS:* doi: 10.1073/pnas.1320008111.

Gunther KP, Dahn HG, Ludeker W. 1994. Remote-sensing vegetation status by laser-induced fluorescence. *Remote Sensing of Environment* **47** 10-17.

Haboudane D, Miller JR, Pattey E, Zarco-Tejada PJ, Strachan IB. 2004. Hyperspectral vegetation indices and novel algorithms for predicting green LAI of crop canopies: Modeling and validation in the context of precision agriculture. *Remote Sensing of Environment* **90** 337-352.

Hasanuzzaman M, Nahar K, Alam MM, Roychowdhury R, Fujita, M. Roychowdhury R, Fujita, M.Roychowdhury R, Fujita, M. 2013. Physiological, biochemical, and molecular mechanisms of heat stress tolerance in plants. *International Journal of Molecular Sciences* **14** 9643-9684.

Havaux M, Strasser RJ, Greppin H. 1991. Effects of incident light intensity on the yield of steady-state chlorophyll fluorescence in intact leaves. An example of bioenergetic homeostasis. *Environmental and Experimental Botany* **31** 23-32.

Homolová L, Malenovský Z, Clevers JGPW, García-Santos G, Schaepman ME. 2013. Review of optical-based remote sensing for plant trait mapping. *Ecological Complexity* **15** 1-16.

Houborg R, Boegh E. 2008. Mapping leaf chlorophyll and leaf area index using inverse and forward canopy reflectance modeling and SPOT reflectance data. *Remote Sensing of Environment* **112** 186-202.

Houborg R, Cescatti A, Migliavacca M, Kustas WP. 2013. Satellite retrievals of leaf chlorophyll and photosynthetic capacity for improved modeling of GPP. *Agricultural and Forest Meteorology* **177** 10-23.

Jacquemoud S, Baret F. 1990. PROSPECT: A model of leaf optical properties spectra. *Remote Sensing of Environment* **34** 75-91.

Joiner J, Guanter L, Lindstrot R, Voigt M, Vasilkov AP, Middleton EM, Huemmrich KF, Yoshida Y, Frankenberg C. 2013. Global monitoring of terrestrial chlorophyll fluorescence from moderate spectral resolution near-infrared satellite measurements: methodology, simulations, and application to GOME-2. *Atmospheric Measurement Techniques Discussions* **6** 3883-3930.

Joiner J, Yoshida Y, Vasilkov AP, Middleton EM, Campbell PKE, Yoshida Y, Kuze A, Corp LA. 2012. Filling-in of near-infrared solar lines by terrestrial fluorescence and other geophysical effects: simulations and space-based observations from SCIAMACHY and GOSAT. *Atmospheric Measurement Techniques* **5** 809-829.

Joiner J, Yoshida Y, Vasilkov AP, Yoshida Y, Corp LA, Middleton EM. 2011. First observations of global and seasonal terrestrial chlorophyll fluorescence from space. *Biogeosciences* **8** 637-651.

Jovanic BR, Dramicanin MD. 2003. In vivo monitoring of chlorophyll fluorescence response to low-dose y-irradiation in pumpkin (*Cucurbita pepo*) leaves. *Luminescence* **18** 274-277.

Jovanic BR, Radenkovic B, Despotovic-Zrakic M, Bogdanovic Z, Panic B. 2012. Impact of nuclear radiation on plants photosynthesis and chlorophyll content after bombing with U-238 enriched bombs. *American-Eurasian Journal of Sustainable Agriculture* **6** 33-43.

Kancheva R, Borisova D, Iliev I, Yonova P. 2007. Chlorophyll fluorescence as a quantitative measure of plant stress. In: Bochenek Z (ed.) *New Developments and Challenges in Remote Sensing*, pp. 37-43. Rotterdam: Millpress.

Kattge J, Knorr W. 2007. Temperature acclimation in a biochemical model of photosynthesis: a reanalysis of data from 36 species. *Plant Cell and Environment* **30** 1176-1190.

Kattge J, Knorr W, Raddatz T, Wirth C. 2009. Quantifying photosynthetic capacity and its relationship to leaf nitrogen content for global-scale terrestrial biosphere models. *Global Change Biology* **15** 976-991.

Kebabian PL, Theisen AF, Kallelis S, Freedman A. 1999. A passive two-band sensor of sunlight-excited plant fluorescence. *Review of Scientific Instrumentation* **70** 4386-4393.

Keller M, Schimel DS, Hargrove WW, Hoffman FM. (2008). A continental strategy for the National Ecological Observatory Network. *Frontiers in Ecology and the Environment* **6** 282–284.

Kosugi Y, Shibata S, Kobashi S. 2003. Parameterization of the CO_2 and H_2O gas exchange of several temperate deciduous broad-leaved trees at the leaf scale considering seasonal changes. *Plant, Cell & Environment* **26** 285-301.

Kozlowski TT, Pallardy SG. (eds.) 1997. Nitrogen metabolism. In: *Physiology of Woody Plants*, Second Edition, pp. 189-209. Academic Press.

Krajicek V, Vrbova M. 1994. Laser-induced fluorescence spectra of plants. *Remote Sensing of Environment* **47** 51-54.

Krause GH, Weis E. 1991. Chlorophyll fluorescence and photosynthesis: the basics. *Annual Reviews of Plant Physiology* **42** 313-349.

Kuckenberg J, Tartachnyk I, Noga G. 2009. Detection and differentiation of nitrogen-deficiency, powdery mildew and leaf rust at wheat leaf and canopy level by laser-induced chlorophyll fluorescence. *Biosystems Engineering* **103** 121-128.

Larcher W. 1994. Photosynthesis as a tool for indicating temperature stress events. In: Schulze E-D, Caldwell MM (eds.) *Ecophysiology of Photosynthesis*, pp. 261-277. Springer.

Lausch A, Pause M, Schmidt A, Salbach C, Gwillym-Margianto S, Merbach I. 2013. Temporal hyperspectral monitoring of chlorophyll, LAI, and water content of barley during a growing season. *Canadian Journal of Remote Sensing* **39** 191-207. DOI: 10.5589/m13-028.

Lazar D, Jablonsky J. 2009. On the approaches applied in formulation of a kinetic model of photosystem II: Different approaches lead to different simulations of the chlorophyll a fluorescence transients. *Journal of Theoretical Biology* **257** 260-269.

Lebedeva GV, Belyaeva NE, Demin OV, Riznichenko GY, Rubin AB. 2002. Kinetic model of primary photosynthetic processes in chloroplasts. Description of the fast phase of chlorophyll fluorescence induction under different light intensities. *Biophysics* **47** 968-980.

Lee JE, Frankenberg C, van der Tol C, Berry JA, Guanter L, Boyce CK, Fisher JB, Morrow E, Worden JR, Asefi S, Badgley G, Saatchi S. 2013. Forest productivity and water stress in Amazonia: observations from GOSAT chlorophyll fluorescence. *Proceedings of the Royal Society of London Series B* **280** doi:10.1098/rspb.2013.0171.

Lee WS, Alchantis V, Yang C, Hirafuji M, Moshou D, Li C. 2010. Sensing technologies for precision specialty crop production. *Computers and Electronics in Agriculture* **74** 2-33.

Leufen G, Noga G, Hunsche M. 2013. Physiological response of sugar beet (*Beta vulgaris*) genotypes to a temporary water deficit, as evaluated with a multiparameter fluorescence sensor. *Acta Physiologiae Plantarum* 35: 1763-1774.

Leuning R. 1995. A critical appraisal of a combined stomatal-photosynthesis model for C3 plants. *Plant, Cell and Environment* **18** 339–355.

Levitt J. 1980. *Responses of Plants to Environmental Stresses. Vol.II. Water, Radiation, Salt and Other Stresses*. Academic Press.

Lichtenthaler HK, Hak R, Rinderle U. 1990. The chlorophyll fluorescence ratio F690/F730 in leaves of different chlorophyll content. *Photosynthesis Research* **25** 295-298.

Lichtenthaler HK, Rinderle U. 1988. The role of chlorophyll fluorescence in the detection of stress conditions in plants. *CRC Critical Reviews in Analytical Chemistry* **19** 29-85.

Lipucci di Paola M, Mazzinghi P, Pardossi A, Vernieri P. 1992. Vegetation monitoring of chilling stress by chlorophyll fluorescence ratio. *EARSeL Advances in Remote Sensing* **1** 2-6.

Liu L, Cheng Z. 2010. Detection of vegetation light-use efficiency based on solar-induced chlorophyll fluorescence separated from canopy radiance spectrum. *IEEE Journal of Selected Topics in Applied Earth Observations and Remote Sensing* **3** 306-312.

Liu L, Zhao J, Guan L. 2013. Tracking photosynthetic injury of Paraquat-treated crop using chlorophyll fluorescence from hyperspectral data. *European Journal of Remote Sensing* **46** 459-473.

Liu LY, Zhang YJ, Wang JH, Zhao CJ. 2005. Detecting solar-induced chlorophyll fluorescence from field radiance spectra based on the Fraunhofer line principle. *IEEE Transactions in Geoscience and Remote Sensing* **43** 827-832.

Lloyd J, Farquhar GD. 1994. ^{13}C discrimination during CO_2 assimilation by the terrestrial biosphere. *Oecologia* **99** 201-215.

Louis J, Cerovic ZG, Moya I. 2006. Quantitative study of fluorescence excitation and emission spectra of bean leaves. *Journal of Photochemistry and Photobiology B: Biology* **85** 65-71.

Louis J, Ounis A, Ducruet J-M, Evain S, Laurila T, Thum T, Aurela M, Wingsle G, Alonso L, Pedros R, Moya I. 2005. Remote sensing of sunlight-induced chlorophyll fluorescence and reflectance of Scots pine in the boreal forest during spring recovery. *Remote Sensing of Environment* **96** 37-48.

Lu CM, Zhang JH. 2000. Photosynthetic CO_2 assimilation, chlorophyll fluorescence and photoinhibition as affected by nitrogen deficiency in maize plants. *Plant Science* **151** 135-143.

Magnani F, Dayyoub A. 2014. Modelling chlorophyll fluorescence under ambient conditions. *New Phytologist* (in preparation).

Magnani F, Olioso A, Demarty J, Germain V, Verhoef W, Moya I, Goulas Y, Cecchi G, Agati G, Zarco-Tejada P, Mohammed G, Van der Tol C. 2009. Assessment of Vegetation Photosynthesis Through Observation of Solar Induced Fluorescence from Space. ESTEC Contract No. 20678/07/NL/HE, Final Report.

Magnani F, Raddi S, Mohammed G, Middleton EM. 2014. Let's exploit available knowledge on vegetation fluorescence. *Proceedings of the National Academy of Sciences of the USA* www.pnas.org/cgi/doi/10.1073/pnas.1406600111.

Maier SW. 2000. Modelling the Radiative Transfer in Leaves in the 300 nm to 2.5 □m Wavelength Region Taking into Consideration Chlorophyll Fluorescence. The Leaf Model SLOPE. PhD Thesis, Technischen Universität München.

Malenovský Z, Mishra KB, Zemek F, Rascher U, Nedbal L. 2009. Scientific and technical challenges in remote sensing of plant canopy reflectance and fluorescence. *Journal of Experimental Botany* **60** 2987-3004.

Mann HB, Whitney DR. 1947. On a test of whether one of 2 random variables is stochastically larger than the other. *Annals of Mathematical Statistics* **18** 50-60.

Marschner H. 1986. Functions of mineral nutrient: macronutrients. In: *Mineral Nutrition of Higher Plants*, pp. 195-267. Academic Press.

Marshall HL, Geider RJ, Flynn KJ. 2000. A mechanistic model of photoinhibition. *New Phytologist* **145** 347-359.

Mayer DG, Butler DG. 1993. Statistical validation. *Ecological Modelling* **68** 21-32.

McFarlane JC, Watson RD, Theisen AF, Jackson RD, Ehrler WL, Pinter PJ, Idso SB, Reginato RJ. 1980. Plant stress detection by remote measurement of fluorescence. *Applied Optics* **19** 3287-3289.

McMurtrey III JE, Chappelle EW, Kim MS, Meisinger JJ, Corp LA. 1994. Distinguishing nitrogen fertilization levels in field corn (*Zea mays* L.) with actively induced fluorescence and passive reflectance measurements. *Remote Sensing of Environment* **47** 36-44.

Medrano H, Escalona JM, Bota J, Gulias J, Flexas J. 2002. Regulation of photosynthesis of C_3 plants in response to progressive drought: stomatal conductance as a reference parameter. *Ann Bot* (Lond) **89** 895-905.

Meroni M, Barducci A, Cogliata S, Castagnoli F, Rossini M, Busetto L, Migliavacca M, Cremonese E, Galvagno M, Colombo R, di Cella UM. 2011. The hyperspectral irradiometer, a new instrument for long-term and unattended field spectroscopy measurements. *Rev. Sci. Instrum*. **82** 043106.

Meroni M, Colombo R. 2006. Leaf level detection of solar induced chlorophyll fluorescence by means of a subnanometer resolution spectroradiometer. *Remote Sensing of Environment* **103** 438-448.

Meroni M, Panigada C, Rossini M, Picchi V, Cogliati S, Colombo R. 2009. Using optical remote sensing techniques to track the development of ozone-induced stress. *Environmental Pollution* **157** 1413-1420.

Meroni M, Rossini M, Picchi V, Panigada C, Cogliati S, Nali C, Colombo R. 2008. Assessing steady-state fluorescence and PRI from hyperspectral proximal sensing as early indicators of plant stress: The case of ozone exposure. *Sensors* **8** 1740-1754.

Methy M, Olioso A, Trabaud L. 1994. Chlorophyll fluorescence as a tool for management of plant resources. *Remote Sensing of Environment* **47** 2-9.

Middleton EM, Corp LA, Campbell PKE. 2008. Comparison of measurements and FluorMOD simulations for solar-induced chlorophyll fluorescence and reflectance of a corn crop under nitrogen treatments. *International Journal of Remote Sensing* **29** 5193-5213.

Miller J, Berger M, Goulas, Y, Jacquemoud S, Louis J, Mohammed G, Moise N, Moreno J, Moya I, Pedrós R, Verhoef W, Zarco-Tejada P. 2005. Development of a Vegetation Fluorescence Canopy Model. European Space Agency ESTEC Contract No. 16365/02/NL/FF, Final Report.

Mishra KB, Gopal R. 2005. Study of laser-induced fluorescence signatures from leaves of wheat seedlings growing under cadmium stress. *General and Applied Plant Physiology* **31** 181-196.

Mohammed GH, Zarco-Tejada P, Miller JR. 2003. Applications of chlorophyll fluorescence in forestry and ecophysiology. In: DeEll JR, Toivonen PMA (eds.). *Practical Applications of Chlorophyll Fluorescence in Plant Biology*, pp. 80-124. Kluwer.

Morales F, Belkhodja R, Goulas Y, Abadia J, Moya I. 1999. Remote and near-contact chlorophyll fluorescence during photosynthetic induction in iron-deficient sugar beet leaves. *Remote Sensing of Environment* **69** 170-178.

Moya I, Camenen L, Evain S, Goulas Y, Cerovic ZG, Latouche G, Flexas J, Ounis A. 2004. A new instrument for passive remote sensing. 1. Measurements of sunlight-induced chlorophyll fluorescence. *Remote Sensing of Environment* **91** 186-197.

Moya I, Goulas Y, Morales F, Camenen L, Guyot G, Schmuck G. 1995. Remote sensing of time-resolved chlorophyll fluorescence and back-scattering of the laser excitation by vegetation. *EARSeL Advances in Remote Sensing* **3** 188-197.

Myers P, Espinosa R, Parr CS, Jones T, Hammond GS, Dewey TA. 2014. Terrestrial & aquatic biomes of the world. University of Michigan.

Naumann JC, Anderson JE, Young DR. 2010. Remote detection of plant physiological responses to TNT soil contamination. *Plant and Soil* **329** 239-248.

Nichol CJ, Pieruschka R, Takayama K, Förster B, Kolber Z, Rascher U, Grace J, Robinson SA, Pogson B, Osmond B. 2012. Canopy conundrums: building on the Biosphere 2 experience to scale measurements of inner and outer canopy photoprotection from the leaf to the landscape. *Functional Plant Biology* **39** 1-24.

Niinemets U. 2010. Responses of forest trees to single and multiple environmental stresses from seedlings to mature plants: Past stress history, stress interactions, tolerance and acclimation. *Forest Ecology and Management* **260** 1623-1639.

Nishiyama Y, Allakhverdiev SI, Murata N. 2011. Protein synthesis is the primary target of reactive oxygen species in the photoinhibition of photosystem II. *Physiologia Plantarum* **142** 35-46.

Olioso A, Methy M, Lacaze B. 1992. Simulation of canopy fluorescence as a function of canopy structure and leaf fluorescence. *Remote Sensing of Environment* **41** 239-247.

Öquist G, Huner NPA. 2003. Photosynthesis of overwintering evergreen plants. *Annual Review of Plant Biology* **54** 329-355.

Ounis A, Evain S, Flexas J, Tosti S, Moya I. 2001. Adaptation of a PAM-fluorometer for remote sensing of chlorophyll fluorescence. *Photosynthesis Research* **68** 113-120.

Panigada C, Busetto L, Meroni M, Amaducci S, Rossini M, Cogliati S, Boschetti M, Picchi V, Marchesi A, Pinto F, Rascher U, Colombo R. 2010. EDOCROS: Early detection of crop water and nutritional stress by remotely sensed indicators. 4th International Workshop on Remote Sensing of Vegetation Fluorescence, 15-17 November 2010, Valencia, Spain.

Pedrós R, Goulas Y, Jacquemoud S, Louis J, Moya I. 2010. FluorMODleaf: A new leaf fluorescence emission model based on the PROSPECT model. *Remote Sensing of Environment* **114** 155-167.

Peguero-Pina JJ, Morales F, Flexas J, Gil-Pelegrin E, Moya I. 2008. Photochemistry, remotely sensed physiological reflectance index and de-epoxidation state of the xanthophyll cycle in *Quercus coccifera* under intense drought. *Oecologia* **156** 1-11.

Perez-Priego O, Zarco-Tejada PJ, Miller JR, Sepulcre-Canto G, Fereres E. 2005. Detection of water stress in orchard trees with a high-resolution spectrometer through chlorophyll fluorescence in-filling of the O-2-A band. *IEEE Transactions in Geoscience and Remote Sensing* **43** 2860-2869.

Peterson RB, Oja V, Laisk A. 2001. Chlorophyll fluorescence at 680 and 730 nm and leaf photosynthesis. *Photosynthesis Research* **70** 185-196.

Pfundel E. 1998. Estimating the contribution of Photosystem I to total leaf chlorophyll fluorescence. *Photosynthesis Research* **56** 185-195.

Porcar-Castell A. 2011. A high-resolution portrait of the annual dynamics of photochemical and non-photochemical quenching in needles of Pinus sylvestris. *Physiologia Plantarum* **143** 139-153.

Porcar-Castell A, Juurola E, Ensminger I, Berninger F, Hari P, Nikinmaa E. 2008b. Seasonal acclimation of photosystem II in Pinus sylvestris. II. Using the rate constants of sustained thermal energy dissipation and photochemistry to study the effect of the light environment. *Tree Physiology* **28** 1483-1491.

Porcar-Castell A, Juurola E, Nikinmaa E, Ensminger I, Berninger F, Hari P. 2008a. Seasonal acclimation of photosystem II in *Pinus sylvestris.* I. Estimating the rate constants of sustained thermal energy dissipation and photochemistry. *Tree Physiology* **28** 1475-1482.

Pretzsch H, Biber P, Schütze G, Bielak K. 2014. Changes of forest stand dynamics in Europe. Facts from long-term observational plots and their relevance for forest ecology and management. *Forest Ecology and Management* (In Press)

Pury DD, Farquhar GD. 1997. Simple scaling of photosynthesis from leaves to canopies without the errors of big-leaf models. *Plant, Cell & Environment* **20** 537-557.

Rascher U, Agati G, Alonso L, Cecchi G, Champagne S, Colombo R, Damm A, Daumard F, de Miguel E, Fernandez G, Franch B, Franke J, Gerbig C, Gioli B, Gomez JA, Goulas Y, Guanter L, Gutierrez-de-la-Camara O, Hamdi K, Hostert P, Jimenez M, Kosvancova M, Lognoli D, Meroni M, Miglietta F, Moersch A, Moreno J, Moya I, Neininger B, Okujeni A, Ounis A, Palombi L, Raimondi V, Schickling A,

Sobrino JA, Stellmes M, Toci G, Toscano P, Udelhoven T, van der Linden S, Zaldei A. 2009. CEFLES2: the remote sensing component to quantify photosynthetic efficiency from the leaf to the region by measuring sun-induced fluorescence in the oxygen absorption bands. *Biogeosciences* **6** 1181-1198.

Rascher U, Alonso L, Burkart A, Cogliati S, Colombo R, Damm A, Guanter L, Julietta T, Moreno J, Pinto F, Rossini M, Schickling A. 2013. Mapping sun-induced fluorescence using the high performance imaging spectrometer HyPlant: Understanding spatio-temporal variations in vegetation stress response and functional adaptation of photosynthesis. EUROSPEC Conference, 6-8 November 2013, Trento, Italy.

Reich PB, Ellsworth DS, Walters MB. 1998. Leaf structure (specific leaf area) modulates photosynthesis–nitrogen relations: evidence from within and across species and functional groups. *Functional Ecology* **12** 948-958.

Rivera JP, Verrelst J, Muñoz-Marí J, Moreno J, Camps-Valls G. 2014. Toward a semiautomatic machine learning retrieval of biophysical parameters. *IEEE Journal of Selected Topics in Applied Earth Observation and Remote Sensing* (in press).

Rodriguez JM, Ustin SL, Riano D. 2011. Contributions of imaging spectroscopy to improve estimates of evapotranspiration. *Hydrological Processes* **25** 4069-4081.

Rohacek K, Soukupova J, Bartak M. 2008. Chlorophyll fluorescence: A wonderful tool to study plant physiology and plant stress. In: Schoefs B (ed.) *Plant Cell Compartments - Selected Topics,* pp. 41-104. Kerala, India: Research Signpost.

Rosema A, Cecchi G, Pantani L, Radicati B, Romuli M, Mazzinghi P, Vankooten O, Kliffen C. 1992. Monitoring photosynthetic activity and ozone stress by laser-induced fluorescence in trees. *International Journal of Remote Sensing* **13** 737-751.

Rosema A, Snel JFH, Zahn H, Buurmeijer WF, Van Hove LWA. 1998. The relation between laser-induced chlorophyll fluorescence and photosynthesis. *Remote Sensing of Environment* **65** 143-154.

Rosema A, Verhoef W, Schroote J, Snel JFH. 1991. Simulating fluorescence light canopy interaction in support of laser-induced fluorescence measurements. *Remote Sensing of Environment* **37** 117-130.

Ross ON, Moore M, Suggett DJ, McIntyre HL, Geider RJ. 2008. A model of photosynthesis and photo-protection based on reaction center damage and repair. *Limnology and Oceanography* **53** 1835-1852.

Rossini M, Meroni M, Migliavacca M, Manca G, Cogliati S, Busetto L, Picchi V, Cescatti A, Seufert G, Colombo R. 2010. High resolution field spectroscopy measurements for estimating gross ecosystem production in a rice field. *Agricultural and Forest Meteorology* **150** 1283-1296.

Saito Y, Saito R, Kawahara TD, Takeda S. 2000. Development and performance characteristics of laser-induced fluorescence imaging lidar for forestry applications. *Forest Ecology and Management* **128** 129-137.

Saltelli A, Annoni P, Azzini I, Campolongo F, Ratto M, Tarantola S. 2010. Variance based sensitivity analysis of model output. Design and estimator for the total sensitivity index. *Computer Physics Communications* **181** 259-270.

Saltelli A, Tarantola S, Chan K. 1999. A quantitative, model independent method for global sensitivity analysis of model output. *Technometrics* **41**: 39-56.

Schreiber U, Bilger W, Neubauer C. 1994. Chlorophyll fluorescence as a non-intrusive indicator for rapid assessment of in vivo photosynthesis. *Ecological Studies* **100** 49-70.

Sobol' IM. 2001. Global sensitivity indices for nonlinear mathematical models and their Monte Carlo estimates. *Mathematics and Computers in Simulation* **55** 271- 280.

Soukupová J, Cséfalvay L, Urban O, Kosvancová M, Marek M, Rascher U, Nedbal L. 2008. Annual variation of the steady-state chlorophyll fluorescence emission of evergreen plants in temperate zone. *Functional Plant Biology* **35** 63-76.

Srivastava A, Greppin H, Strasser RJ. 1995a. The steady state chlorophyll a fluorescence exhibits in vivo an optimum as a function of light intensity which reflects the physiological state of the plant. *Plant and Cell Physiology* **36** 839-848.

Srivastava A, Zeiger E. 1995b. Guard cell zeaxanthin tracks photosynthetically active radiation and stomatal apertures in *Vicia faba* leaves. *Plant Cell and Environment* **18** 813-817.

Srivastava P, Pandey J. 2012. LICF spectrum as a fast detector of chlorophyll damage in safflower growing under mutagenic stress. *World Journal of Agricultural Sciences* **8** 322-325.

Stirbet A., Govindjee. 2011. On the relation between the Kautsky effect (chlorophyll a fluorescence induction) and Photosystem II: Basics and applications of the OJIP fluorescence transient. *Journal of Photochemistry and Photobiology B: Biology* **104** 236-257.

Suarez L, Berni JAJ. 2012. Spectral responses of citrus and their application to nutrient and water constraints diagnosis. In: Srivastava AK (ed.) *Advances in Citrus Nutrition*, pp.125-141. Springer.

Suarez L, Zarco-Tejada PJ, Sepulcre-Canto G, Perez-Priego O, Miller JR, Jimenez-Munoz JC, Sobrino J. 2008. Assessing canopy PRI for water stress detection with diurnal airborne imagery. *Remote Sensing of Environment* **112** 560-575.

Subhash N. 1995. Detection of vegetation stress from laser-induced fluorescence signatures. International Centre for Theoretical Physics (Trieste, Italy), LAMP Series Report, LAMP/95/4, June 1995.

Subhash N, Mohanan CN. 1997. Curve-fit analysis of chlorophyll fluorescence spectra: Application to nutrient stress detection in sunflower. *Remote Sensing of Environment* **60** 347-356.

Subhash N, Mohanan CN. 1994. Laser-induced red chlorophyll fluorescence signatures as nutrient stress indicator in rice plants. *Remote Sensing of Environment* **47** 45-50.

Takahashi S, Badger MR. 2011. Photoprotection in plants: a new light on photosystem II damage. *Trends in Plant Science* **16** 53-60.

Theisen AF. 2002. Detecting chlorophyll fluorescence from orbit: The Fraunhofer Line Depth Model. In: Muttiah RS (ed.) *From Laboratory Spectroscopy to Remotely Sensed Spectra of Terrestrial Ecosystems*, pp. 203-232. Netherlands: Kluwer Academic.

Theisen AF, Rock BN, Eckert RT. 1994. Detection of changes in steady-state chlorophyll fluorescence in Pinus strobus following short-term ozone exposure. *Journal of Plant Physiology* **144** 410-419.

Thoren D, Schmidhalter U. 2009. Nitrogen status and biomass determination of oilseed rape by laser-induced chlorophyll fluorescence. *European Journal of Agronomy* **30** 238-242.

Thoren D, Thoren P, Schmidhalter U. 2010. Influence of ambient light and temperature on laser-induced chlorophyll fluorescence measurements. *European Journal of Agronomy* **32** 169-176.

Timmermans J, Su Z, Verhoef, W, Van der Tol C. 2011. Coupling optical and thermal directional radiative transfer to biophysical processes in vegetated canopies. Enschede, University of Twente Faculty of Geo-Information and Earth Observation (ITC), ITC Dissertation 193, ISBN: 978-90-6164-313-5.

Tremblay N, Wang Z, Cerovic ZG. 2012. Sensing crop nitrogen status with fluorescence indicators: A review. *Agronomy for Sustainable Development* **32** 451-464.

Treshow M, Anderson FK. 1989. *Plant Stress from Air Pollution*. John Wiley & Sons.

Tyystjärvi E, Aro E-M. 1996. The rate constant of photoinhibition, measured in lincomycin-treated leaves, is directly proportional to light intensity. *Proceedings of the National Academy of Sciences of the USA* **93** 2213-2218.

Tyystjärvi E, Hakala M, Sarvikas P. 2005. Mathematical modelling of the light response curve of photoinhibition of Photosystem II. *Photosynthesis Research* **84** 21-27.

Valentini R, Cecchi G, Mazzinghi P, Scarascia Mugnozza G, Agati G, Bazzani M, De Angelis P, Fusi F, Matteucci G, Raimondi V. 1994. Remote sensing of chlorophyll *a* fluorescence of vegetation canopies: 2. Physiological significance of fluorescence signal in response to environmental stresses. *Remote Sensing of Environment* **47** 29-35.

Van der Tol C. 2014. SCOPE version 1.53 user manual, 15 March 2014.

Van der Tol C, Berry J. 2012. Biochemical model in SCOPE. KISS Photosynthesis Workshop, 26-31 August 2012, Pasadena, California.

Van der Tol C, Berry JA, Campbell P, Rascher U. 2014. Steady state leaf chlorophyll fluorescence yield is related to the rate and the relative light saturation of photosynthesis. *Journal of Geophysical Research: Biogeosciences* (submitted).

Van der Tol C, Verhoef W, Rosema A. 2009a. A model for chlorophyll fluorescence and photosynthesis at leaf scale. *Agricultural and Forest Meteorology* **149** 96-105.

Van der Tol C, Verhoef W, Timmermans J, Verhoef A, Su Z. 2009b. An integrated model of soil-canopy spectral radiances, photosynthesis, fluorescence, temperature and energy balance. *Biogeosciences* **6** 3109-3129.

Verhoef W. 2011. Modelling vegetation fluorescence observations 7th EARSEL workshop of the Special Interest Group in imaging spectroscopy, 11-13 April 2011, Edinburgh, UK, pp. 41-42

Verhoef W. 2010. Vegetation fluorescence signal modelling from photosystem level to TOA radiance spectra. 4th Intl. Workshop on Vegetation Fluorescence, 15-17 November 2010, Valencia, Spain.

Verhoef W. 2004. Extension of SAIL to model solar-induced canopy fluorescence spectra. Proc. 2nd International Workshop on Remote Sensing of Vegetation Fluorescence, 17-19 November 2004, St-Hubert (Quebec), Canada.

Verhoef W. 1998. Theory of radiative transfer models applied in optical remote sensing of vegetation canopies. PhD Thesis, Wageningen Agricultural University.

Verhoef W. 1984. Light scattering by leaf layers with application to canopy reflectance modelling: the SAIL model. *Remote Sensing of Environment* **16** 125-141.

Verhoef W, Bach H. 2007. Coupled soil-leaf-canopy and atmosphere radiative transfer modeling to simulate hyperspectral multi-angular surface reflectance and TOA radiance data. *Remote Sensing of Environment* **109** 166-182.

Verhoef W, Jia L, Xiao Q, Su Z. 2007. Unified optical-thermal four-stream radiative transfer theory for homogeneous vegetation canopies. *IEEE Transactions in Geoscience and Remote Sensing* **45** 1808-1822.

Verhoeven AS, Demmig-Adams B, Adams III WW. 1997. Enhanced employment of the xanthophyll cycle and thermal energy dissipation in spinach exposed to high light and N stress. *Plant Physiology* **113** 817-824.

Verrelst J, Alonso L, Delegido J, Camps-Valls G, Moreno J. 2012. Retrieval of canopy parameters using Gaussian Processes techniques. *IEEE Transactions on Geoscience and Remote Sensing* **50** 1832-1843.

Verrelst J, Rivera JP. 2014a. A-SCOPE v1.53 installation guide. March 2014.

Verrelst J, Rivera JP. 2014b. A-SCOPE v1.53 manual. March 2014.

Verrelst J, Rivera JP. 2014c. Verification report on the functioning of SCOPE v1.53 / A-SCOPE v1.53. 14 March 2014, 2012 FLEX/Sentinel-3 Tandem Mission Photosynthesis Study, ESTEC Contract No. 4000106396/12/NL/AF.

Verrelst J, Rivera JP, Alonso L, Moreno J. 2011. ARTMO: an Automated Radiative Transfer Models. Operator toolbox for automated retrieval of biophysical parameters through model inversion. EARSeL 7th SIG-Imaging Spectroscopy Workshop, 11-13 April 2011, Edinburgh, UK.

Verrelst J, Rivera JP, Camps-Valls G, Moreno J. 2013. Recent advances in biophysical parameter retrieval methods - opportunities for Sentinel-2. In: ESA Living Planet Symposium 2013, 09-13 September, Edinburgh, UK.

Verrelst J, Romijn E, Kooistra L. 2012. Mapping vegetation structure in a heterogeneous river floodplain ecosystem using pointable CHRIS/PROBA data. *Remote Sensing* **4** 2866-2889.

Von Caemmerer S. 2013. Steady-state models of photosynthesis. *Plant, Cell & Environment* **36** 1617-1630.

Von Caemmerer S. 2000. *Biochemical Models of Leaf Photosynthesis*. CSIRO Publishing.

Wallace JS, Verhoef A. 2000. Modelling interactions in mixed-plant communities: light, water and carbon dioxide. pp. 204-250 In: Marshall B, Roberts JA (eds.) *Leaf Development and Canopy Growth*. Sheffield Academic Press.

Wallach D, Goffinet B. 1989. Mean squared error of prediction as a criterion for evaluating and comparing system models. *Ecological Modelling* **44** 299-306.

Weis E, Berry JA. 1987. Quantum efficiency of Photosystem II in relation to 'energy'-dependent quenching of chlorophyll fluorescence. *Bioenergetics* **894** 198-208.

Willmott CJ. 1981. On the validation of models. *Physical Geography* **2** 184-194.

Wilson KB, Baldocchi DD, Hanson PJ. 2001. Leaf age affects the seasonal pattern of photosynthetic capacity and net ecosystem exchange of carbon in a deciduous forest. *Plant, Cell & Environment* **24** 571-583.

Wong SC, Woo KC. 1986. Simultaneous measurements of steady state chlorophyll a fluorescence and CO_2 assimilation in leaves. *Plant Physiology* **80** 877-883.

Wullschleger SD. 1993. Biochemical limitations to carbon assimilation in C3 plants—a retrospective analysis of the A/Ci curves from 109 species. *Journal of Experimental Botany* **44** 907-920.

Wunch D, Toon GC, Blavier J-F L, Washenfelder RA, Notholt J, Connor BJ, Griffith DWT, Sherlock V, Wennberg PO. 2011. The Total Carbon Column Observing Network. *Philosophical Transactions of the Royal Society A: Mathematical, Physical and Engineering Sciences* **369** 2087–2112.

Yin X, Sun Z, Struik PC, Van der Putten PEL, Van Leperen W, Harbinson J. 2011. Using a biochemical C4 photosynthesis model and combined gas exchange and chlorophyll fluorescence measurements to estimate bundle-sheath conductance of maize leaves differing in age and nitrogen content. *Plant Cell and Environment* **34** 2183-2199.

Zaks J, Amarnath K, Kramer DM, Niyogi KK, Fleming GR. 2012. A kinetic model of rapidly reversible nonphotochemical quenching. *Proceedings of the National Academy of Sciences of the USA* **109** 15757-15762.

Zarco-Tejada PJ, Berni JAJ, Suarez L, Sepulcre-Canto G, Morales F, Miller JR. 2009. Imaging chlorophyll fluorescence with an airborne narrow-band multispectral camera for vegetation stress detection. *Remote Sensing of Environment* **113** 1262-1275.

Zarco-Tejada PJ, Catalina A, Gonzalez MR, Martin P. 2013a. Relationships between net photosynthesis and steady-state chlorophyll fluorescence retrieved from airborne hyperspectral imagery. *Remote Sensing of Environment* **136** 247-258.

Zarco-Tejada PJ, Gonzalez-Dugo V, Berni JAJ. 2012. Fluorescence, temperature and narrow-band indices acquired from a UAV platform for water stress detection using a micro-hyperspectral imager and a thermal camera. *Remote Sensing of Environment* **117** 322-337.

Zarco-Tejada PJ, Miller JR, Pedrós R, Verhoef W, Berger M. 2006. FluorMODgui V3.0: A graphic user interface for the spectral simulation of leaf and canopy chlorophyll fluorescence. *Computers & Geosciences* **32** 577-591.

Zarco-Tejada PJ, Morales A, Testi L, Villalobos FJ. 2013b. Spatio-temporal patterns of chlorophyll fluorescence and physiological and structural indices acquired from hyperspectral imagery as compared with carbon fluxes measured with eddy covariance. *Remote Sensing of Environment* **133** 102-115.

Zarco-Tejada PJ, Pushnik JC, Dobrowski S, Ustin SL. 2003. Steady-state chlorophyll a fluorescence detection from canopy derivative reflectance and double-peak red-edge effects. *Remote Sensing of Environment* **84** 283-294.

Zhang Y-J, Huang W-J, Wang J-H, Liu L-Y, Ma Z-H, Li F-L. 2007. Chorophyll fluorescence sensing to detect stripe rust in wheat (*Triticum aestivum* L.) fields based on Fraunhofer lines. *Scientia Agricultura Sinica* 2007-01, doi: CNKI:ISSN:0578-1752.0.2007-01-010.

Zhu XG, Govindjee, Baker NR, deSturler E, Ort DR, Long SP. 2005. Chlorophyll a fluorescence induction kinetics in leaves predicted from a model describing each discrete step of excitation energy and electron transfer associated with photosystem II. *Planta* **223** 114-133.

8. Acronynms & Abbreviations

A	photosynthesis	**FFR**	far-red fluorescence
Actot	net photosynthesis of canopy (parameter)	**FFRc**	far-red fluorescence, control value
Adj R^2	adjusted coefficient of determination	**F-GPP**	fluorescence – gross primary productivity
AL	asymmetric leaf	**F_I or F_{II}**	Fluorescence weight I or II
APAR	absorbed photosynthetically active radiation	**FIS**	Fluorescence Imaging System
APARChl	absorbed PAR by chlorophyll	**FLD**	Fraunhofer Line Discrimination
ARTMO	Automated Radiative Transfer Models Operator	**FLEX**	FLuorescence EXplorer
A-SCOPE	Automated SCOPE	**FLEX/S3**	Fluorescence Explorer/Sentinel-3
ASFY	apparent spectral fluorescence yield	**FLIDAR**	fluorescence lidar
ATP	adenosine triphosphate	**FLORIS**	FLuORescence Imaging Spectrometer
beta (β)	fraction of photons partitioned to PSII	**Fluortot**	total fluorescence emitted at top of canopy [W m^{-2}]
Ca	atmospheric CO_2 concentration	**Fluoryield**	fluorescence yield: Fluortot/aPAR_energy units [W W^{-1}]
Cab	chlorophyll a&b content	**FLUSS**	Atmospheric Corrections for Fluorescence Signal and Surface Pressure Retrieval Over Land (Study)
Cal/Val	calibration/validation	**FOV**	field of view
Cdm	dry matter content	**FR**	fluorescence ratio; or far-red fluorescence
CEFLES 2	CarboEurope, FLEX and Sentinel-2	**FRc**	red fluorescence, control value
CF	chlorophyll fluorescence	**F_S**	steady-state fluorescence (from active sensors)
CFM	Cost function minimization	**FSD**	fast and slow fluorescence dynamics
Chl	chlorophyll content	**Ft**	fluorescence at time *t* (from active sensors)
Chl a:b	chlorophyll a:b ratio	**Fv/Fm**	variable to maximal fluorescence (dark-adapted)
Ci	intercellular carbon dioxide	**GOME**	Global Ozone Monitoring Experiment
CO_2	carbon dioxide	**GOSAT**	Greenhouse Gases Observing Satellite
Cs	senescent material fraction	**GPP**	gross primary productivity (or production)
Cw	leaf water equivalent layer	**GPR**	Gaussian processes regression
d	LIDFa-LIDFb	**gs**	stomatal conductance
DART	a 3-D radiative transfer model	**GSA**	global sensitivity analysis
deltaF/F	quantum yield of PSII in the light (ΔF/Fm' or Φ_F of PSII)	**GUI**	Graphic User Interface
DEPS	(xanthophyll) de-epoxidation state	**hc**	vegetation height
DPD	double-peak detection	**Jmax**	maximum electron transport rate
DPi	Double-Peak Index	**KM**	Kubelka-Munk
ea	atmospheric vapour pressure	**kNPQs**	rate constant of sustained thermal dissipation (non-photochemical quenching)
ESA	European Space Agency	**kV**	extinction coefficient for Vcmo in the vertical
ETR	electron transport rate	**LAI**	leaf area index
F	steady-state chlorophyll fluorescence (from active or passive sensors)	**LIDF**	leaf inclination parameter (LIDFa or LIDFb)
***f*APAR**	fraction of absorbed photosynthetically active radiation	**LIF**	laser-induced fluorescence
FD	fast (OJIP) fluorescence dynamics	**LIFIS**	Laser-Induced Fluorescence Imaging System
FFS	fixed fluorescence spectrum	**LiFS**	Literature on Fluorescence and Stress (database of publications)

LIFT	Laser-Induced Fluorescence Transients	**R_{in}**	incident shortwave radiation
LUE	light use efficiency	**R_{li}**	broadband incoming longwave radiation
LUT	lookup table	**RT**	radiative transfer
m	Ball-Berry stomatal conductance parameter	**RMSE**	root mean square error
MCARI2	Modified Canopy Adjusted Ratio Index 2	**RTMf**	radiative transfer module for chlorophyll fluorescence
MD12	Magnani-Dayyoub 2012 model	**RTMo**	radiative transfer module for incident solar and sky radiation
MF	modulated fluorescence	**RTMt**	radiative transfer module for thermal radiation
MSE	mean square error	**s**	LIDFa+LIDFb
MSE_S	systematic mean square error	**S-3**	Sentinel-3
MSE_U	unsystematic mean square error	**SCOPE**	Soil Canopy Observation of Photochemistry and Energy fluxes (model)
MTCI	MERIS Terrestrial Chlorophyll Index	**SEN2FLEX**	Sentinel-2 and FLEX Experiment
N	leaf thickness parameters in SCOPE	**SF**	spectrofluorometer
NDVI	Normalized Difference Vegetation Index	**S_i**	first order sensitivity index
NEON	National Ecosystem Observatory Network	**SIF**	sun- or solar-induced fluorescence (passive sensors)
NIR	near infra-red	**SIFI**	Stress Intensity Fluorescence Index
NLIN	non-linear regression	**SIFLEX**	Solar Induced Fluorescence Experiment
NPC	net photosynthesis of canopy	**SL**	symmetric leaf
NPP	net primary production (or productivity)	**SLSTR**	Sea and Land Surface Temperature Radiometer
NPQ	non-photochemical quenching	**SS**	steady-state fluorescence
NRMSE	normalized root mean square error	**ST_i**	total effect sensitivity index
NSFI	Nitrogen Stress Fluorescence Index	**stressfactor**	stress factor to reduce Vcmo
O_2-A, O_2-B	oxygen A(B) band	**SVAT**	soil-vegetation-atmosphere transfer
OCO-2	Orbiting Carbon Observatory-2	**TTCON**	Total Carbon Column Observing Network
OLCI	Ocean and Land Colour Imager	**Tyear**	mean annual temperature
p	air pressure	**u**	wind speed at height z
PAM	pulse-amplitude modulated	**T**	temperature (C)
PAR	photosynthetically active radiation	**Ta**	air temperature
PARCS	Performance Analysis and Requirement Consolidation Study	**TB-12**	Tol-Berry 2012 leaf biochemical model
PB	process-based	**TB-12(D)**	Tol-Berry 2012 (Drought) leaf model
PEP	phosphoenolpyruvate	**Tc**	canopy temperature
PFS	Plant Fluorescence Sensor	**TOA**	top of atmosphere
PFT	plant functional type	**TOC**	top of canopy
p_{LAI}	transformed LAI	**TRF**	time-resolved fluorometer
PQ	photochemical quenching	**TS**	time series
PRF	polynomial and rational functions	**TSFI**	Temperature Stress Fluorescence Index
PRI	Photochemical Reflectance Index (or Physiological Reflectance Index)	**tto**	observation zenith angle (parameter)
psi	azimuthal difference between solar and observation angle (parameter)	**tts**	solar zenith angle (parameter)
PSI or **PSII**	photosystem I or II	**Vcmo**	maximum carboxylation capacity at optimum temperature (also V_{cmax})
Q	incoming PAR	**VFS**	variable fluorescence spectrum
Qa	primary quinine electron acceptor of PSII)	**VIS**	visible spectrum
qLs	fraction of functional reaction centres	**V_{pm}**	PEP carboxylation rate
Rd	respiration rate in the light	**WSFI**	Water Stress Fluorescence Index

9. Appendices

9.1 Team involvements

Activity	Participants
Management & coordination of activities	**Task Leader: G. Mohammed**
Study activity website and services	D. Pernokis
Overall study management & coordination	G. Mohammed
Interface & coordination with other FLEX studies & campaign activities	G. Mohammed
Datasets and model availability review: model/module assessment, comparison, and gap analysis	**Task Leader: F. Magnani**
Review and comparison of existing models	F. Magnani, A. Volta, C. van der Tol, W. Verhoef
Database generation	Y. Goulas, F. Magnani
Testing and verification of modules: A-SIF	F. Magnani, S. Raddi
Testing & verification of modules: radiative transfer and SIF upscaling	C. van der Tol, W. Verhoef
Model design framework	F. Magnani, C van der Tol, W. Verhoef
Model implementation, validation, sensitivity analysis and error quantification	**Task Leader: J. Moreno**
Model implementation	J. Verrelst, J Pablo Rivera, C van der Tol, F. Magnani, J. Moreno
Model validation based on consistency tests and statistical properties on input/output data	F. Magnani
Model validation based on field measurements and external reference information	F. Daumard, Y. Goulas
Model consolidation	C. van der Tol, W. Verhoef, G. Mohammed
Sensitivity analysis based on Jacobians	C. van der Tol, J. Verrelst, M. van der Tol, F. Magnani, W. Verhoef, G. Mohammed
Sensitivity analysis based on Monte Carlo distributions	J. Verrelst, J Pablo Rivera, C. van der Tol
Error quantification for output variables vs uncertainties in input data	Y. Goulas, F. Daumard
Final software implementation and documentation	J. Verrelst, J Pablo Rivera, J. Moreno, C. van der Tol, F. Magnani
Algorithm development based on models	**Task Leader: Y. Goulas**
Model inversion	J. Verrelst, J Pablo Rivera
Statistical algorithm based on model and/or observations	Y. Goulas, F. Daumard
Algorithms based on simple F-GPP relationships	F. Magnani, S. Raddi
Simplified algorithms based on health or stress indicators	Y. Goulas, F. Daumard
Strategies integration and development of a prototype algorithm	Y. Goulas, F. Daumard
Fluorescence as an indicator of vegetation health and stress resilience	**Task Leader: J. Olejníčková**
Database of stress responses	A. Gallé, U. Rascher
Potential for the novel signal	A. Gallé, J. Olejníčková, A. Ač, U. Rascher
Knowledge gap analysis	Z. Malenovský
Conceptual framework for use with FLEX	G. Mohammed, D. Pernokis
Conclusions and recommendations	**Task Leader: G. Mohammed**
Final report and recommendations	G. Mohammed, Team
Final presentation	G. Mohammed
Technical data package (TDP)	D. Pernokis

9.2 Study meeting dates

Meeting name	Acronym	Location	Date
Kick-Off Meeting	KO	Telecon	05 July 2012
Progress Meeting 1	PM1	Italy (U. Bologna)	26 October 2012
Progress Meeting 2	PM2	Telecon	17 January 2013
Progress Meeting 3	PM3	ESTEC	28 May 2013
Mid-Term Review	MTR	ESTEC	18 October 2013
Final Review	FR	ESTEC	02 July 2014

9.3 Publications & Conference presentations

Ač A, Malenovský Z, Olejníčková J, Gallé A, Rascher U, Mohammed G. 2014. Meta-analysis assessing potential of steady-state chlorophyll fluorescence for remote sensing detection of plant water, temperature and nitrogen stress. *Remote Sensing of Environment* (submitted).

Malenovský Z, Ač A, Olejníčková J, Gallé A, Rascher U, Mohammed G. 2014. Knowledge gap analysis assessing steady-state chlorophyll fluorescence as an indicator of plant stress status. 5th International Workshop on Remote Sensing of Vegetation Fluorescence, 22-24 April 2014, Paris, France.

Mohammed G, Ač A, Daumard F, Drusch M, Gallé A, Goulas Y, Magnani F, Malenovský Z, Moreno J, Olejníčková J, Pernokis D, Rascher U, Rivera JP, Van der Tol C, Verhoef W, Verrelst J, Volta A. 2014. FLEX / Sentinel-3 Tandem Mission Photosynthesis Study – An investigation of steady-state chlorophyll fluorescence and photosynthesis in terrestrial vegetation. 5th International Workshop on Remote Sensing of Vegetation Fluorescence, 22-24 April 2014, Paris, France.

Van der Tol C, Verhoef W, Berry J, Rascher U, Campbell P, Verhoef A, Timmermans J, Vilfan NR, Mohammed G, Su B. 2014. SCOPE model: overview and sensitivity. 5th International Workshop on Remote Sensing of Vegetation Fluorescence, 22-24 April 2014, Paris, France.

Van der Tol C, Verhoef W, Verrelst J, Magnani F, Mohammed G, Moreno J, Berry J. 2014. Sensitivity of SCOPE modelled GPP and fluorescence for different Plant Functional Types. Whispers, 6th Workshop on Hyperspectral Image and Signal Processing: Evolution in Remote Sensing, 24-27 June 2014, Lausanne, Switzerland.

Verrelst J, Rivera JP, Van der Tol C, Magnani F, Mohammed G, Moreno J. 2014. A-SCOPE: automating fluorescence modeling in support of FLEX. 5th International Workshop on Remote Sensing of Vegetation Fluorescence, 22-24 April 2014, Paris, France.

Verrelst J, Rivera JP, Van der Tol C, Magnani F, Mohammed G, Moreno J. 2014. Global sensitivity analysis of the A-SCOPE model in support of future FLEX fluorescence retrievals. Whispers, 6th Workshop on Hyperspectral Image and Signal Processing: Evolution in Remote Sensing, 24-27 June 2014, Lausanne, Switzerland.

9.4 Errata

Revision 1.8 — 15 January 2015:

The citation "Guanter et al. 2014" was corrected to "Guanter et al. 2012" in four locations of this document (Pages 15, 90, 93, and 136) and in the standalone version of the Executive Summary (Page 7).